Insights into the tectonic evolution of the North China Craton through comparative tectonic analysis: A record of outward growth of Precambrian continents

Ali Polat

Accepted Manuscript

Insights into the Tectonic Evolution of the North China Craton Through Comparative Tectonic Analysis: A Record of Outward Growth of Precambrian Continents

¡!–¡QUERY id="Q14" type="boolean" replies="Yes—No" name="Spice3G"¿¡ce:para¿The author names have been tagged as given names and surnames (surnames are highlighted in teal color). Please confirm if they have been identified correctly.¡/ce:para¿¡/QUERY¿–¿T.M. Kusky, A. Polat, B.F. Windley, K.C. Burke, J.F. Dewey, W.S.F. Kidd, S. Maruyama, J.P. Wang, H. Deng, Z.S. Wang, C. Wang, D. Fu, X.W. Li, H.T. Peng

PII: S0012-8252(16)30283-5
DOI: doi:10.1016/j.earscirev.2016.09.002
Reference: EARTH 2312

To appear in: *Earth Science Reviews*

Received date: 3 June 2016
Revised date: 31 August 2016
Accepted date: 4 September 2016

Please cite this article as: Kusky, ¡!–¡QUERY id="Q14" type="boolean" replies="Yes—No" name="Spice3G"¿¡ce:para¿The author names have been tagged as given names and surnames (surnames are highlighted in teal color). Please confirm if they have been identified correctly.¡/ce:para¿¡/QUERY¿–¿T.M., Polat, A., Windley, B.F., Burke, K.C., Dewey, J.F., Kidd, W.S.F., Maruyama, S., Wang, J.P., Deng, H., Wang, Z.S., Wang, C., Fu, D., Li, X.W., Peng, H.T., Insights into the Tectonic Evolution of the North China Craton Through Comparative Tectonic Analysis: A Record of Outward Growth of Precambrian Continents, *Earth Science Reviews* (2016), doi:10.1016/j.earscirev.2016.09.002

Insights into the Tectonic Evolution of the North China Craton Through Comparative Tectonic Analysis: A Record of Outward Growth of Precambrian Continents

Kusky, T.M.,[1,2*] Polat, A.,[3,1] Windley, B.F.,[4,1] Burke, K.C.,[5] Dewey, J.F.,[6] Kidd, W.S.F.,[7] Maruyama, S.,[8,1], Wang, J.P.,[1] Deng, H.,[1] Wang, Z.S.,[1] Wang, C.,[1] Fu, D.,[1] Li, X.W., Peng, H.T.,[1]

[1] *Center for Global Tectonics, School of Earth Sciences, ChinaUniversity of Geosciences, Wuhan, 430074*

[2] *State Key Lab for Geological Processes and Mineral Resources, ChinaUniversity of Geosciences, Wuhan, 430074*

[3] *Department of Earth and Environmental Sciences, University of Windsor, Ontario, Canada*

[4] *Department of Geology, University of Leicester, U.K.,*

[5] *Department of Geosciences, University of Houston, TX, USA*

[6] *University of CaliforniaDavis, and UniversityCollege, Oxford.*

[7] *Department of Atmospheric and Environmental Sciences, University at Albany, USA*

[8] *Earth-Life Institute, Tokyo Institute of Technology*

Earth Science Reviews, submitted, Jan. 8, 2016

Revision Submitted 6/3/2016

Preamble

"Looking back dispassionately into the history of geology it is interesting to observe how deeply conservatism appears to have become entrenched. Particular theories have come to be so widely accepted, that any doubts regarding their validity are apt to be overlooked. Indeed there is some danger lest the science become stereotyped through too close adherence to accepted beliefs…" Alex du Toit, 1937, Our Wandering Continents.

Abstract

Archean cratons have map patterns and rock associations that are diagnostic of the Wilson Cycle. The North China Craton (NCC) consists of several distinctly different tectonic units, but the delineation and understanding of the significance of individual sutures and the rocks between them has been controversial. We present an actualistic tectonic division and evolution of the North China Craton based on Wilson Cycle and comparative tectonic analysis that uses a multi-disciplinary approach in order to define sutures, their ages, and the nature of the rocks between them, to determine their mode of formation and means of accretion or exhumation, and propose appropriate modern analogues. The eastern unit of the craton consists of several different small

blocks assembled between 2.6 and 2.7 Ga ago, that resemble fragments of accreted arcs from an assembled archipelago similar to those in the extant SW Pacific. A thick Atlantic-type passive margin developed on the western side of the newly assembled Eastern Block by 2.6-2.5 Ga. A >1,300 km- long arc and accretionary prism collided with the margin of the Eastern Block at 2.5 Ga, obducting ophiolites and ophiolitic mélanges onto the block, and depositing a thick clastic wedge in a foreland basin farther into the Eastern Block. This was followed by an arc-polarity reversal, which led to a short-lived injection of mantle wedge-derived melts to the base of the crust that led to the intrusion of mafic dikes and arc-type granitoid (TTG) plutons with associated metamorphism. By 2.43 Ga, the remaining open ocean west of the accreted arc closed with the collision of an oceanic plateau now preserved as the Western Block with the collision-modified margin of the Eastern Block, causing further deformation inthe Central Orogenic Belt. 2.4-2.35 Ga rifting of the newly amalgamated continental block formed a rift along its center, and new oceans within the other two rift arms, which removed a still-unknown continental fragment from its northern margin. By 2.3 Ga an arc collided with a new Atlantic-type margin developed over the rift sequence along the northern margin of the craton, and thus was converted to an Andean margin through arc-polarity reversal.

Andean margin tectonics affected much of the continental block from 2.3 to 1.9 Ga, giving rise to a broad E-W swath of continental margin magmas, and retro-arc sedimentary basins including a foreland basin superimposed on the passive northern margin. The horizontal extent of these tectonic components is similar to that across the present-day Andes in South America. From 1.88 to 1.79 Ga a granulite facies metamorphic event was superimposed across the entire continental block with high-pressure granulites and eclogites in the north, and medium-pressure granulites across the whole craton to the south. The scale and duration of this post-collisional event is similar to that in Central Asia that resulted from the Cenozoic India-Asia collision. The

deep crustal granulites and volcanic rocks on the surface today, interpreted to be anatectic melts from deep crustal granulites, are similar to high-grade metamorphic rocks and partial melts presently forming at mid-crustal levels beneath Tibet. Structural fabrics in lower-crustal migmatites related to this event reveal that they flowed laterally parallel to the collision boundary, in a way comparable to what is speculated to be happening in the deep crust of the Himalayan/Tibetan foreland. We relate this continent-continent collision to the collision of the North China Craton with the postulated Columbia (Nuna) Continent. The NCC broke out of the Columbia Continent between 1753-1673 Ma, as shown by the formation of a suite of anorthosite, mangerite, charnockite, and alkali-feldspar granites in an ENE-striking belt along the northern margin of the craton, whose intrusion was followed by the development of rifts and graben, mafic dike swarms, and eventually an Atlantic-type passive margin that signaled the beginning of a long period of tectonic quiescence and carbonate deposition for the NCC during Sinian times, which persisted into the Paleozoic. The style of tectonic accretion in the NCC changed at circa 2.5 Ga, from an earlier phase of accretion of arcs that are presently preserved in horizontal lengths of several hundred kilometers, to the accretion and preservation of linear arcs several thousand kilometers long with associated oceanic plateaus, microcontinents, and accretionary prisms. The style of progressively younger and westward outward accretion of different tectonic components is reminiscent of the style of accretion in the Superior Craton, and may signal the formation of progressively larger landmasses at the end of the Archean (perhaps like the Kenorland Continent), then into the Paleoproterozoic, culminating in the assembly of the Columbia (Nuna) Continent at 1.9-1.8 Ga.

Keywords: North China Craton; Precambrian; Tectonic Analysis; Ophiolite; arc-continent collision; Andean Arc; Continental Growth

1. Introduction

It is not easy to recognize suture zones and records of past Wilson Cycles that may be preserved in ancient high-grade metamorphic rocks that lack fossils, and from which it is not possible to obtain reliable paleomagnetic data. However, if methods of tectonic analysis such as delineation of regional tectonic zonation, sedimentology, structural analysis, geochronology, geochemistry of magmatic rocks, and metamorphic petrology are mutually combined, a robust tectonic analysis can ensue. Studies that rely solely on one or two methodologies are unlikely to generate sufficient fundamental data to be able to produce meaningful results. In this work we apply all these methods of tectonic analysis to the North China Craton (NCC hereafter) in order to document the presence of sutures, the nature of different units that were mutually sutured, the geometry of subduction that led to the suturing, and we examine how these processes may or may not have changed with time from the Archean to the present and from the low-grade upper crust to the high-grade lower crust. For the NCC there are considerable data, but also many controversies about the tectonic sub-divisions, the location and ages of sutures and orogens, the polarity of interpreted subduction zones, the presence of collisional orogens and sutures, and the meaning of metamorphic trajectories. We shed light on these problematic interpretations through copious use of global comparisons between Archean examples and Phanerozoic analogues. This major craton preserves a record of 3.8 billion years of geological activity. We use the methods of tectonic analysis and comparative tectonics to test whether or not there has been any secular change in tectonic style during its long history.

The NCC is divisible into several different tectonic units (Fig. 1), the boundaries of which and the timing and significance of their formation are under lively discussion. The Eastern Block consists of Neoarchean tonalite-trondhjemite-granodiorite (TTG gneisses, granitoids), and greenstone belts variously interpreted as arcs, ophiolites, relict rifts, or products of plume-related volcanism, and older crustal remnants that date back to circa 3.8 Ga. The Eastern Block has been interpreted to consist of several different microblocks, or a larger terrain that was later dismembered, that amalgamated between ~ 2.7 and 2.6 Ga (Zhai et al., 2010; Zhai and Santosh, 2011; Zhai, 2014; Santosh et al., 2016). These rocks were metamorphosed in the Archean and Paleoproterozoic. The eastern part of the craton was "decratonized" in an "orogen-craton-orogen" cycle (Kusky et al., 2007a) in the Mesozoic, when large parts of the sub-continental lithospheric mantle root were lost (Menzies et al., 1992; Griffin et al., 1998; Zhai et al., 2007; Windley et al., 2010; Zhu et al., 2012, and references therein). A central zone (alternatively referred to as the Central Orogenic Belt (COB), or Trans-North China Orogen (TNCO) has been considered to be an orogen, but its borders change in different models, and the collisional ages of various units are dissimilar in successive models (e.g., Zhao et al., 2005; Kusky, 2011a, b). The Western Block is generally regarded as a typical Archean craton, with low heat flow, a thick mantle root, and few earthquakes; however, its detailed geology is little known because it is almost completely covered by thick Precambrian-Quaternary sediments. Kusky and Mooney (2015) suggested that the Ordos Basin may be floored by a trapped Archean oceanic plateau that evolved through later tectono-magmatic events into a stable craton. The northern part of the craton is marked by a Paleoproterozoic orogen, named the Inner Mongolia-Northern Hebei Orogen (or just North Hebei Orogen in some works), which contains several lithotectonic units including the so-called Khondalite Belt, and the Yinshan "Block"; in the west it continues as the "Alxa (also called Alashan) Block." We consider these northern units to belong to an accretionary ribbon-like orogen along the margin of the craton. The eastern side of the craton is occupied by the Paleoproterozoic Jiao-Liao-Ji deformed volcano-sedimentary belt (Fig. 1).

Fig 1 near here – map of NCC

In this contribution we first review the principles of tectonic analysis used in the search for ancient sutures. We then assess the essential aspects of the geology, geochemistry, metamorphic history, and geophysical characteristic of the NCC, applying methods of plate tectonic analysis to this ancient high-grade metamorphic terrane, in order to show how the records of plate tectonics including vestiges of ancient Wilson Cycles can be recognized in ancient cratons. In this analysis we use worldwide examples of many ages of comparable tectonic settings assigned to the NCC at different stages of its evolution. We examine the nature of the boundaries between the different tectonic units in the NCC, and propose a comprehensive actualistic model for the craton's evolution based on current understanding of the construction of the plate tectonic paradigm. We then examine whether or not the tectonic history of the NCC is similar to or different from modern-style plate tectonics.

2. GEOLOGIC METHODS OF MAPPING SUTURES IN PRECAMBRIAN TERRANES

2.1 How are sutures recognized in old high-grade metamorphic terranes?

Sutures mark places where oceans have opened, and then closed in the Wilson Cycle, and where two once-widely-separated tectonic blocks (arcs, continents, plateaus, etc.) have collided. Since the classic paper “Suture zone complexities” by Dewey (1977), sutures have been recognized and defined on the basis of geological relationships, and differences in the geologic, structural, magmatic, sedimentary, and metamorphic histories of the tectonic blocks on either side. Sutures are characterized by complex structures, but there is a boundary within suture zones that separates rocks formed on one plate from those formed on the other plate, and this boundary zone is typically characterized by structurally complex, thrust-imbricated rocks such as mélanges, dismembered ophiolites and ocean plate stratigraphy that were scraped off the intervening oceanic plate during convergence and collision of the two tectonic blocks (Fig. 2). A fundamental current problem is that early work on sutures was in upper crustal rocks such as the Appalachians and Alps (e.g., Dewey, 1969; Bird and Dewey, 1970; Dewey et al., 1973; Windley, 1995) for which there are modern analogues, but much later work has been in lower crustal rocks, but few deep crustal levels of modern orogens are exposed today. Thus the more deeply buried and highly metamorphosed a suture zone becomes, the harder it is to recognize it as a suture, until at some point - typically at granulite facies level – a suture becomes cryptic, and might only be recognized by “a few specks of fuchsite” along a shear zone (Burke et al., 1976). For instance, boundaries between different tectonic blocks in the Archean craton of West Greenland are marked by up to 200 meter wide mylonitic, amphibolite facies volcanic and sedimentary rocks and serpentinites. These have been interpreted to represent the roots of Archean suture zones (Nutman and Friend, 2007; Windley and Garde, 2009; Polat et al., 2015). One of the goals of this paper is to use modern understanding of suture zones based on young orogens such as shown in Figure 2 to test whether or not we can recognize any similar patterns in the ancient North China Craton, and then compare this with other Archean terranes world-wide to define criteria about how to recognize sutures in ancient high-grade rocks.

Fig. 2 near here, cross-section of orogen

Suture zones are commonly overprinted by later events, and thus become even harder to recognize. For example, and compared with the NCC, in the Appalachians (Fig. 3) the Ordovician Taconic suture between the North American passive margin and an accreted island arc is marked by a few mélanges and shear zones, a series of allochthonous nappes of continental rise sedimentary rocks, rare ophiolitic fragments, and it is strongly overprinted by younger, stronger tectonic events related to a later Acadian continental collision (e.g., Rowley and Kidd, 1981; Bosworth and Kidd, 1985). However, detailed geological mapping and structural analysis has revealed the presence and position of the older Taconic suture (e.g., Kidd et al., 1995; Lim et al., 2005). Figure 3 shows part of New England and eastern USA, where tectonic zones demarcating the Ordovician Taconic orogen can be clearly defined. The Taconic thrust front is typically located in flysch sediments shed from the advancing Taconic allochthons and deposited in a trench, and the allochthons, comprised of continental rise meta-sediments, are bound by thrusts with displacements of approximately 120 km (e.g. Rowley, 1982). Moving eastwards from the belt of allochthons and deformed accreted oceanic rocks, a discontinuous belt of Precambrian (Grenvillian) basement domes, uplifted in the Devonian Acadian orogeny, have penetrated through the Ordovician tectonic zones; these are succeeded eastwards by younger sedimentary basins that were deformed during the Devonian Acadian orogeny (e.g., Bradley, 1983; van Staal et al., 2012). The next belt is the main Ordovician Taconic arc, which is only a few tens of km wide and strongly deformed. Even though it is clear that the Taconic orogeny occurred in the mid-Ordovician, the Taconic orogen was strongly affected by younger tectonic events. The presence of younger and stronger metamorphic overprints from the Acadian orogeny (continent – continent collision) has not obliterated the evidence that the Taconic orogeny took place in the Ordovician. The presence of younger sedimentary basins within the boundaries of the original Taconic orogen, many bound by faults, has not obscured the deformation that took place during the Acadian orogeny.

The same general principles can be applied to older Precambrian terranes, such as the Archean NCC, and to Proterozoic high-grade terranes such as the Gondwanan basement of

Madagascar (e.g., Collins et al., 2000; Kröner et al., 2000; Raharimahefa and Kusky, 2006, 2009; Ishwar-Kumar et al., 2015). Below we examine the field, structural, sedimentary, petrological, geochronological, and metamorphic evidence for a 2.5 Ga suture between the Eastern Block of the NCC, and an accreted arc preserved in the COB of the craton, and we will compare these with comparable features in other orogenic belts of different ages world-wide. Note that the scale and overall tectonic zonation of the COB are remarkably similar to those of the Taconic Orogen (Fig. 3), briefly described above.

2.2 Recognizing vestiges of ancient Wilson Cycles in Precambrian Orogens

Modern plate tectonic processes observable in the present plate mosaic serve as examples of the complexities that might be anticipated in assessment of the presence or absence of Wilson Cycles in ancient cratons. Consider, for instance, a simple Wilson Cycle, which describes the geologic consequences of plate separation and later convergence and collision (e.g., Polat, 2014). When a continent breaks up, the two initially contiguous pieces move apart, their rifted margins thermally subside, and any rift-related volcanic or sedimentary rocks are covered by sandstones, shales, and carbonates of a passive margin. This rock sequence can be recognized in a later-formed orogen, and constitutes a diagnostic time-and-space series of specific rock units that relate to the sequential history of the final orogeny (e.g. Wakita et al., 2013).

At some stage, arcs develop in a closing ocean, particularly due to changes in plate motion that cause a ridge or fracture zone to be converted to a subduction zone (e.g. Casey and Dewey, 1984; Stern, 2004). As the new arc moves towards one of the continental margins, an accretionary wedge typically develops in a trench in front of that arc. The accretionary wedge is characterized by specific rock types, such as olistostromes, mélanges, turbidites, and material scraped off the down-going plate such as cherts, hemipelagic muds, fragments of ocean floor, ophiolitic mélanges, and in some places ophiolites, which constitute oceanic plate stratigraphy (OPS), which reflects the depositional history of an oceanic plate as it moves from a ridge to an accretionary wedge at a trench, and is recognizable as piles of imbricated thrust duplexes (e.g. Fujisaki et al., 2015) in many accretionary wedges of all ages around the world (Kusky et al., 2013). Many accretionary wedges are affected by episodes of ridge subduction, which typically add a distinctive suite of magmas and anomalous deformation that are diachronous along strike in the wedge (e.g., Bradley et al., 2003). When an arc is moving across an ocean, it grows through magmatic and accretionary processes, and later is deformed when it is accreted. When arcs and continents collide, they overthrust or underthrust each other, and some are subducted (e.g., Yamamoto et al., 2009), undergoing multiple deformational, metamorphic, and partial melting processes.

When the arc and the accretionary wedge collide with a continent, slab pull forces and the load of the thrust-imbricated orogen cause the continental margin to subside, and a distinctive sedimentary sequence of black shales, then graywackes, then coarse-grained clastic rocks are deposited in a craton-moving flexural foreland basin (e.g., Dewey, 1969; Bradley and Kusky, 1986), and are often deformed in emplacement-related melanges (Festa et al., 2012). The accretionary wedge and arc are thrust upon the continent, and a very distinctive tectonic zonation is developed from the craton, to the foreland basin overlying the rift-passive margin sequence, to the mélange-bearing accretionary prism, through ophiolite belts in some cases, into the core or root of the arc, which is typically at high metamorphic grade (Fig. 2). In many cases high-pressure or ultra-high pressure metamorphic rocks such as eclogites are exhumed (e.g., Hsu, 1991). Following their accretion, fragments of arcs, accretionary prisms and ophiolites are further deformed, dismembered and dispersed by strike-slip faults. It is imperative to recognize a suture in this geological / tectonic scenario. The suture marks the zone that separates rocks that were deposited on one continent from an accretionary prism and arc-related rocks on the other.

Fig. 3 near here map of NE Appalachians

After the arc collides with the continent, the trench is consumed, and the subduction zone typically steps outboard towards the ocean, dipping under the continent and accreted arc terrane (e.g., Clift et al., 2003; Deng et al., 2013; Wang et al., 2015). This is because convergence still continues between the continent and the remaining open part of the ocean, and the back of the arc is the weakest part of the system. Therefore, the simple tectonic zonation described above begins to be overprinted, and the arc may even become dismembered into smaller fragments as in the Timor-Australian collision zone (Rutherford et al., 2001). New continental- margin arc magmas intrude the collision-modified continental margin, and most importantly, another arc or continent will eventually collide with this margin. So now there are two accretionary wedges in this accretionary orogen, which become overprinted by processes associated with the conversion from an accretionary orogen to a collisional orogen. In the case of the Appalachian orogen, the younger accretionary wedge(s) related to closure of the Acadian Ocean is preserved in the Merrimack Synclinorium (Fig. 3), whereas the older accretionary wedge related to closure of the Iapetus Ocean during the Taconic orogeny is preserved farther inboard. Thus, two sutures can be drawn on the map of New England (Bradley, 1983). During continent/continent collision, deformation and metamorphism can be intense, typically up to granulite facies, and new plutons of crustal melt granites intrude the structurally complex package. Acadian plutons are widespread throughout the northern Appalachians (Fig. 3), whereas Taconic-aged plutons are rare. The high-grade metamorphism resulting from the terminal continent-continent collision overprints and typically obliterates much of the lower-grade metamorphism of the earlier Taconic arc-continent collision, which is why most metamorphic studies in the Appalachians reveal just Devonian metamorphic peaks and P-T-t paths, and only very detailed structural/metamorphic study together with geochronology can reveal the earlier events (e.g., Tremblay et al., 2000; Castonguay et al., 2012; de Souza et al., 2014). In following sections we use a holistic tectonic approach, as described above, to define Precambrian suture zones in the NCC, and to test for records of Wilson Cycles and the operation of plate tectonics during the craton's long evolution (eg. Kusky et al., 2014).

3. TRACING ARCHEAN SUTURES IN THE NORTH CHINA CRATON

3.1 Geological Zonation of the NCC at 2.5 Ga: Tracing an Archean Suture

In this section we attempt to explain the clear differences in Archean geology between the Eastern Block, the COB, and the Western Block (Fig. 1) (using terminology of Kusky and Li, 2003; Kusky et al., 2007a; Kusky and Santosh, 2009; Kusky, 2011a,b). We next examine the geology of the boundary between the Eastern Block of the NCC and what we interpret as an accreted Archean arc terrane (Wutai/Fuping arc) within the COB, to determine the nature of rock units, structures, and metamorphism on either side, to determine the time of suturing of these two terranes, and to trace this suture across the NCC. Note that the cross-strike scale of the COB is similar to that of the Taconic orogen in eastern North America (compare Fig. 1 with Fig. 3), but the original length of the COB can only be estimated as greater than 1,300 km.

In a direct application of the Burke et al. (1976) model of microblock accretion for the Archean, it has been proposed that there are several different microblocks within the Eastern Block that amalgamated between 2.7 and 2.6 Ga (Zhai et al., 2000, 2010; Zhai, 2014; Zhai and

Santosh, 2011), but the boundaries of these blocks are not well-defined (if they even exist), and the geometry, timing, and mechanism of these proposed events are not yet well-established (Yang et al., 2015, Li et al., 2015, Santosh et al., 2015), and it is not clear if they represent primary microblocks, or a single terrane latter dismembered by younger tectonics, as in the case of Indonesia which has developed its present short arcs since the Australian collision with Timor about 18 Ma ago (Rutherford et al., 2001). In addition, the purported "Neoarchean ophiolite" located near one of these boundaries (Santosh et al., 2016) is only about 100 meters thick, and consists only of very altered rocks interpreted as hornblende norite, hornblende-OPX-lherzolite, gabbroic hornblendite, hornblendite, hornblende-gabbro, and granite. It is not laterally extensive, lacks deep-water sedimentary deposits, has no pillow lavas, no sheeted dike complex, no layered gabbros or cumulates, nor harrzburgite tectonites; it only consists of a suite of deformed mafic-ultramafic rocks of uncertain origin within a contemporaneous pluton. It is not clear if this is a "micro-ophiolite", an ophiorag (sensu Sengör and Natal'in, 2004), or just a mafic-ultramafic phase of the enclosing pluton. Therefore, we refrain from speculation on these purported microblocks and the nature of their boundaries, and begin our analysis at the time when the western margin of the Eastern Block was covered by a thick passive margin (from > 2.6-2.5 Ga).

3.2 Zanhuang Massif

The Zanhuang Massif (Figs. 1, 4) is located in the south-eastern COB along its border with the Eastern Block of the NCC. It consists of three main tectonic zones (Trap et al., 2009, 2012), which can each be subdivided into Domains (Wang, J.P. et al., 2013). The Eastern Domain consists of TTG gneiss and migmatite of the Eastern Block of the NCC, and is overlain in the west by a sequence of metasandstone, marble, and metapelite, grading up into a metagraywacke-pelite unit, then more younger sediments. This zone is interpreted as the older continental crust of the Eastern Block overlain by a passive margin sequence, then by a foreland basin with flysch sediments followed by a superimposed retroarc basin sequence (Kusky and Li, 2003; Li and Kusky, 2007; Wang, J.P. et al., 2013, 2016).

The Western Domain of the Zanhuang Complex consists of tonalitic gneisses with ages of 2692+/- 12 Ma (Yang CH et al., 2013), as well as a suite of hornblende-bearing plutons dated at 2511+/-36 Ma and 2528+/-18 Ma (Wang J.P. et al., in press). The Western Domain was correlated with the Wutai/Fuping Arc (Fuping Block) in the COB by Kusky and Li (2003), Trapp et al (2009, 2012), Wang, J.P. et al. (2013) and Deng, H. et al. (2013), and is considered to be an island arc with magmatic ages of circa 2.7-2.5 Ga. The Central Domain of the Zanhuang Massif consists of a complex mixture of metapelites, metapsammites, metabasalts, metagabbros, and rare ultramafic rocks, forming a structurally complex mélange (Wang, J.P. et al., 2013, 2016; Figs. 5, 6). The mélange belt shows consistent sense of shear indicators of thrusting from the NW to the SE, but the mélange shows at least two generations of similarly-oriented fault sets, suggesting a complex tectonic history (Figs. 5, 6) (Trap et al., 2009a). We interpret this zone to be a subduction/ accretion/ collisional mélange (Wang, J.P. et al., 2016), related to the closure of the ocean between the Eastern Block and the Wutai/Fuping arc in the COB, and final collision of the Western Zanhuang Domain (the Wutai/Fuping arc) with the passive continental margin of the Eastern Block. It thus represents the suture between the Eastern Block and an arc that collided with it. The clear tectonic zonation within the Zanhuang Domain fits the formal criteria for defining a suture zone, as discussed in section I.

Fig. 4 near here map of Zanhuang massif

The timing of suturing of the Wutai/Fuping arc with the Eastern Block has been controversial. Kusky and Li (2003), Kusky et al. (2007a), Kusky (2011a,b), Polat et al. (2005, 2006) have all suggested that this collision occurred around 2.5 Ga, because of the overwhelming geological and geochronological evidence for accretionary and collisional tectonic events at that time. However, Zhao et al. (2001, 2009, etc.) have consistently argued for a circa 1.85 Ga collision, based on their interpretation of P-T-t paths and recrystallized zircons from metamorphic rocks. The problem was solved by Wang, J.P. et al. (2013) and Deng, H. et al. (2013), who reported zircon ages of circa 2.5 Ga on granitic plutons and pegmatites that cut the fabrics in the mélange, clearly showing that the accretion and collision took place before 2.5 Ga. The Zanhuang (or Taihanghshan) suture thus formed at circa 2.5 Ga or earlier. This does not mean, however, that rocks of the COB failed to experience younger sedimentation, deformation, and metamorphic events; just as the Taconic orogen was overprinted by the stronger effects of the Acadian orogeny in New England, as discussed above. So the COB was affected by younger and stronger (early Paleoproterozoic) events.

Deng, H. et al. (2013) reported geochemical data from two suites of mafic rocks from the Zanhuang massif, including older blocks in mélange, and a younger suite of cross-cutting but deformed dikes. These dikes are in turn cut by undeformed 2.5 Ga granite dikes and pegmatites. To explain this, Deng, H. et al. (2013) and Wang, J.P. et al. (2015, 2016) suggested that after the circa 2.5 (or slightly older) arc/continent collision, the arc polarity was reversed from westward-dipping, to eastward dipping under the newly collision-modified margin of the Eastern Block, converting this margin for a short time into an Andean-type arc. In consequence, subsequent sedimentation, deformation, and metamorphic events in the COB could be related to deformation and magmatism in this arc, collision of outboard terranes, closure of the ocean on the outboard side of the accreted Wutai/Fuping arc (along the Trans-North China suture of Trap et al., 2012), or more regional events such as the postulated collision of the amalgamated NCC with the Columbia (Nuna) Continent along the northern margin of the craton at circa 1.85 Ga.

Fig. 5, 6 near here, Zanhuang

We next present structural details of this suture zone as they are not commonly discussed, and yet it is important to work out the different types of structures, their kinematics, and their orientations, because they provide key information about the geometry of accretionary and collisional events. Trap et al. (2012) proposed a model for the Zanhuang-Wutai-Hengshan Complexes in which two oceans, the Luliang and Taihang, opened at 2.2-2.3 Ga from a previously amalgamated NCC, and closed in two continental collision events between 1900-1800 Ma, paradoxically thrusting circa 2.5 Ga oceanic assemblages out of these closing oceans, and stacking them as piles of ductile nappes within the collision zone. In the Trap et al. model, D1 is recorded by a penetrative S1 foliation with a NW trending lineation, and top-to-the-SE kinematics. The D1 fabrics are best-preserved in the Longquanguan Thrust, Upper Wutai Thrust, and at the base of the Low-Grade Mafic Unit (LGMU) and Orthogneiss-Volcanite Unit (OVU) nappes (Fig. 7). Wang, J.P. et al. (2013, 2016) recognized an earlier fabric than the D1 of Trap et al. (2012), characterized by a scaly low-grade mélange fabric and intense imbrication of many structural slices in the Central Zanhuang mélange belt, and suggest that the D1 structures of Trap et al. (2012) are later cross-cutting high-grade shear zones. The D1 of Trap et al. (2012) therefore corresponds to D2 or D3 of Wang, J.P. et al. (2013, 2016).

D2 of Trap et al. (2012) is recognized as folds with NW-dipping axial surfaces and an S2 cleavage in the Hutuo Group, which unconformably overlies the Wutai and Fuping Complexes and is only weakly metamorphosed, so must be relatively young. D3 is attributed to normal shearing with localized S3 foliation developed along normal-sense shear zones such as the Pinshan low-angle normal shear zone. The S3 foliation is associated with an L3 lineation; these are considered to be late extensional structures formed after crustal thickening. D4 is attributed to late strike slip shearing, best exemplified by the km-scale, EW-striking, sinistral Zhujiafang Shear Zone (Fig 7). The structural history of Trap et al. (2012) is internally consistent, but did not consider the earlier events described by Kusky and Li (2003), Wang, J.P. et al. (2013, 2015, 2016) and Deng, H. et al. (2013, 2014).

Trap et al. (2012) constructed a quantitative P-T-t-D path with their D1-D4 representing the second major tectonic event. Their D1 metamorphic assemblage of qz+bi+mu+st+g+ky yields P-T conditions between 6.8 and 7.8 kb (with a range of 7-9.2 kb) and 650-660°C (however, they excluded the core 18% of the garnet from the analysis, which naturally would be expected to contain the earliest metamorphic assemblages), with a U-Th/Pb EPMA age from unzoned monazite of 1887+/- 4 Ma (Trap et al., 2007). Interestingly, the D1 - M1 assemblage of Trap et al. (2012) is significantly different from the M1 assemblage of Xiao, L.L. et al. (2014) who used non-oriented inclusions in garnet cores including an assemblage of qz+bi+plag+ilmenite+magnetite+rutile+apatite that yields M1 conditions of 4.5-5.9 kb and 551-596°C at 2507 Ma. Xiao et al. (2014) calculated M2 “peak” assemblages of qz+bi+plag+kyanite+ilmenite+magnetite+Kspar, corresponding to 9.6-12.3 kb at 1839 Ma.

Thus, it is clear that the D1 event of Trap et al. (2012) corresponds to D2 or D3 higher-grade events of Wang, J.P. et al. (2013, 2016), and the M1 event of Trap et al. (2012) corresponds to the higher grade and younger M2 event of Xiao, L.L. et al. (2014). Thus, the well-constrained CW P-T-t-D path of Trap et al. (2012) corresponds to the second major tectonic event in the so-called TNCO, and does not include the earlier, perhaps more significant, accretionary events related to the collision of the Wutai/Fuping Arc with the Eastern Block of the NCC.

3.3 Wutaishan and Fuping Complexes (Wutai/Fuping Arc)

The Wutai Complex is located NW of the Zanhuang Complex and lies in the center of the COB (Fig. 7). The main rocks of the complex include a suite of 2.55-2.50 Ga metamorphosed bi-modal mafic-felsic volcanic (mainly mafic), siliciclastic sedimentary rocks, and banded iron formations with volcanogenic massive sulfide (VMS) deposits (Bai, 1986; Tian, 1991; Huang. et al., 2004), together with a few older ~2.7 Ga gneisses (Kröner et al., 2005b). Circa 2.7 Ga xenocrystic zircons are also found in the Longquanguan augen granite and granite gneiss (Wilde, 2002b). A tectonic mélange with blocks of podiform chromite-bearing harzburgite and dunite in a metasedimentary matrix underlies these strongly deformed rocks (Wang, K. et al., 1996; Kusky and Li, 2003). These units are all intruded by circa 2.56-2.52 Ga TTG orthogneisses (Zhao and Kröner, 2002; Liu, S. et al., 2004; Polat et al., 2005; Wilde et al., 2005).

Zhang et al. (2012) worked out the structural sequence of the Wutai Complex, demonstrating that early D1 fabrics characterized by NE/SW-striking foliations with NW-SE lineations and associated tight-to-isoclinal folds indicate an early NW-SE contractional event. The D1 event is associated with low-grade greenschist facies metamorphism shown best by inclusion trails in garnet porphyroblasts (Zhang et al., 2012), but this M1 event remains undated in the Wutai Complex. In contrast, in the Zanhuang Complex the M1 event is dated at 2507 Ma (Xiao et al., 2014). Thus, although Zhao et al. (1999) interpret M1 in the Wutai Complex as one point on a continuous P-T-t path related to a circa 1.85 Ga collision, we instead relate it to an earlier tectonic event at circa 2.5 Ga. D2 overprints D1 structures with ENE-WSW ductile shear zones, tight-to-isoclinal folds with associated foliation, and thrust faults and folds that verge to the NW in the NW, and to the SE in the SE (Zhang et al., 2012), deforming the older orogenic wedge into a fan-shaped geometry during doubling of the crustal thickness. Although Zhang et al.

(2012) claim that the basal Hutuo Group is deformed by D1 and D2, the earliest structures preserved in the basal conglomerates (circa 2.18 Ga; Liu et al., 2011) are the D2-related folds (their Figs. 9a and 9b). Metamorphic grades during this event reached amphibolite facies, the highest event recorded in the Wutai Complex (Zhang et al., 2012). D3 represents late structures that formed WNW-ENE-striking open folds that lack any axial planar fabrics, kink bands, and normal faults and metamorphic textures including symplectic coronas around garnets that were derived from earlier M2 mineral assemblages, that shows near-isothermal decompression, which Zhang et al. (2012) and Zhao et al. (1999) relate to post-collisional exhumation of the belt.

We interpret the Wutai greenstone belt as part of an arc that collided with the Eastern Block of the NCC at circa 2.5 Ga forming the D1 structures of Zhang et al. (2012), and then deformed again during later tectonism at circa 1.85 Ga related to events along the northern margin of the craton, forming the D2 and D3 structures of Zhang et al. (2012).

The question then is: what is the origin of the high-grade TTG gneisses of the Fuping and Hengshan Complexes, their sedimentary cover, and the mélange that separates the Fuping Complex from the Wutai greenstone belt? Is the suture between the Eastern Block and the 2.5 Ga arc that is preserved to the southeast in the Zanhuang Complex repeated by a major thrust along the NW side of the Fuping Complex (the Longquanguan or Dragon Spring Shear Zone (Li, J.H. and Quan, X.L., 1991; Kusky and Li, 2003), or is the Fuping Complex part of the arc that collided with the Eastern Block at 2.5 Ga? We test these possibilities using structural geology, sedimentology, geochronology, and geophysical profiles.

The Fuping Complex mostly comprises amphibolite-facies TTG gneisses with inclusions of mafic granulites, and it is characterized by multiple phases of deformation forming fold interference patterns (e.g., Zhang, J. et al., 2009, 2012; Li S.Z. et al., 2010). It is intruded by circa 2077-2024 Ma monzogranites and granodiorites (Zhao et al., 2002c). Zhang J. et al. (2009)

documented three phases of deformation in the Fuping Complex. D1 deformation includes rarely-preserved tight-to-isoclinal folds with associated axial planar fabrics and mineral lineations in mafic to pelitic rocks, which have variable orientations because of later overprinting deformations. L1 lineations are defined by syn-kinematic aggregates of clinopyroxene or hornblende and, although overprinted, indicate a NW-SE sense of thrusting and shearing on the S1 planes (Zhang et al., 2009). D2 strongly overprints D1 structures and formed meter- to kilometer-scale tight to isoclinal folds with an associated axial planar fabric. The folds are asymmetric and overturned, and associated with thrust faults, with SSE-to-E vergence and have hinges that plunge SW-NE, indicating NW-SE shortening (Zhang J. et al., 2009). Mylontic and augen-gneisses of the ductile Longquanguan Shear Zone (Li and Qian, 1991; Dragon Spring Shear Zone – Fig. 7) formed during D2, and were responsible for thrusting the Wutai Complex over the Fuping Complex. The relative timing of D1 and D2 is well-constrained by two leucocratic dikes that underwent D2 deformation but did not experience D1 deformation. The dikes have SHRIMP zircon ages of 1843 +/- 12 Ma and 1844 +/- 18 Ma, indicating that D1 predates ~ 1.85 Ga. We relate D1 to the circa 2.5 Ga events documented elsewhere in the COB. Two other post-D2 dikes have yielded ages of 1817 +/- 14 Ma and 1815 +/- 45 Ma, showing that D2 occurred around 1843-1815 Ma (Zhang et al., 2009). D3 produced regional WNW/ESE-striking open folds and low-angle detachment faults, which Zhang et al. (2009) related by M3 metamorphism to isothermal decompression and exhumation of the complex.

The Fuping Complex is overlain by the Wanzi metasedimentary/volcanic assemblage that includes pelitic gneisses and schists, marbles, calc-silicate rocks, and amphibolites, all metamorphosed to amphibolite facies (Liu, S.W. and Liang, H.H. 1997; Zhao et al., 2002; Kusky and Li, 2003). These rocks appear superficially similar to the shelf sequence deposited on the western edge of the Eastern Block, as described from the Zanhuang Complex. If true, then the

Fuping Complex could represent a piece of the Eastern Block, repeated along major thrusts, with the Longquanguan Thrust representing a repeat of the Zanhuang (Taihangshan) Suture (e.g., Kusky and Li, 2003). However, Zhao et al. (2002b, c) and Zhang, J. et al. (2009) reported that a zoned zircon from a metapelite from the Wanzi assemblage has a near-concordant U-Pb zircon age of 2.11 Ga, which shows that the Wanzi sequence is much younger than the shelf sequence deposited on the western margin of the Eastern Block. Thus, we retain the interpretation that the Fuping Complex represents a deeper arc root to the 2.7-2.5 Ga arc, and that the Wutai volcanic and plutonic rocks represent higher levels of this same arc. This may be an entirely intra-oceanic arc, or it may represent an older microcontinent rifted from an unknown continent on the other side of the Luliang Ocean of Faure et al. (2007). Future geochronological studies should be able to resolve this issue. The young circa 2.11 Ga zircon crystal from the overlying Wanzi assemblage must be related to a younger event, just as in the Appalachians (see Fig. 3), where Devonian sediments overlie Ordovician arc rocks, and both were metamorphosed together in the Devonian Acadian orogeny. The Longquanguan shear zone may be an intra-arc structure or a post-collisional thrust formed during the 2.5, 2.4, 2.1, or 1.85 Ga tectonic events, or could be a hint that the Wutai/Fuping Arc is compound with different inter-arc elements sutured along this zone.

Fig. 7 near here- Wutai-Fuping map

3.4 Eastern Hubei: Zunhua – Structural belt / suture/ Qinglong foreland basin fold belt

The eastern Hebei area contains a well-exposed cross-section of Archean crust that changes from a fore-arc accretionary complex containing ophiolitic mélanges and slivers, through a foreland fold-thrust belt, to a little deformed foreland basin that is cut by 2.4 Ga granitoids. A late Archean suture is preserved in the Zunhua mélange belt that separates the fore-arc accretionary complex from gneisses of the late Archean Taipingzai enderbitic – charnockitic gneiss complex (Fig. 8). The late Archean rocks of this belt are referred to as the Zunhua-Qinglong Structural Belt (Li, J.H. et al., 2002 a,b), or more simply as the Zunhua Structural Belt (ZSB: Kusky and Li, 2010). The ZSB comprises highly-strained metasedimentary gneiss, numerous tectonic slices of 2.6-2.5 Ga greenstones (mostly amphibolite facies metabasalts, gabbros, and ultramafic rocks with minor andesite and dacite), banded iron formations, and ophiolitic mélanges with metamorphosed blocks of basalt, gabbro, ultramafic rocks including harzburgite tectonite, dunite, and podiform chromite-bearing serpentinites (Li, J.H. et al., 2002; Huang et al., 2004; Kusky et al., 2007, Kusky, 2011a). Algoma-type banded iron formations (BIFs) that are interpreted to have formed in a fore-arc environment at 2541 +/- 21 Ma to 2553 +/- 31 Ma contain zircons with metamorphic rims yielding ages of 2512+/- 13 and 2510 +/- 10 Ma (Zhang., L.C. et al., 2012). The ZSB exhibits many east-vergent folds with west-dipping axial surfaces, sliced by numerous NE-striking shear zones. The belt is intruded by numerous 2.6-2.5 Ga tonalite-trondhjemite-granodiorite rocks that are now gneisses, by 2.5 Ga granites, and is transected by numerous ductile shear zones. The whole complex is thrust over the Taipingzhai gneiss complex, and the linear structural patterns in the ZSB are clearly discordant with the more domal-style structural fabric of the early Archean granulite – gneiss dome of the Taipingzhai complex (Fig. 8). The Paleoproterozoic Chengde-Hengshan high-pressure granulite belt overprints the northwestern part of the belt, and is cut by numerous circa 300 Ma plutons.

The ZSB is noteworthy for two remarkable features: two large circa 2.5 Ga ophiolitic slices (NW Belt and Shangyin slices of the Dongwanzi Ophiolite, DWO), and the 2.5-2.6 Ga Zunhua podiform chromite bodies (Figs. 8, 9) in an ophiolitic mélange (Kusky et al., 2001; Li et al., 2002a; Huang et al., 2004). Since the original defininton of the DWO in 2001, the Central

Belt has been shown to consist mostly of circa 300 Ma Paleozoic plutonics (Kusky et al., 2004; Zhao et al., 2007; Kusky and Zhai, 2012) with a few rafts of the older Archean and Proterozoic basement, so we drop the former, now defunct, Central Belt from the DWO, and just include the SE belt (the Shangyin ophiolitic sheet) and the NW belt in our classification of the DWO. However, it must be empahsized that even though the DWO is cut by some younger plutonic rocks, the the NW Belt and the Shangyin ophiolitic sheets have Archean ages, and represent well-preserved relicts of a dismembered and metamorphosed Neoarchean ophiolite (Kusky and Zhai, 2012).

Fig 8 near here – Eastern Hebei map

The Shangyin ophiolitic sheet has a preserved basal thrust zone, which includes an ophiolitic mélange along the base that grades up to a harzburgite tectonite and a mantle transition zone with a well-exposed Moho (Julian Pearce, pers. comm., 2014). The mantle transition zone consists of a circa 2-km thick interlayered harzburgite, mafic and ultramafic cumulates, and gabbro. This in turn grades up into gabbro, then high level gabbros with local dike complexes, and these are in structural contact with several tens of meters of well-preserved pillow lavas, with rare inter-pillow cherts, and with fault slices of BIF (Fig. 10; Kusky et al., 2001, 2004).

Southwestwards the Shangyin ophiolitic sheet is imbricated by shear zones that continue into the Zunhua ophiolitic mélange belt (Figs. 8, 9). In the southern part of the ZSB near Zunhua, the ophiolitic mélange contains blocks of harzburgite tectonite, dunite, podiform chromite, cumulate gabbro, isotropic gabbro, and lenticular amphibolitic units that were likely original pillow lavas and/or dike complexes. In the Shangying ophiolitic sheet these units are better preserved with magmatic transitions from the cumulate ultramafic rocks to gabbro, to gabbro intruded by contemporaneous dikes, to amphibolite facies metabasites including basaltic flows and pillows. Small pods and beds of silica (Fig. 10) are interpreted as interpillow cherts, and beds of BIF as volcanogenic exhalative deposits (e.g., Li. J.H. et al., 2004). The podiform chromites (Fig. 11) are unique because they preserve some of the best nodular and orbicular textures in any Archean ophiolite and are very similar to those in ophiolites such as Semail in Oman, Troodos in Cyprus, and Josephine in the California Coast Ranges (Li, J.H. et al., 2002a).

Figs, 9, 10, 11 near here

The ages of the Shangyin ophiolitic sheet and associated Zunhua podiform chromites are well-constrained (Fig. 12). U-Pb ages from gabbros from the Shangyang ophiolitic sheet yield ages for the gabbro section of 2505+/- 2 Ma (Kusky et al., 2001), and Re-Os ages on chromites from the Zunhua podiform deposits yield ages of 2.5-2.6 Ga (Kusky et al, 2007c). Peridotites from the base of the Shangyang sheet and Zunhua also yield Lu-Hf ages of 2.55 Ga (Polat et al, 2006), showing that the mantle and crustal sections of the DWO and Zunhua podiform chromitites are contemporaneous. Claims that the DWO cannot be an ophiolite, because it is cut by circa 300 Ma mafic to felsic magmatic intrusive rocks (Zhao et al., 2007), are not supported by the exposed field relations and high-precision isotopic dates of Archean age on well-characterized samples from the Shangyin ophiolitic sheet (Kusky et al., 2001, 2007; Kusky and Li, 2008; Polat et al., 2006), and it can be clearly shown that every other Precambrian unit in the region is also intruded by such younger magmatic rocks (Fig. 8). The chemistry of the chromites in the Zunhu Structural Belt has also been debated. Li et al. (2002) reported orbicilar and nodular textures in podiform chromites (Figs. 11, 12), and noted that these texture are only known from ophiolites of any age on the planet. Zhang et al. (2003, 2004) reported that the chemistry of the chromites in the Zunhua-Structural Belt was more like that of a continental intrusion rather than an Alpine-type peridotite. However, analyses of chromites from the Zunhua belt by Polat et al. (2006), which excluded chromites of uncertain age from the younger pluton in the central belt of Dongwanzi, and did not include portions of the chromites altered to ferrit-chromite, all plot within the characteristic fields of chromites and spinels in ophiolites. The samples of Zhang et al. (2003, 2004) have no specified locations, no associated field studies, and appear to have analytical defects since they scatter widely over the Cr/(Cr=Al) vs. Fe2+/(Fe2+=Mg) discrimination plots (Polat et al., 2006, Fig. 7). The podiform chromites from Zunhua have nodular and orbicular textures (Fig. 11). The podiform chromites from Zunhua have nodular and orbicular textures (Fig. 11) only found in ophiolitic chromitites, and their ages are the same as those in the crustal section. The Eastern Hebei area (and its extensions to Liaoning to the north and Wutai Shan to the south) is also host to large banded iron formations (BIFs; Zhai and Windley, 1989). Zhang L.C. et al. (2012) examined the giant Shirengou BIF in the Zunhua Structural Belt of eastern Hebei, which is associated with hornblende plagiogneiss, magnetite quartzite, and plagioclase-amphibolite metabasite. The metabasite and gneiss yield ages of 2541+/- 21 and 2553 +/- 31 Ma. Using the field relationships, along with oxygen isotope systematics, Zhang et al. (2012) concluded that the Shirengou BIF is an Algoma-type deposit formed in a submarine volcanic setting related to Archean subduction. This setting is consistent with their close association with the Zunhua ophiolitic mélange, and formation in an Archean sea-floor exhalative setting. Li J.H. et al. (2004) and Li Y.H. et al. (2014) reached a similar conclusion that BIF in Eastern Hebei and Fuping are also products of submarine hydrothermal exhalation.

The ZSB is bounded to the east by less-deformed circa 2.5-2.4 Ga sedimentary rocks of the Qinglong Basin, which is cut by voluminous 2.4 Ga diorites. The Qinglong Basin is structurally underlain by the Luxiang Group (Wu, C.H. et al., 1998), which contains a lower unit of metabasalt and tuff interpreted to be rift-related, succeeded by shallow water sedimentary strata including quartz-mica schist, marble, sandstone, and banded iron formation that Kusky and Li (2003) and Li and Kusky (2007) interpreted as a remnant of the 2.7-2.5 Ga passive margin developed on the western margin of the Eastern Block. The main sedimentary fill of the Qinglong Basin is called the Qinglong Group, the lower part of which consists of interbedded meta-shales and graywackes with well-preserved Bouma sequences, siltstones, and BIF, and an upper part of coarser-grained conglomerates and sandstones. Pebbles in the upper unit consist of mafic volcanics, vein-quartz, granodiorite, andesite, quartz diorite, and metasediments (Qi, H.L. et al., 1999) and the conglomerate is several meters to 400 meters thick. Pebbles are coarser in the western side of the basin, suggesting derivation from the west, and sedimentary analysis suggests that the basin was bound by thrusts in the west, and deepened in that direction (Bai, J., et al., 1996). This sequence was interpreted as a flysch-to- molasse transition by Kusky and Li (2003) and Li, J.H. and Kusky (2007), and alternatively as a rift sequence by Lv, B. et al., (2012). Kusky and Li (2003) and Li and Kusky (2007) correlated the Qinglong foreland basin with rocks of the Hutuo Group in Wutaishan, but more recent work (Wilde et al., 2004; Liu, C.H. et al., 2011) has shown that the Hutuo Group is much younger, so we abandon this correlation and relate the Hutuo Group to younger events, discussed below.

The Qinglong Basin (Fig. 8) is deformed by asymmetric, tight to isoclinal east-vergent folds with a penetrative axial planar cleavage, is cut by two major west-dipping thrusts (Qi, H.L., et al., 1999), and pebble-elongation lineations as well as stretching lineations plunge westwards, all suggesting that this basin is a foreland basin derived from erosion of the orogenic belt to the west. Sedimentary rocks of the Qinglong Basin are cut by abundant circa 2.4-2.5 Ga diorites (Li, J.H. and Kusky, 2007), and are overthrust by the 2.54 – 2.64 Ga Shuangshanzi Group, the 2.51

Ga Dongwanzi ophiolite, and the 2.55-2.51 Ga Zunhua Mélange to the west. The Qinglong Basin therefore records the history of rifting of the western margin of the Eastern Block sometime between 2.7 and 2.5 Ga, the development of a thin passive margin sequence, then deposition of a foreland basin with a flysch-to -molasse transition by 2.5 Ga during emplacement of a fore-arc accretionary wedge bearing ophiolitic slivers and mélanges. The boundary between the foreland basin (and underlying shelf) and the accretionary wedge marks the suture between the Eastern Block and the COB, and the entire sequence represents a classic record of a Wilson Cycle preserved in an Archean suture zone. Geological relationships in Eastern Hebei are similar to those farther south in the Zanhuang massif, so we correlate this Zunhua suture with the Zanhuang suture (Taihang suture of Trap et al., 2012), and recognize it as the leading edge of the late Archean arc-continent collision between the Eastern Block of the NCC and the Wutai/Fuping Arc terrane in the COB.

3.5 North Liaoning

Tracing circa 2.5 Ga events north of the Zunhua Structural Belt is difficult, because of the intense re-working of the northern margin of the craton in Proterozoic and Paleozoic times in the Inner Mongolia - North Hebei Orogen (Wan, B. et al., 2015) (Fig. 1) and in the Central Asian Orogenic Belt (e.g., Zhang, S.H. et al., 2014). Despite this, some remnants of the late Archean events are preserved in places such as the Jianping Complex (Fig. 13).

Fig. 13. Near here. Jianping map

The Jianping Complex includes Archean and Paleoproterozoic rocks best-exposed in the Nulu'arhu Mountains in western Liaoning Province. It is bound on the southeast by the Jianping-

Xiguanyingzi Fault, which is offset by several younger NNE-striking faults, overlain by extensive Proterozoic to Mesozoic sedimentary and volcanic rocks (Fig. 13), and intruded by late Paleozoic gabbroic, dioritic and granitic plutons (Zhang et al., 2007), similar to those farther south in the Zunhua Structural Belt. The volcano-sedimentary rocks of the Jianping Complex were deposited between 2.55-2.52 Ga and have detrital zircons with ages ranging from 2.7—2.55 Ga (Kröner et al., 1998), intruded by a TTG suite at 2.54-2.50 Ga, metamorphosed to granulite facies at 2.49 Ga, and then intruded by post-tectonic granitoids at 2.47 Ga (Lin, B.Q. et al., 1997; Kröner et al., 1998; Liu, S.W. et al., 2011a, b; Wang W., et al., 2015). Interestingly, the Jianping Complex contains belts of mélange that contain blocks of harzburgite, and podiform chromite with nodular and orbicular textures (Fig. 13; Li et al., 2002b). This suggests that this part of the Jianping Complex may correlate with the ophiolitic mélanges in the Zunhua Structural Belt, the Wutai/Fuping arc, and the Zanhuang complex.

The main rocks in the Jianping Complex (Figs. 13, 14) include metasedimentary rocks that now consist of two-pyroxene granulites, garnet-clinopyroxene amphibolites, felsic gneisses, garnet quartzites, and BIF with beds of magnetite quartzite and magnetite pyroxenite (Liu, S.W., et al., 2011a, b; Wang W. et al., 2015). Enderbitic gneisses (derived from the TTG suite) and their metasedimentary counterparts (similar to the metasedimentary rocks of the Khondalite Belt) were all metamorphosed to granulite facies (i.e. indicated by the presence of hypersthene), and interpreted by Kröner et al. (1998) as a circa 2.49 Ga high-grade metamorphic event. A study by Liu, S.W. et al. (2011a, b) suggested a multiphase metamorphic evolution, with four groups of metamorphic ages including 2512±12 to 2469±6 Ma, 2458±12 to 2449±5 Ma, 2435±27 to 2385±7 Ma and 1862±30 Ma. These ages are in agreement with inferred metamorphic ages farther south in the COB, which include the circa 2.5 Ga arc/continent collision between the Wutai/Fuping Arc and the Eastern Block, and the younger circa 1.9-1.85 Ga amalgamation of the

NCC with the Columbia (Nuna) Continent along the northern margin of the craton in the Inner Mongolia - Northern Hebei Orogen (Wan, B. et al., 2015).

Fig 14 near here.

Based on the rock types, depositional and intrusion ages, and the timing and grade of metamorphism, we suggest that the Jianping Complex is comparable to the Wutai and Dengfeng Complexes, and represents part of the arc complex that collided with the Eastern Block of the NCC at circa 2.5 Ga. The 2.5 Ga suture therefore lies farther to the east of the Jianping Complex. The presence of podiform chromites in blocks of dunite/harzburgite in a metasedimentary mélange belt in the Jianping Complex (Li JH et al., 2002a) suggests that this belt is similar to the Zunhua Structural Belt, and that the suture is not far away to the east in the subsurface.

The 1.86 Ga metamorphism demonstrates that rocks in the eastern part of the NCC, far east of Zhao et al.'s (2009) boundary of the "Khondalite Belt", were affected by the high-grade 1.9-1.85 Ga event, which included the formation of charnockites, enderbites, and khondalites, and that the boundary of the Inner Mongolia - Northern Hebei Orogen continues past Datong and continues to overprint the COB and northern margin of the Eastern Block (Fig. 1). This means that the Eastern and Western Blocks were already amalgamated before the 1.9-1.85 Ga collision with the Nuna-Columbia Continent. Traces of this event continue into the Tarim Craton (Kusky and Santosh, 2009), so the Inner Mongolia-Northern Hebei Orogen associated with the 1.9-1.85 collision on the northern margin of the craton extends for several thousand kilometers in an E-W direction.

3.6 South: Denfeng Complex

The Dengfeng Complex in the southern part of the COB contains a mixture of TTG gneisses, metamorphosed Archean diorites, meta-sandstones and metapelites (Figs. 15, 16) with interspersed lenses of amphibolite-facies metabasites in a possible mélange (Diwu, C.Z. et al., 2011). U-Pb (zircon) and Hf isotopic data indicate that the magmatic rocks are juvenile and formed at circa 2547-2504 Ma. Diwu, C.Z. et al. (2011) suggested, from geochemistry, that the TTGs were generated by partial melting of a subducted slab, and the chemistry of the metadiorites is similar to that of sanukitoids, which Martin et al. (2010) considered were derived from partial melting of a metasomatized mantle wedge above a subducting slab. Furthermore, the geochemistry of the metabasites interspersed with the metasediments are of two types, MORB and arc-like, leading Diwu, C.Z. et al. (2011) to interpret this part of the complex as a tectonic mélange. Examination of the map (Fig. 15) shows that the metasediments and metabasites form discontinuous belts that are truncated in places by faults, and folded, in a style reminiscent of accretionary prism complexes. We accordingly interpret the Dengfeng Complex as part of an arc (correlated with the Wutai/Fuping Arc, and Western Zone of the Zanhuang Complex) and accretionary prism. Thus, the suture with the Eastern Block must lie some tens or more km to the east in areas with poor exposure.

Deng, H. et al. (2016) reported metamorphic ages of 2507+/- 24 Ma from amphibolite-facies tholeiitic metabasalts from the Dengfeng mélange, and suggested that the basalts formed in a fore-arc setting and were metamorphosed during collision of an arc to the west with the Eastern Block to the east. Late undeformed granitic dikes cutting the fabrics of the mélange yield ages of 2492 +/- 35 Ma (Deng., H. et al., 2016), consistent with a late Archean collision between an arc terrane in the COB and the Eastern Block, and is similar in style and age to the other belts along the suture to the north.

Fig. 15 near here.

Fig. 16 near here.

3.7 Tracing the 2.5 Ga Zunhua-Zanhuang (ZZ) suture in the NCC

Using traditional geological relationships, we are able to use the data discussed above to trace the circa 2.5 Ga suture between the Eastern Block and the accreted Wutai/Fuping Arc in the Central Orogenic Belt (COB) for more than 1,300 km across the NCC. Fig.17 shows the suture extending from north of the the Jianping Complex, to the Zunhua-Dongwanzi belt, across the North China plain to the Zanhuang Massif, then south to just east of the Dengfeng Complex. The evidence that this is an Archean suture is clear, because it includes structural and stratigraphic relationships, tectonic zonations ranging from a foreland basin, to a foreland fold-thrust-belt, into an accretionary mélange with ophiolitic fragments, into arc volcanics and plutonics at higher metamorphic grade, and dated cross-cutting intrusives (Fig. 18). The kinematics, metamorphic histories, the presence of ophiolites and ophiolitic mélanges along the suture, and the geochemistry of blocks of MORB and arc-affinity rocks mixed in an accretionary mélange are all remarkably similar to younger sutures with accretionary mélanges and ophiolites in modern arc/continent collision zones, as in the Ordovician Taconic orogen described at the beginning of this paper (compare Figs 18 and 2). This demonstrates that modern techniques of tectonic analysis and discrimination are able to delineate sutures in old strongly metamorphosed rocks, as much as they can in younger, lower-grade orogens. These conclusions are supported by a compilation of Geng, Y.S. et al. (2012) of more than 2,600 Hf isotopic measurements from rocks of the Eastern Block and "TNCO", which are similar in showing major crustal growth at circa 2.7-2.8 Ga, with only partial melting and re-working of the older juvenile rocks at and after 2.5

Ga. Geng, Y.S. et al. (2012) used the similarities between the Eastern Block and TNCO to suggest that they were together by the end of the Neoarchean.

Fig. 17 near here.

This suture, which we previously named the Zunhua-Zanhuang Suture (e.g., Kusky, 2011; Kusky et al., 2012), and Trap et al. (2012) alternatelynamed the Taihangshan suture, has been widely agreed to separate a circa 1,300 km long arc terrane (the Wutai/Fuping Arc) in the COB (with an east-vergent accretionary wedge attached to its eastern side) from the Eastern Block of the NCC (e.g., Kusky, 2011a,b; Kusky et al., 2001, 2004, 2007a,b,c, 2013; Li et al., 2002; Li and Kusky, 2007; Kusky and Li, 2003; Polat et al., 2005, 2006; Deng et al., 2013, 2014. 2016; Wang W. et al., 2013, 2015). The idea that the Wutai/Fuping Arc, and its extensions elsewhere in the COB (Figs. 17, 18), formed above a west-dipping subduction zone and collided with the Eastern Block of the NCC at circa 2.5 Ga has recently been corroborated by Wang W. et al. (2015), who examined the Fuxin greenstone belt in the Jianping Complex. This Fuxin belt consists of voluminous circa 2640-2522 Ma metabasalts and andesites intruded by 2521-2495 granitoids, then metamorphosed up to granulite facies at 2485 Ma and retrogressed to amphibolite facies at 2450-2401 Ma. In their petrological study Wang W. et al. (2015) report that these rocks formed in an evolving intra-oceanic arc system with five different magmatic suites with affinities to MORBs, island arc tholeiites (IAT), calc-alkaline basalts (CAB), high-magnesium andesites (HMA), and adakites. They relate this to an evolving intra-oceanic arc system that was initiated by partial melting of depleted to slightly enriched asthenospheric mantle at a spreading center that generated the MORB. Incipient intra-oceanic subduction at ~2550 Ma metasomatized the mantle and generated the IAT, CAB, HMA and adakites (Fig. 18), and high-Mg TTGs from

2550 to 2506 Ma, and partial melting of the arc root by underplated mafic melts generated a suite of low-Mg TTGs (Wang et al., 2015). Collision of the arc with the Eastern Block at 2490 Ma caused the regional granulite facies metamorphism and also generated K-rich granitoids from crustal anataxis (Wang et al., 2015). Following the models of Kusky and Li (2003) and Kusky (2011, and references therein), Wang et al. (2015) correlated the arc-rocks in this Fuxin greenstone belt with others in the COB, all the way south to the Wutaishan belt, and suggested that this was a large intra-oceanic arc system that collided with the Eastern Block above a west (or NW)-dipping subduction zone (e.g., Fig. 18).

There are hints that there may be significant along-strike variations in the accreted Wutai/Fuping Arc system in the COB. For instance, Kröner et al. (2005b) described small amounts of circa 2.7 Ga TTG gneisses from the Wutai Greenstone Belt, and Wilde (2002b) reported xenocrystic zircons with ages of 2.7 Ga from the Longquanguan gneiss also in the Wutai Greenstone Belt, suggesting that there may be an older basement in the root of the arc, or that zircon-bearing sediments eroded from an older orogen or craton were deposited in the trench, subducted, and incorporated into the arc magmas. Thus, it is likely that the Wutai/Fuping Arc system in the COB had significant along-strike variations in basement character, or that the COB contains a more complex system of amalgamated arcs of different origins. Alternatively it is possible that this arc system resembled the present-day Aleutians, where an oceanic arc merges along strike into an arc built on older accreted continental crust (e.g., Kay et al., 1982).

Thus, through a combination of mainly structural and field-based studies (our work), and petrological-geochemical-geochronological studies (Wang et al., 2015, and references therein), coupled with a robust geochronological database (e.g., Kröner et al., 1998, 2000, 2005a, 2006; Wilde, 1998; Wilde et al., 2002, 2003, 2004, 2005a; Wang J.P. et al. 2015; Deng et al., 2016) it is well-established that the Zunhua-Zanhuang Suture (Figs. 17, 18) represents a circa 2.5 Ga suture between the Eastern Block of the NCC, and a late Archean arc terrane. This suture zone is similar to other modern arc-continent collision zones, in which accretionary prism rocks, locally containing ophiolitic slivers and ophiolitic mélanges (as at Dongwanzi, Zunhua, Wutai, and Zanhuang) are thrust over and imbricated with a passive margin on an older continent (Fig. 18). In the other direction towards the hinterland of the orogen, the accretionary wedge rocks pass, through structural imbrication, into the allochthonous arc sequence (e.g., compare Figs. 2 and 18).

Fig. 18 near here, cross sections at 2.55 and 2.5 Ga

3.8 The style of the 2.5 Ga metamorphism in the COB

Circa 2.5 Ga metamorphism is well documented in the North China Craton (Zhai, M.G. 2014). Nearly all the Archean rocks in the NCC underwent a strong ca. 2.52-2.55 Ga metamorphism from amphibolite to granulite facies (Zhai, M.G. 2004, 2011). However, Zhao et al. (2013) claimed that rocks in the Eastern and Western Blocks of the NCC underwent greenschist to granulite facies metamorphism (with CCW P-T-t paths) at 2.6-2.5 Ga, whereas rocks of their "TNCO" only experienced regional metamorphism at circa 1.85 Ga (with CW P-T-t paths). Zhao and Zhai (2013) suggested that this is because both the Eastern and Western blocks were located above separate mantle plumes at circa 2.6-2.5 Ga, whereas the "TNCO" was not metamorphosed until 1.85 Ga during a continent/continent collision between the two separate, plume-impinged blocks at that time. Here, we list data that show that rocks of the "TNCO" (roughly corresponding to the COB) did indeed experience regional high-grade metamorphism at circa 2.5 Ga, which can be related to an arc/continent collision at that time. Descriptions of the widespread circa 2.5 Ga event in the Eastern Block are abundant and can be found in Pidgeon, (1980), Jahn, B.M., and Zhang, Z.Q., (1984), Jahn, B.M., et al. (1988, 2008), Wan, Y.S., et al. (2001, 2005), Geng, Y.S., et al. (2006), Jahn, B.M., et al. (2008), Yang, J.H., et al. (2008), Grant et al. (2009), Zhao (2009), Geng, Y.S., et al. (2010, 2012), Li, T.S., et al. (2010b), Liu et al. (2011a,b), Nutman et al. (2011), Zhang, X.J., et al. (2011), Dong et al. (2011, 2012, 2013), Liu, C.H. et al., 2011a), Jian, P., et al. (2012), Zhang et al. (2012c),and Zhang, L.C., et al. (2013). A possible tectonic origin for this CCW metamorphism in the Eastern Block was discussed by Wang et al. (2015) who suggested that following an arc-polarity reversal event, mantle-derived magmas impinged on the base of the lithosphere of the Eastern Block causing the widespread magmatism and intrusion of granitoid plutons.

Neoarchean-Paleoproterozoic granulite facies metamorphic conditions in the Central Orogenic Belt were first confirmed by Kröner et al. (1998), who documented circa 2.49 Ga granulite facies assemblages from the Jianping Complex in the NE part of the belt. Li, X.P. et al. (2010) and Zhai, M.G. (2014) later suggested that mafic rocks throughout the COB, which have Nd and Hf model ages ranging from 2.9 to 2.7 Ga, yield consistent metamorphic zircon U/Pb ages of 2.6 to 2.5 Ga.

Metamorphic rims on zircons from amphibolite and gneiss in the Zunhua Structural Belt have ages of 2512+/- 13 Ma and 2510+/-21 Ma (Zhang et al., 2012). SHRIMP zircon ages of amphibolites and hornblendite from the Miyun Geopark in the northern part of the COB northeast of Beijing also show metamorphic peaks at ca. 2.5, 2.44, 1.92 and 1.82 Ga (Shi, Y.R. et al., 2012). Xiao, L.L. et al. (2014) recently documented M1 (first stage) metamorphic assemblages from garnet-bearing metapelites from the Zanhuang massif, and calculated conditions of 4.5-5.9 kb and 551-596 C at 2507 Ma. Deng et al. (2016) reported circa 2507+/- 24 metamorphic overgrowths on zircons from the Dengfeng Complex in the southern part of the COB, showing that this metamorphic event stretches the entire length of the COB from Jianping in the north to Denfeng in the south, a distance of more than 1,300 km (see Supplementary Data Table 1 for details).

Based on the few, but well-documented ages of 2.5 Ga for the M1 metamorphism in the COB, we discount the many other descriptions where M1 is undated and yet used to suggest a prograde section of a 1.85 Ga CW P-T-t path in order to support a tectonic model of a continental collision between the Eastern and Western Blocks at that time (e.g. Zhao et al., 1999, 2001, 2005, 2012; Zhao, 2009; 2011; Zhao and Zhai, 2013). There are no unambiguous data to support the prograde part of the 1.85 Ga metamorphic event, except for that of Trap et al. (2012) from amphibolite-facies deformation during their D1 at 1880 Ma (our D2 or D3), and an $^{40}Ar/^{39}Ar$ age of 1804 +/- 13 Ma from a muscovite that grew during their D4 deformation along the Zhujiafang Shear Zone, and an age of 1802 +/- 13 Ma from a garnet-bearing gneiss in the Fuping Block. As far as we know, these are the best constraints on the timing and duration of the second major tectonic event that affected the Zanhuang-Wutai-Hengshan area of the COB.

Thus, the metamorphism in the COB is more complex than most workers on the NCC have reported, because there are at least two or more different P-T-t paths needed for the different orogenic events. It is inappropriate to force all the data into a single P-T-t path that fits a pre-determined tectonic history. Collisions are not associated with 700 Ma + P-T-t histories (e.g., Dewey, 2005). The so-called paths are, we suggest, different points representing the approximate peak metamorphic conditions of a 2.5 Ga orogenic event, a 1.8 Ga orogenic event, and either a younger event or the retrograde path of the M2 assemblage.

3.9 Reversal of Subduction Polarity?

It has recently been proposed that, after the Wutai/Fuping Arc collided with the Eastern Block at ca. 2.5 Ga, the subduction polarity was quickly reversed from west-dipping to east-dipping (Kusky, 2011; Deng, H. et al., 2013; Wang, J.P. et al., 2013, 2015) with a new subduction zone developed on the back side (western margin) of the Wutai/Fuping Arc (Fig. 18b). Subduction polarity reversal events are common after arc/continent collisions, as demonstrated by examples from the Philippines (Pubellier et al., 1999), northern New Guinea (Cooper and Taylor, 1987; Dewey and Bird, 1970), Solomons, (Draper et al., 1996), Caribbean (LeBron et al., 1993), Taiwan-Luzon (Clift et al., 2003), and elsewhere (see review by Wang, J.P. et al., 2015). An active example of arc-polarity reversal is taking place where the eastern Sunda Arc is colliding with the NW Australian continental margin, and a back-thrust (Flores Thrust) has formed in the back-arc region, marking the initiation of subduction-polarity reversal (Fig. 19), which is propagating westward as the collision progresses, and is happening only a few millions to tens of millions of years after the initial collision of the Sunda Arc with Australia (e.g., Reed et al., 1987; Rutherford et al., 2001). On Fig. 19, note the remarkable similarity of scale and geometry between the Sunda Arc/Australia collision and arc-polarity reversal, and that proposed here for the Wutai/Fuping Arc collision with the NCC and its arc-polarity reversal.

This subduction-polarity reversal event released slab-derived melts beneath the collision-modified margin of the Eastern Block, initially generating mafic dike swarms (Deng, H. et al., 2013, 2014), which in turn added heat to the base of the crust, which led to a suite of granitoids across the Eastern Block (Wang, J.P. et al., 2015). The heat from this mafic underplating and the granitoids associated with it, are here suggested to be responsible for the widespread HT - LP metamorphism, (with CCW paths) in many places in the Eastern Block (see references above). Lu et al. (2008), Wu et al. (2012), Zhao and Cawood, 2012) suggested that the heat for this metamorphism was from a mafic underplate related to a mantle plume, but we suggest that it was from a mafic underplate derived from fluids that induced partial melting of the underlying metasomatized mantle wedge (Fig. 18b), or from slab melting, and thus a consequence of the arc-polarity reversal. In either case, the resulting PT-t paths would be similar, showing a CCW trend, so it is difficult to differentiate between these models using only PT-t paths and without a regional tectonic synthesis. Whilst there was an ocean behind the accreted Wutai arc (named the Luliang Ocean by Trap et al. (2009)), the western margin of the Eastern Block was an active continental margin, or an Andean-style arc, as envisioned by Zhao et al. (2001, etc.). However, there is still considerable debate and uncertainty about how long this ocean remained open, whether until 1.85 Ga (Zhao et al., 2001, etc.), 2.4, 2.3 or 2.1 Ga (Trap et al., 2007, 2008, 2009a, b, 2012; Wang, Y.J. et al., 2004; Wang Z.H., et al.; 2010; Wang, Z.H., 2009), or only for a short time. We discuss this in the next section on the "Trans North China Suture".

Fig. 19 near here-- Sunda arc.

South of the northern COB in northern Liaoning (Fig 17, NL) Peng, P. et al. (2015) document the petrogenesis of a short-lived continental arc segment within the Qingyuan Greenstone Belt, which includes ca. 2540-2510 Ma ultramafic-mafic and felsic volcanics, a 2570-2510 Ma quartz diorite, and a 2510-2490 Ma quartz monzodiorite. Trace element analysis led Peng, P. et al. (2015) to suggest that this sequence evolved above a "mantle wedge-absent hot subduction zone, in which the ultramafic-mafic rocks originated from undifferentiated mantle, the rhyolite was derived from eclogite-facies crust of the overriding plate, the quartz diorite resulted from mixing of mantle melts and the overriding crust, the TTG suite was derived from partial melting of the subducting slab at amphibolite to amphibole-bearing eclogite facies conditions, and the quartz monzodiorite was generated by melting of the overriding mid-lower crust. The whole history of arc magmatism lasted from 2570 Ma to 2480 Ma, from arc initiation, through maturation, to exhumation presumably during collision, and the magmatic sequence could have formed in a continental arc with special Archean conditions, in which there was slab melting instead of slab dehydration, and hydrous minerals were preserved in the slab through the eclogite facies. If the subducting oceanic slab was thick and had limited dehydration, there would be no modern-style hydrous mantle wedge (c.f. Fig 18b, where we retain the hydrous mantle wedge, but not beneath the accreted arc, as suggested by Peng et al., 2015), and a ‘hot-subduction system” would result, producing the magmatic series documented from the Qingyuan Belt. We suggest that this short-lived Andean-style arc may also have formed after the subduction polarity reversal event (which was slightly earlier in the north than in the center of the COB), and that is the reason why the entire history of the arc, from formation to exhumation lasted only <80 million years.

4. PALEOPROTERZOIC SUTURES OF THE NCC

4.1 Where is the next suture, the Trans North China Suture, and how old is it?

Little is known about when the remaining open part of the “Luliang” Ocean (Trap et al., 2012) closed, since most workers in China have simply assumed that the borders of the TNCO as defined by Zhao (2001) represent the borders along which the eastern and western blocks collided at 1.85 Ga. However, a few studies have looked deeper into this “second suture”, and found several features that indicate that the closure time was, may be, at 2.5-2.4, 2.3, 2.1, or 1.85 Ga.

Faure et al. (2007) and Trap et al. (2007, 2008, 2009a, b, 2012) provided detailed structural documentation of a suture that they termed the “Trans North China Suture” along the western side of the accreted Wutai/Fuping Arc terrane. This suture is best exposed in the Luliang

Massif (LL on Fig. 17) where it crops out as greenschist facies metasedimentary rocks mixed with mafic and ultramafic rocks, which have an oceanic affinity (Trap et al., 2009b; 2011; Polat et al., 2005). Trap et al. (2011) included the flysch, mafic rocks, pillow basalts and other sedimentary rocks of the Wutai Greenstone Belt in an allochthonous unit (called the Low Grade Mafic Unit, LGMU in their terminology) that was extruded from the Trans North China Suture and thrust over TTGs and migmatites of the Fuping Block (Fig. 7). Interestingly, the pillow basalts, gabbros, and felsic volcanic rocks in this suite have ages of 2.530-2.515 Ga (Wilde et al., 2005) whereas the underlying TTG gneisses of the Fuping Complex have ages of 2.560-2.515 Ga (Wilde et al., 2005). This in turn implies that the Luliang Ocean closed not too long after 2.5 Ga, since it is unusual for oceanic-affinity rocks in sutures to be older than the ocean formation age, and most are obducted soon after they form (Burke et al., 1977; Dewey, 1977). Strangely, Trap et al. (2012) interpreted these rocks to have formed in a basin that rifted from a previously amalgamated NCC at 2.3-2.2 Ga, and therefore the Luliang Ocean closed at circa 1880 Ma.

It is clear that there were significant magmatic and partial melting events between 2.3 and 2.1 Ga in the Fuping, Wutai, and Hengshan areas, and also along the northern margin of the NCC, Ordos Block, Alxa Block, and Eastern Block (Fig. 17). In the Fuping/Wutai/Hengshan areas these events include evidence for anatectic melting from the Fuping Complex at 2193 +/- 15 Ma (Wang ZH et al., 2010), 2.06-2.08 Ga anatectic melts in the Fuping Complex (Cheng Y.Q. et al., 2001), and 2.25-2.11 Ga anatectic granites from the Hengshan Complex (Kröner et al. 2036 +/- 19 Ma 2008). Trap et al. (2012) interpreted these to reflect a regional anatectic melting event within the TNCO, and Zhao et al. (2008, etc.) interpreted them as products of Andean-type arc magmatism related to eastward subduction beneath the TNCO. In contrast, Kusky and Li (2003) interpreted these intrusions to form a wide zone of magmatism related to a convergent margin and Andean arc-related activities stemming from subduction under the northern margin of the craton, 200 km to the north, and stretching 1,600 km EW along the northern margin of the craton. Note that magmatism associated with the present-day Andean arc extends some 500 km from the convergent boundary, so this is not an unusually large distance (Fig. 17). In recent papers Wan, Y.S., et al. (2013) and Zhang, C.L., et al. (2015) reported U-Pb ages and chemical data from circa 2.2-2.0 Ga granitic gneisses from boreholes in the Ordos basement, and interpreted them to be part of a continental margin arc. This is in perfect agreement with the interpretation that the northern margin of the craton was an Andean-style arc at this time (Kusky and Li, 2003, Kusky, 2011a), but it would have been impossible to produce, if the TNCO had not closed by then, and the Andean arc was located above an east-dipping subduction zone beneath the eastern NCC (e.g., Zhao et al., 2001, etc).

Very little happened between 2.4 and 2.3 Ga, suggesting that the Luliang Ocean closed very soon after the collision of the Fuping arc with the Eastern Block. This may be reflected in the ca. 2512±12 to 2469±6 Ma, 2458±12 to 2449±5 Ma, 2435±27 to 2385±7 Ma metamorphic ages obtained from the Jianping Complex (Liu, S.W., et al., 2011), the 2.44 Ga metamorphic ages from the Minyun Geopark (Shi, Y.R. et al., 2012), reflecting the initial collision of the Wutai/Fuping arc with the Eastern Block, a subduction polarity reversal, then closure of the remaining open part of the “Luliang Ocean” some 70 Ma after the initial collision (Fig, 20). This agrees with data from the Zanhuang Massif, where granite plutons and pegmatites that cut the fabrics in the mélange have yielded ages of 2493 +/- 22 Ma, 2540 +/- 23 Ma, and 2539 +/- 44 Ma (Wang J.P. et al., 2013), which also cut mafic dikes that cut the mélange fabric with ages of 2535 +/- 30 Ma, and have metamorphic zircons with ages of 2.1 (with a large error) and 1.85 Ga (Deng, H. et al., 2014). We therefore suggest, based on this limited information, that the Luliang Ocean closed by 2435 Ma, and the Eastern and Western Blocks were amalgamated at this time (Fig. 20).

The magmatic gap from 2435-2300 Ma represents the time between closure of the "Luliang" Ocean, and when the Andean arc was set up along the northern margin of the craton.

The nature of the basement to the Western Block is enigmatic, since it is largely covered by late Archean to modern sedimentary rocks. However, Kusky and Mooney (2015) synthesized geophysical, geological, and geochronological data on the nature of the Ordos (part of the Western Block) basement, and suggested that it is likely an oceanic plateau that was accreted (Fig. 20a, b), and experienced several periods of later differentiation during younger subduction and collision events along the northern margin of the craton.

Fig. 20 near here. Cross sections at 2.43 and 2.3 Ga

4.2 Post-orogenic extension and rifting at 2.4 Ga

There has been much recent work along the northern margin of the NCC, focusing on the ages and PT conditions of HP and UHT metamorphism (e.g., Guo, J.H., et al., 2006; Santosh and Sajeev, 2006; Santosh et al., 2007a, b; Wan, Y.S., et al., 2009; Santosh and Kusky, 2010; Li et al., 2011; Zhai and Santosh, 2011 and references therein; Guo et al., 2012; Peng, P. et al., 2012; Yin, C.Q et al., 2009, 2011; Wan, B. et al., 2015), but a paucity of geological mapping for tectonic discrimination.

Kusky and Li (2003) and Zhai and Santosh (2011) suggested that, following the amalgamation of the East and West Blocks through accretion of the Ordos Oceanic Plateau (Kusky and Mooney, 2015), which we now regard as completed by 2435 Ma, the COB and the northern margin of the craton underwent post-collisional rifting by 2400 -2350 Ma. These rifts include: the Luliang, Zhongtiao, South Taihang, and Hutuo, in which Proterozoic sediments unconformably overlie the Neoarchean basement. They are concentrated in the Fengzhen Belt on the NW margin of the craton, and in the Jinyu Belt that strikes NE through the center of the craton (Zhai, M.G. and Santosh, 2011). The basal-lower unit in these rifts generally consists of bimodal volcanic and immature clastic sedimentary rocks, overlain by an upper unit of argillites, carbonates, and flood basalts.

Kusky and Li (2003) suggested that the well-preserved N-S rift in the COB connected with two arms of a triple-junction style rift along the northern margin of the craton, and that the rift along the northern margin led to the formation of an ocean to the north, rifting away any fragments of the NCC that were originally continuous with the Eastern and Western Blocks and the COB along the present northern margin of the craton. After the rifting, sediments and volcanics were deposited, the rifts went into thermal subsidence mode, and a series of shallow water sediments including aluminous muds, shallow-water sands, graphitic muds, feldspathic arenites, siltstones, and carbonates were deposited along the northern margin of the craton, forming a shelf sequence, which during younger collisional events would become metamorphosed to granulite conditions and become incorporated into the older parts of the Khondalite Belt (see detailed description of the Khondalite Belt below, in section 4.3). However, parts of the Khondalite Belt are younger, and there is currently some confusion on the age range of deposition and metamorphism of the various rocks in it, since there has been very little systematic geological or structural work on these rocks, and most zircon isotopic ages have come from samples with little or no field context. For instance, from the Daqingshan area, Wan, Y.S. et al. (2006), Zhao et al. (2010) and Dong, C.Y. et al. (2012) reported that that khondalites have detrital and metamorphic zircons of 2.0, and 1.95-1.83 Ga, whereas Wan, Y.S. et al. (2006, 2008, 2009), Wu, C.H. et al. (2006), Santosh et al. (2007, 2009a), Zhong, C.T. et al. (2007), Zhao et al. (2010), Li, X.P. et al. (2010), Liu S.J. et al. (2012), Ma, M.Z., et al. (2012a,b), Dong, C.Y. et al. (2012, 2013) reported metamorphic ages from these rocks of 2.6, 2.5, 2.45, 2.37, 2.3 to 2.0, and

1.95 to 1.85 Ga. These data are clearly inconsistent, and reflect the fact that samples were collected before their field context was well understood. We therefore stand by our hypothesis that rocks of the Khondalite Belt (and its equivalents to the east) represent a thick sequence of metasedimentary rocks deposited on the Ordos Block after rifting at 2.4 Ga, and before or during final collision along the north margin of the craton at 1.85 Ga. Meta-sedimentary rocks similar to those in the Khondalite Belt are now known from drill-core data to extend at least half-way across the Ordos Block (Fig. 16) (Wan, Y.S. et al., 2013; Wang, W et al., 2014; Zhang, C.L. et al., 2015) consistent with them representing a regional shelf sequence deposited on top of the enigmatic Ordos basement (Kusky and Mooney, 2015). They therefore should have a complex age mixture of detrital zircons. These rocks unconformably overlie the older basement of the Western Block and the NW part of the Eastern Block, show geochemical evidence for derivation from cratonic sources, and are thought to have originally been 1-3 km thick (Condie et al., 1992; Qian, X.L. and Li, J.H. 1999; Zhao et al., 2001). Not long after the rifting and ocean formation, an arc formed in this ocean, and would soon collide with the northern margin of the craton converting the northern margin into an active continental margin. These events would have emplaced an accretionary prism and associated fore-deep sediments on top of the shelf sequence, adding another complex component to the protoliths of the Khondalite Belt. Even younger sediments could have been shed into this basin during Andean-margin tectonic activity, as discussed below.

4.3 Events along the northern margin from 2.35-1.92 Ga: Andean Margin Tectonics

4.3.1 The Inner Mongolia – Northern Hebei Orogen (IMNHO)

Kusky and Li (2003) initially suggested that a belt of ca. 2.49-2.45 Ga tonalites-trondhjemites, 2.48-2.40 Ga diorite – gabbro complexes associated with ultramafic rocks, 2.45-2.33 Ga turbidites, BIF, and biotite-hornblende gneisses intruded by 2393+/- 3 Ma trondhjemites in the Guyang and Chifeng Metamorphic Complexes represent an arc sequence built on older basement and an accretionary wedge that collided with the NCC at approximately 2.3 Ga, after which time the subduction polarity reversed, from northwards to southwards, converting the northern margin of the craton to an Andean margin. They named this belt and its extensions the Inner Mongolia-Northern Hebei Orogen (IMNHO), simplified to the Northern Hebei Orogen in some publications, with an expanding definition that included the Khondalite Belt in the foreland of the orogenic system (Kusky et al., 2007a, b; Kusky and Santosh, 2009). Zhao and Wilde (2002) also recognized this belt, but suggested that it was older than the collision of the Eastern and Western Blocks. Condie (1992) referred to a belt of granulite facies meta-pelitic rocks intruded by S-type granites south of this belt as the “Khondalite Belt”, also taken up by Zhao et al. (2009). Rocks in parts of the IMNHO have also been referred to as the “Yinshan Block” (Zhao and Wilde, 2002; Zhai and Santosh, 2011), separated from the Ordos Block by the Khondalite Belt (which has also been called the “Inner Mongolia Suture Zone” (Santosh, 2010).

The northern part of the IMNHO is a strongly tectonized metasedimentary belt that consists of deformed shallow water sedimentary rocks, to the south of which is a predominantly plutonic belt including TTG-quartz diorite plutons, and younger granodiorite, metamorphosed to greenschist through amphibolite facies (Li, J.H. et al., 2000a,b; Kusky and Li, 2003; Kusky et al., 2007b). South of this is another metasedimentary belt that is intruded by gabbro and diorite complexes, metamorphosed to amphibolite facies. Kusky and Li (2003) suggested that these represent an accretionary wedge, Andean-style arc, and a closed back-arc basin, or a foreland basin built on top of an older shelf sequence. At present it is only possible to identify basic elements of this continental margin convergent orogen, and more field, structural, geochronological, petrological, and geochemical work is clearly needed if this major orogen can be fully understood. In this contribution we include the Yinshan ribbon continent with younger arc-related intrusions, the metasedimentary rocks to the north, and the metasedimentary rocks intruded by S-type granites in the "Khondalite Belt" all within the IMNHO, representing different components of a continental margin magmatic arc, similar in scale to the Andes of South America (e.g., Dewey and Lamb, 1992). It is important to note that our inclusion of the Khondalite Belt in the IMNHO does not mean that the entire belt is allochthonous. Southern portions of it (and its possible extensions to the east) represent a series of orogenic basins in the foreland possibly including a <2.4 Ga passive margin, and 2.3 – 1.85 Ga retro-arc and foreland basins. Thus, on Fig. 17 we draw a dashed line indicating the approximate known southern extent of the Khondalite Belt, and note that it merges with the allochthonous parts of the IMNHO near the Xuanhua Complex, and still has remnants preserved within the hinterland of the orogen in places to the east such as the Jianping Complex. In addition, isolated exposures of khondalites with detrital zircons of circa 2200-2178 Ma have been identified along the southern margin of the craton (Li N., et al., 2015), and like other metapelites across the craton, were metamorphosed to granulite facies between 1.95 and 1.85 Ga.

Fig. 21 Cordilleran ribbon microcontinent

4.3.2 The Yinshan Ribbon Micro-continent

The "Yinshan Ribbon Micro-Continent (or Block)" contains a basement that is typical of Archean cratons, (Jian, P., et al., 2005, 2012; Chen, L. 2007, Ma, X. et al., 2013a, b: Zhang et al., 2014), including TTGs and greenstones comprised of Neoarchean mafic-ultramafic complexes (Wang D. et al., 2015; Ma et al., 2015) with a subduction-related signature. The Guyang and Wuchang Metamorphic Complexes in the "Yinshan Ribbon Micro-Continent" include a greenstone sequence (sometimes called the Wulashan Group) that has a lower unit of Neoarchean komatiite-bearing mafic and ultramafic rocks (Chen, L., 2007), a middle unit with calc-alkaline felsic rocks, volcaniclastic meta-sediments, tholeiitic basalts, meta-sandstone and limestone, overlain by an upper unit of felsic volcanoclastic and immature clastic rocks (Jian, P. et al., 2012; Zhang, X.H., et al., 2014). Other components of the Guyang and Wuchang Complexes include charnockite, enderbite, mafic granulite, and amphibole gneiss, intruded by a TTG suite and high-Mg diorite of the sanukitoid and adakite suites (Jian, P. et al., 2012; Ma, M.Z. et al., 2012, 2013a,b; Zhang, X.H. et al., 2014). These are all covered by Mesoproterozoic low-grade rocks of the Zhaertai and Bayan Obo Groups (Li et al., 2007). These complexes experienced granulite-facies metamorphism at 1935-1790 Ma (Peng, P. et al., 2014). We regard the Yinshan Block as a ribbon micro-continent incorporated into the greater IMNHO (e.g., Kusky and Mooney, 2015), upon which a younger arc sequence was built. This kind of relationship is common in many younger orogens such as the American Cordillera and the Central Asian Orogenic Belt (e.g., Sengor and Natal'in, 2004; Johnston, 2008; Xiao, W.J. et al., 2015). Further work is needed to delineate the lateral extent of the Yinshan Ribbon Micro-Continent beyond the Guyang and Wuchang Complexes.

For comparison, Fig. 21 shows a palinspastic reconstruction of the North American Cordilleran Ribbon Continent, prior to its collision with North America. Superimposed on this map is an outline of the NCC, with the southern part of the craton superimposed on cratonic North America, and the outline of the IMNHO drawn over the Cordilleran Ribbon Continent. Note the similarities in composite nature of the ribbon continents (including older continental slivers, arcs, ophiolites, accretionary prisms, and platforms), and the scales of the pre-collisional orogens.

Rocks of the IMNHO appear to extend all the way to the western part of the craton in the Alxa Block (also called the Alashan Block). Zhang, J.X. et al. (2013) report U-Pb zircon and Hf isotope data from the westernmost NCC in the Beidashan Complex in the Alxa block, in which TTG gneisses have εHf(t) model ages of 2.6-2.8 Ga indicating crustal growth, and circa 2.5 Ga magmatic zircons with 2.5 Ga metamorphic rims, indicating a closely-spaced magmatic and metamorphic event. A second metamorphic age of 1.85 Ga is interpreted as related to the circum-NCC high-grade metamorphic event. Igneous protoliths of the Longshoushan Complex in the Alxa Block formed at circa 2.4-2.0 Ga (Xiu, Q.Y. et al., 2004; Gong, J.H. et al., 2011), and were strongly metamorphosed at 1.93-1.85 Ga (Zhang, J.X. et al., 2013). Zhang, J.X. et al. (2013) conclude that “the present dataset seems to support the idea that the Alxa Block is part of the Paleoproterozoic IMNHO”, and the similarities between the Beidashan Complex and the Guyang and Wuchang Complexes also suggest that the Yinshan Ribbon Micro-Continent extends all the way to the Alxa (Alashan) Block.

4.3.3 The Khondalite Belt

The Khondalite Belt (Condie et al., 1992) forms the southern margin of the IMNHO, but the southern margin of the Khondalite Belt is currently unknown because its buried equivalents extend at least half way across the Ordos Basin (Wan YS et al., 2013; Wang W et al., 2014; Zhang CL et al., 2015). A > 1.90 Ga molasse basin lies along the northern margin of the Khondalite Belt, separating it from the Yinshan Ribbon Micro-Continent. Granulites of the Khondalite Belt are best-exposed in the Jining, Liangcheng, Fenzhen, Daqingshan, Wulashan, and Helanshan Massifs (Fig. 17), and include assemblages of khondalite, charnockite, and metagabbro, intruded by S-type granites which have yielded U-Pb ages between 1.97-1.83 Ga (Guo et al., 1999; Kusky and Santosh, 2009). The major rock types include granulite facies garnet-sillimanite-bearing metapelites, quartz-feldspar-garnet-bioite gneisses, marbles, and calc-silicate rocks. The protoliths of these rocks are considered to be interlayered pelitic, psammitic, calcareous, and carbonaceous sediments, typical of shallow cratonic shelf sediments and foreland basins. Foliations are generally E-W striking, and a component of sinistral shear may be related to the emplacement of S-type granites (Kusky and Santosh, 2009). Zircons from the Khondalite Belt include at least two different populations, including an older group with ages between 2.3 and 2.6 Ga, and a younger group of 1.85-2.0 Ga (considered to be metamorphic by Kusky and Santosh, 2009). Dong, C.Y. et al. (2012) reported detrital zircons with a range of 2.0-1.95 Ga. We suggest therefore that the Khondalite Belt and its equivalents to the east preserve several superimposed basins, whose development predated granulite facies metamorphism, including a passive margin deposited on the northern margin of the NCC, a foreland basin related to collision of the arc in the Yinshan Block and later retro-arc foreland basins (e.g., Figs. 21, 22); all these rocks and units represent an Andean-style arc on the northern margin of the craton active from 2.3-2.0 Ga.

South of the Yinshan Block in the northern part of the Khondalite Belt (Fenzhen Belt), the Halaqin volcano-sedimentary sequence includes circa 1910-1880 Ma basalts, andesites, dacites and rhyolites. Peng et al. (2011) suggested that the basalts and andesites are the extrusive equivalents of the Xuwujia gabbronorites (Peng et al., 2010), which they related to circa 1.92 Ga ridge subduction beneath an Andean arc on the northern margin of the craton, and that the dacites and rhyolites are upper crustal equivalents of the nearby Liangcheng granitoids (Peng P. et al., 2012a). The Halaqin volcano-sedimentary sequence includes the Erdaowa Group consisting of metamorphosed pebbly sandstones, sandstones, pelites, marbles and volcanic rocks in tectonic contact with the underlying basement of the Yinshan ribbon microcontinent. Peng et al. (2011) noted that the Halaqin volcano-sedimentary sequence is highly deformed, including ductile thrusts, isoclinal folds and sheath folds, and that the whole succession is a thick tectonic pile thrust from the SE to the NW over the Yinshan Ribbon Micro-Continent, and that it likely represents an accretionary wedge in the Khondalite Belt located between the accreted Yinshan Block and the amalgamated Eastern Block/Wutai/Fuping Arc (Huai'an terrane). They emphasized, however, that no modern structural studies have been undertaken on these complex rocks.

Fig 22 Comparison of NCC with Andes near here

4.3.4 Andean arc-related magmatism

Andean-style magmatism affected much of the northern, central, western (including the Alxa Block), and northern part of the eastern NCC from 2.3-1.88 Ga (see Zhao et al., 2005, 2008, 2010, 2012; Zhao and Zhai et al., 2005, 2010, Peng et al., 2012b; Zhai and Santosh, 2013; Yang and Santosh, 2015), with a strong magmatic pulse that affected regions as far south as the central Ordos Block from 2.2-2.0 Ga (Wan Y.S. et al., 2013; Zhang C.L. et al., 2015, and references therein; Fig. 17). These rocks include lavas and tuffaceous rocks, granitic plutons, mafic dikes, sills and plutons. The volcanic rocks are very variable in thickness and include a suite of basalts, andesites, dacites, and rhyolites, including pillow lavas, flows, and subaerial tuffaceous rocks, and are typically intercalated with clastic and carbonate sedimentary rocks (Du et al., 2010, 2011; Geng et al., 2000; Jiang, 1987; Li et al., 2012; Liu et al., 2011, 2012; Lu et al., 2006; Peng et al., 2011; Sun and Hu, 1993; Wilde et al., 2003; Yu et al., 1997; Zhang et al., 2010; Zhao et al., 2008b; Peng et al., 2012). This suite of rocks has a continental arc geochemical signature (Zhang et al., 2015), including variable Hf isotopic compositions similar to continental margin arc rocks in the Central Zone and Eastern Block. Their presence throughout the Western Block does not support the tectonic model (Zhao et al., 2001, 2005, 2009, 2012) that the "TNCO" closed by eastward subduction of an oceanic plate attached to the Western Block beneath an Andean arc developed on the Eastern Block, since the arc-related magmas are now known to extend in a broad E-W arc that perpendicularly crosses the proposed 1.85 Ga suture of the TNCO (Fig. 22c).

Circa 2300-1880 Ma plutonic rocks including granodiorites, tonalites, monzogranites, biotite granites, garnet-sillimanite granites, and charnockites are widely distributed across the northern half of the craton (Geng et al., 2000; Guo and Li, 2009; Kröner et al., 2005; Li and Zhao, 2007; Li et al., 2012; Liu et al., 2009b; Lu et al., 2004a,b; Peng et al., 2012a, b; Wan et al., 2006; Wang and Wilde, 2002; Wang et al., 2010c; Wilde, 1998; Wu et al., 2007; Yang et al., 2009, 2011; Zhao et al., 2002a, 2006, 2008a,b, 2011) and extend a few hundred km south (see Fig. 22c). Some of these are deformed into granitic gneisses, whereas others are relatively undeformed.

Peng et al. (2012b) described several circa 2.3-1.88 Ga suites of magmatic rocks in the eastern and north-central NCC, including A-type granites, S-type granites, rare carbonatite dikes, and several mafic dike swarms including the circa 2147 Ma Hengling mafic dike/sill swarm, the 2060 Ma Yixingzhai mafic dike swarm, and the circa 1973 Ma Xiwangshan mafic dike swarm. The dikes are tholeiitic in composition and were interpreted by Peng et al. (2012b) to have been derived from the Archean sub-continental lithospheric mantle, perhaps in a rift setting. However, A-type granites and the other igneous rocks in this suite can also form in Andean-arc settings, especially in places where the arc is fairly mature and the granites are derived from crust that has already produced a suite of orogenic granites, leading to the formation of A-type granites (e.g., Pearce et al., 1984). In the case of the NCC, the arc had been active for 150-200 Ma before the dikes intruded, so the crust had already produced numerous melts. From different Andean settings "from Antarctica to Alaska", Kay and Rapela, (1990) have shown that it is difficult to assign A-type granites and other subduction-related magmas to specific tectonic settings based on geochemistry, since magmatism in one setting, such as a volcanic arc, rift, continental collision, etc., may overlap in composition considerably and many different types may occur in a single subduction-related setting based on the relative proportion of crustal material involved in the magma genesis.

The Inner Mongolia – Northern Hebei Orogen also contains an assortment of TTG to dioritic gneisses, 2.2-1.9 Ga granites, metasedimentary and metavolcanic rocks, and rare gabbroic to ultramafic intrusions (Kusky and Li, 2003; Wang et al., 2015). Deformation is characterized by roughly EW-striking shear zones and folds that extend at least as far south as the Hengshan, which is cut by the E-W striking Zhujifang and Datong-Chengde Shear Zones (Fig. 17) which disappear under young cover of the Ordos Basin. Geophysical studies reveal a series of NE-striking faults in the basement beneath the cover of the Ordos Basin, and it is possible (although speculative) that some of these may be reactivated extensions of the Zhujifang fault (Figs. 17, 22) or the Datong – Chengde Shear Zones.

In the Jiao-Liao Ji Belt in the Eastern Block (Fig. 22), a group of magnetite monzogranites intruded at circa 2176-2166 Ma, and a suite of hornblende-biotite monzogranites was emplaced between 2150 and 2143 Ma (Li S.Z. et al., 2007). Nd isotope geochemistry reveals that the monzogranites have model ages (TDM) of 2.4-2.6 Ga (Li S.Z. et al., 2006) and show evidence of derivation from a source that includes partial melting of the Archean crustal basement. The magmatism is associated with a group of volcaniclastic sediments, pelites, and flood basalts, , that we relate to processes in a retro-arc foreland basin in the next section.

4.3.5 Tectonics

The northern part of the IMNHO was thrust to the south and SE over the NCC (Kusky and Li, 2003; Peng et al., 2011), forming widespread south-vergent folds and thrusts in the Khondalite Belt and intrusion of numerous S-type granites between 2.2 and 1.90 Ga (Kusky and Li, 2003). In the current interpretation, the Yinshan Ribbon Micro-Continent is part of the accretionary orogen of the IMNHO, and the accretionary wedge and arc built on the microcontinent were thrust over the shelf sequence, shedding flysch, later to become the so-called Khondalite Belt (Kusky and Mooney, 2015). Zhai and Peng (2007) suggested that events in this time period (previously referred to as the Luliang Movement) can be divided into a Wilson Cycle sequence of events from rifting at 2350 Ma, followed by subduction and collision by 1970 Ma, then a regional high-grade metamorphic event at 1950-1820. The former phases of Zhai and Peng's orogenic cycle correspond to the events proposed by Kusky and Li (2003), and Kusky (2011a, b), and the regional high-grade event likely records the incorporation of the NCC into the Columbia (Nuna) Continent (Kusky and Santosh, 2009; Wan et al., 2015).

4.3.6 Events further inboard from the Andean margin

In Wutaishan, the Hutuo Group has historically been regarded as Archean in age, but more recent geochronological studies have shown that it is much younger and corresponds in age to the magmatism associated with the Andean arc on the northern margin of the craton. The Hutuo Group (Fig. 23) contains basal sandstones and conglomerates of the Doucun Subgroup, clastic sediments, dolostones, and basalts of the Dongye Subgroup, phyllites and dolostones of the Upper Dongye Subgroup, topped by coarse-grained sandstones and conglomerates (molasse) of the Guojiazhai Subgroup. Wilde et al. (2004) analyzed a tuff from the Hutuo Group and obtained two zircon populations, including 2180+/- 5 Ma, and 2087 +/- 9 Ma. Liu C.H. et al. (2011b) obtained detrital zircons from the Doucun, Lower and Upper Dongye, and Guojiazhai Subgroups, yielding concordant $^{207}Pb/^{206}Pb$ ages of 2.11-3.88 Ga, 2.10-2.84 Ga, 1.88-2.72 Ga, and 1.92-2.65 Ga. The ages of the younger zircons in each subgroup are similar to the ages obtained from the Wanzi stratified assemblage in the Fuping Complex (described above), suggesting that the depositional basin was of wide extent.

Fig. 23 near here. Hutuo Group Strat

Flood basalt layers in the Hutuo Group have yielded Sm-Nd ages of 2369 +/- 30 Ma, U-Pb ages of 2366+/- 103-94 Ma, 2358 Ma, whereas similar units from Taihang Mountain have yielded Pb-Pb ages of 2300 Ma (Wang K. et al., 1997, Wu J.S. et al., 1986). These ages come into question, with recent results by Liu C.H. et al. (2011) who documented detrital zircons below and between the volcanic flows with ages as young as 2010 Ma (Fig. 23). Thus, the Hutuo Group basalts, previously regarded as circa 2.3-2.4 Ga old, must be related to younger tectonic activity, or the Hutuo Group is much more structurally complex, with a mixture of different units, than currently appreciated.

In the Jiao-Liao-Ji Belt (Figs. 22, 24) a group of sedimentary and volcanic rocks known as the North and South Liaohe Groups is in structural contact with a suite of monzogranites, gabbros, and dolerites (Li S.Z. et al., 2007). The monzogranites have ages of 2176-2143 Ma (Li S.Z. et al., 2007) and show derivation from partial melting of the lower crust. The basal volcano-sedimentary sequence includes a basal clastic section with bi-modal volcanic rocks that grade up into carbonates, then an upper metapelite unit. The Jia-Liao-Ji Belt contains significant magnesite, Pb-Zn, and boron deposits (Li, S.Z. and Zhao, G.C. 2007), and the northern boundary is interpreted through non-seismic geophysical methods as a fault (Peng, C. et al., 2015). A N-S residual gravity profile (Peng C et al., 2015; Fig. 24) shows that the basin thickens to the north and shows obvious N-over-S thrust structures, but Peng C. et al. (2015) concluded that the basin-bounding fault may have had an earlier history as a normal fault. Luo Y. et al (2004) analyzed detrital zircons from the lower part of the Liaohe Group, and found that all concordant igneous-sourced zircons have ages between 2100-2000 Ma, suggesting that, like the Hutuo Group, at least parts of the Jiao-Liao Ji Belt may have been deposited in a retro-arc foreland basin (Fig. 22). This is supported by more recent dating, which shows that the Liaohe Group has isotopic ages between 2214-1970 Ma (reported in Zhai and Santosh, 2011), and was metamorphosed at 1850-1800 Ma. Interbedded clastic rocks, metapelites, and carbonates interlayered with mafic volcanic rocks in the lower part of the sequence were interpreted as a turbidite sequence by Zhai and Santosh (2011), whereas the Upper Liaohe Group, consisting of boron-rich volcanic rocks and magnesite-rich metasedimentary rocks metamorphosed to amphibolite-granulite facies had protoliths of shallow-water, marine sediments interbedded with intermediate to felsic, and minor mafic, volcanic rocks. We suggest that this sequence is consistent with deposition in a retro-arc foreland basin, situated near sea level, in which the clastic sediments derived from the arc and underlying basement were interbedded with volcanic flows and volcaniclastic debris, and interbedded with marine sediments deposited during sea level high stands. The volcaniclastic sequence was deposited before it was intruded by the monzogranites, and continued to be deposited after their intrusion, consistent with an Andean-type retro-arc tectonic setting similar to the central Andes (e.g., Ramos et al., 2014).

Fig. 24 near here. Jiao Liao Ji Belt cross section

4.3.7 Comparison with the Andes as a modern analogue

In our current interpretation, we regard the Hutuo Group, parts of the Zanhuang Complex, the Jiao-Liao-Ji Belt, and parts of the Khondalite Belt as successor or retro-arc basins behind the arc developed on the northern margin of the craton, recording sedimentation and deposition of tuffs and eruption of volcanics from this arc. In this sense, the tectonic setting is very similar to retro-arc basins of the Central Andes between 34 and 37 S, just south of the Pampean flat slab subduction segment (Fig. 22). Like the Hutuo and Jiao-Liao-Ji Groups, in this retro-arc foreland basin, the clastic and lake deposit sedimentary rocks of the basins are interlayered with basaltic to rhyolitic flows, agglomerates, tuffs, and volcaniclastic rocks, with the volcanic rocks locally reaching 1,300 meter thickness, and covering an area of 40,000 km^2 (Ramos and Kay, 2006; Ramos and Fulguera, 2011). Interestingly, for comparison, this retro-arc basin is located up to 550 km from the trench (Ramos and Kay, 2006), whereas the Hutuo retro-arc foreland basin is located only 350-400 km from the northern margin of the craton. The Jiao-Liao-Ji and Khondalite Belts are also located in similar retro-arc positions. Ramos et al. (2014) noted that the Andean basin is located in the Payenia paleo-flat-slab subduction segment of the central Andes, and suggested that the basalts were generated during steepening and roll-back of the slab, creating extension and volcanism in the overriding slab. Such a mechanism may also be applicable to the Hutuo Group.

It is interesting to compare the scales of deformation, volcanism, and plutonism in the present-day Andes to the North China Craton in the interval between 2.3-1.95 Ga, when we propose that the northern margin of the craton was an Andean arc with related tectonic belts. Fig.

22a shows a simplified map of the central Andes, with an outline map at the same scale of the NCC plotted over it so that the proposed Andean margins are parallel. Note that in the Andes the magmatism is discontinuous, the deformation front lies 600-1,000 km from the trench, and that much of the region under the Altiplano is characterized by double-thickness crust. Thus, if this crust were isostatically eroded to 35 km normal thickness, we would be looking at the remnants of a widespread granulite facies metamorphic event, affecting an area roughly the size of the whole NCC. Since the width of the area affected by Andean-related tectonism ranges from 600-1,000 km, we show two lines, 600 and 1,000 km away from the northern margin of the craton on Fig. 22c. Note that the 600-km deformation envelope extends south of Wutaishan (350 km from the trench) and south even of the Zanhuang massif. The 1,000 km-long Andean deformation envelope includes nearly the entire NCC. Thus, the patterns of deformation, magmatism, sedimentation, and metamorphism in the NCC in this time interval are consistent with it having lain on the overriding plate of an Andean margin.

4.4 Tectono-thermal events between 1965-1790 Ma

The period 1965-1790 Ma saw the strongest metamorphic overprint on rocks of the NCC, with exposed rocks nearly everywhere recording this event. Most of the metamorphism is concentrated in two pulses; a localized UHT event in the NW (Guo JH et al. 2012, 2012; Santosh, et al., 2006, 2007a, b, 2009; Santosh and Kusky, 2010; Wan B. et al., 2015), and a major "Pan-NCC" granulite (and locally amphibolite) facies event, whose retrograde paths peak at about 1.85-1.80 Ga (Zhai et al., 2003; Kusky and Li, 2003; Kusky et al., 2007a; Zhai et al., 2005, 2010; Peng et al., 2014).

The 1.92 UHT metamorphism is best documented locally in the Alxa area (Wan, B. et al., 2015), and in the Jining complex (in the Bao'an, Hongshaba, Xumayao and Tuguiwula areas) where it appears to be associated with contact metamorphism near large gabbronorite intrusions (Guo J.H. et al., 2012),which in turn may be associated with a ridge subduction event that preceded a major continent-continent collision (Santosh and Kusky, 2010; Peng et al., 2011; and Wang W. et al., 2013). If so, that would mean the Andean arc on the northern margin of the craton was still active at circa 1.92 Ga.

The circa 1.85-1.80 Ga event has been interpreted by most workers in China, following Zhao et al. (2001, 2005, 2009, 2012), to be the result of the "final" amalgamation of the Eastern and Western Blocks along the TNCO. However, this has been debated for years by Kusky (Kusky, 2011; Kusky and Li, 2003, 2010; Kusky et al., 2007a, b, c; Kusky and Santosh, 2009; Kusky and Zhai, 2012; Polat et al., 2005), and more recently by Peng P. et al., (2014) who demonstrated that the metamorphic data (from which this purported orogen is defined) are so similar inside and outside the TNCO that they provide no basis for its definition as a separate orogenic belt. We elaborate on this below, and then provide an alternative, actualistic interpretation of the existing data.

In detailed analyses of Paleoproterozoic metamorphic events across the entire NCC, Kusky (2011) and Peng, P. et al. (2014) concluded that there is no evidence for the existence of the so-called TNCO as a Paleoproterozoic orogenic belt. They noted that the spatial distribution of circa 1950-1800 Ma metamorphic events are widely distributed across the craton, but concentrated, and at higher grade, along the northern margin of the Craton, and along the southern margin (Fig 24). Peng, P. et al. (2014) used statistical analysis of multiple data sets on all reported metamorphic events in this time-frame, building on earlier claims of Kusky and Li (2003), Kusky et al. (2007), Kusky and Santosh, 2009), Zhai and Santosh (2011), and Kusky

(2011a, b) that the metamorphic data are not consistent with a Paleoproterozoic orogen in the boundaries defined as the TNCO (Zhao et al., 2001, etc.). In the Kusky et al (2007a) interpretation, the metamorphism of this age was related to a continent-continent collision along the northern margin of the craton when the already-amalgamated NCC joined the Columbia/Nuna Continent. In the new Peng, P. et al. (2014) interpretation, the metamorphism in this time-frame was related to both a collision along the northern margin of the craton, and another along the southern margin of the craton, suggesting perhaps that the NCC was located in a more interior part of the Columbia Continent than in the reconstructions of Kusky et al. (2007a), Kusky and Santosh, (2009), and Kusky (2011a, b). The above detailed data analysis showed that there is nothing unique in terms of metamorphic history about the so-called TNCO, and that it does not exist as a Paleoproterozoic orogen. The TNCO was defined as on orogen based on the claim that rocks in a N-S striking zone, bound by Mesozoic faults, contained different circa 1.85 Ga CW P-T-t paths than areas outside of these Mesozoic faults, which were claimed to show CCW paths at that time. Even ignoring the fact that orogenic belt boundaries cannot be defined by structures that are 1.7 billion years younger than the deformation and metamorphism, it is now clear that there is nothing distinct about the metamorphic paths, or their timing, in locations within the so-called TNCO and outside it. The circa 1.88-1.79 metamorphic event was a “pan-North China Craton” event that affected the whole craton, and is recognizable almost everywhere that rocks of appropriate age are exposed (Zhai, M.G. 2014). Metamorphic grades are higher in the north, and EW-striking structures place higher P assemblages to the N over lower-grade assemblages to the S (Fig. 25). The delineation of the “TNCO” was based solely on this metamorphic interpretation and recrystallized zircon ages, and did not include any regional analysis of tectonic zonations, structural history, or other types of data used for tectonic analysis and definition of suture zones between different, once-widely-separated terranes. Thus, there is no evidence that a N-S striking

Paleoproterzoic orogen existed within the boundaries of the TNCO as defined by Zhao et al. (Zhao, 2001, 2009, 2011, 2012; Zhao et al., 1999, 2001, 2005; Zhao and Zhai, 2013), and further propagated through the published literature. The term TNCO must be abandoned.

4.4.1 An actualistic interpretation of the circa 1.85 Ga Pan-NCC metamorphic event

The main metamorphic event in the NCC saw granulite facies conditions across much of the craton at 1.85-1.80 Ga, with HP granulites and garnet websterites (2.5 GPa) in the north (Wan, B. et al. 2015), and medium-pressure granulites in the rest of the craton (with the exception of amphibolite facies assemblages preserved in a few locations). Kusky et al., (2007a, b) related this to a continent-continent collision, with the outboard continent representing the Columbia (Nuna) Continent. The scale of this event is immense, but of the same magnitude as the current post-collisional zone in Central Asia that resulted from the India – Asia collision (Fig. 25a) so arguments that "the metamorphism in Hengshan and Wutai could not be caused by a continent - continent collision in the north, because it is 200-300 km away" (Trap et al., 2012) are open to discussion. Several hundred km north of the India-Asia suture today, we find ourselves in Tibet (Hodges, 2000), with a double-thickened crust, partial melting at mid-crustal levels (e.g, Chung SL et al., 2003), and intense deformation with lower crustal flow similar to that documented for the high-pressure Datong-Chengde Granulite Belt (Trap et al., 2011) causing divergent directions of thrusting at the surface (e.g., Royden et al., 1997; Clark and Royden, 2000; Hubbard and Shaw, 2009). For instance, the strike of the Longmenshan, which is being uplifted as a result of the India-Asia collision, is roughly parallel to the motion direction of India into Asia, and the thrusting is at right angles to the convergence direction (e.g. Burchfiel et al., 1995). Thus, having a 10° angle between the northern margin of the craton, and predicted perpendicular thrusting directions in some places such as Wutai or Zanhuang are not unexpected. The same argument applies to much of the deformation across Asia north of Tibet (e.g., Cunningham, 2015).

Fig. 25 compares the scale of the India – Asia collision with that of the NCC at 1.85 Ga. Note that the Tibetan Plateau, underlain by granulites and zones of partial melting, extends for more than 500 km from the India-Asia suture zone in India (Fig. 25b). If the scale of the continent-continent collision that juxtaposed the NCC against the Columbia Continent was comparable to the India-Asia collision, then the entire NCC would have been involved, as is demonstrated by the metamorphic data. It is not confined to a narrow ~200 km wide belt called the TNCO. Note also that the time-scales of the deep metamorphism, melting, and deformation are similar. The India/Asia collision that is uplifting Tibet began more than 50 Ma ago (e.g., Rowley, 1996; Zhu et al., 2005; Ding et al., 2005), and is still on-going to this day (Harrison et al., 1992; Kirby et al., 2003). Thus, the roughly 100 Ma long group of metamorphic events from 1.88 Ga to 1.79 Ga can all be related to different stages of the ancient continent-continent collision initiated along the northern margin of the NCC.

The N-S collision between the NCC and the Columbia/Nuna Continent is supported by a study of Re-Os isotopes from 99 peridotite xenoliths from the Central NCC. Liu JG et al., (2011) reported that peridotites from the northern part of the craton are more fertile than those from the south, and that the peridotites in the north have Os model ages (T_{RD}) of ~ 1.8 Ga, suggesting that the lithospheric mantle in the north is significantly younger than the overlying Archean crust. In contrast, in the south, the (T_{RD}) ages are ~2.1-2.5 Ga, consistent with the collision of the Eastern Block and arcs in the COB in the late Archean-early Proterozoic. Moreover, the lithosphere in the north seems to have been replaced at circa 1.8 Ga, consistent with a “major north-south continent-continent collision that occurred during assembly of the Columbia Supercontinent at ~ 1.8-1.9 Ga” (Liu JG et al., 2011).

Fig. 25 near here. Tibet – NCC comparison

The 1.85 Ga event is recorded in the many metamorphic P-T-t paths so widely reported and interpreted to be a result of continent-continent collision in the TNCO. Unfortunately, nearly all these works (with the exception of Trap et al., 2009a,b, 2012) and Faure et al. (2007) and Zhang et al. (2007, 2009, 2012) lack accompanying detailed field and structural studies, and led only to construction of P-T-t paths. We concur that the P-T-t paths are indicative of a continent - continent collision, but think that collision took place along the northern margin of the Craton (e.g.,Wan, B. et al., 2015), and not along the defunct TNCO.

The circa 1.9-1.85 Ga continent-continent collision is associated with a suite of leucogranites that are distributed across the craton, particularly in its northern half (Fig. 25d, Fig. 26). Many of these are leucocratic veins that are associated with crustal anataxis and cut most of the high-grade metamorphic rocks as in Fig. 25c (Peng et al., 2012a). Other areas contain large bodies of post-tectonic leucogranites with ages between 1880 and 1790 Ma. For instance, a late group of post-tectonic porphyritic monzogranites and granites intruded the Jiao-Liao-Ji Belt at 1875-1856 Ma, and were followed by alkaline syenites at 1857-1843 Ma (Lu et al., 2006; Li S.Z. et al., 2007, 2011 (Fig. 23d). Geng et al. (2004) reported SHRIMP U-P (zircon) ages of circa 1794 +/- 13 Ma for post-tectonic augite-monzonites and circa 1801 +/- 11 Ma granites from the Luliang area in Shanxi Province. Wilde et al. (2002) described a widespread generation of crustal melts across the central part of the craton between 1.88 and 1.79 Ga in the Wutai Complex. In the Hengshan Complex, high-grade metamorphism at circa 1800 Ma is associated with anatectic melting and the production of leucogranites at 1860 Ma (Zhao et al., 2001c). From the Hai'an Complex, Zhao et al. (2008) reported ages of 1849+/-10 Ma from the anatectic Huai'an charnockite, and 1850+/- 17 Ma from the Dapinggou garnet-bearing S-type granite. Other tonalitic, trondhjemitic, and granodioritic gneisses from this complex yield ages of 1847-1842 Ma (Zhao et al., 2008). In North Korea, massive porphyritic post-tectonic monzogranites formed at 1865-1843 Ma (Zhao et al., 2006). We relate these abundant post- tectonic anatectic granitoids to crustal thickening following collision (e.g., Dewey and Burke, 1973) of the NCC with the Columbia/Nuna Continent (Fig. 22d; Fig. 26), and suggest that they are analogous to the Himalayan and Tibetan leucogranites forming today in response to the India-Asia collision (e.g., Le Fort et al., 1987; Yin and Harrison, 2000; Galliard et al., 2004).

4.4.2 High-Pressure granulites, eclogites, and orogen-parallel lower crustal flow in the Hengshan and the northern margin of the NCC: an analog to modern day Tibet

The Hengshan Complex to the north of the Wutai Complex (Figs. 7, 17, 25, 26) contains a suite of circa 2550-2450 Ma tonalitic, trondhjemitic, and granodioritic (TTG) gneisses and granitic gneisses, metamorphosed to granulite facies in the Paleoproterozoic that include numerous boudins of high-pressure mafic granulites, retrogressed eclogites, and high-grade metasedimentary rocks (Li and Qian, 1991; Li, J.H. et al., 2000a,b,c; Wilde et al., 2002;Wilde and Zhao, 2005; Zhao et al., 2002a,b,c, 1999, 1999c, 2005, 2006, 2012; Kröner et al., 2005 a,b, 2006; O'Brien et al., 2005). A major EW-striking ductile shear zone, the Zhujifang Shear Zone cuts the complex in two, with high-pressure granulites confined to north of the shear zone, and medium-pressure granulites and amphibolites only to the south of the shear zone (O'Brien et al., 2005; Kröner et al., 2006; Trap et al., 2011).The high-pressure belt in the north strikes ENE for about 400 km before it disappears under younger cover, and is about 150 km wide in an N-S direction (Figs. 7 and 17).

Zhang et al. (2007) documented a complex deformation history of the Hengshan Complex. Early D1 (maybe not the earliest event) structures include a compositional fabric with small isoclinal rootless intrafolial folds with axial planar transposing intrafolial foliations and mineral lineations. Zhao et al. (2001b) and Zhang et al. (2007) noted that this deformation event may be associated with the earliest metamorphic assemblage preserved in these rocks that includes quartz and rutile inclusions in garnet, and symplectic clinopyroxene-plagioclase intergrowths. There are no constraints on the age or PT conditions of this event, other than that it pre-dates D2. Overprinting D2 structures form the dominant structures in the Hengshan, and include NW-verging, tight to open asymmetric folds a few meters to kilometers in scale, with an axial planar foliation and associated thrusts. D2 structures are associated with the highest-grade assemblages in the rocks. Deformed mafic dikes deformed in D2 have assemblages that yield P-T conditions of 13.4-15.5 kbar and 770-840 C (Zhao et al., 2001), suggesting crustal thicknesses of 55 km at this stage (Zhang et al., 2007). D3 deformation is confined to the NNE-striking Zhaojiayao and related shear zones, which show a transpressional dextral shear event that includes top-to-the-NW oblique-slip shearing and NNE-SSW dextral strike-slip shearing. D4 is represented by formation of the giant 2 km wide Zhujiafang Shear Zone striking E-W for 60 km across the complex until it is buried under younger cover in the east and west. This shear zone separates the high-pressure granulites in the north from medium-pressure granulites to the south (Kröner et al., 2005a; O'Brien et al., 2005). Kinematic indicators in the shear zone including σ–type porphyroclasts and sheath folds are interpreted as indicating dextral shear (Zhang et al. (2007). This shear zone also has many enigmatic shear sense indicators on it, for instance, Trap et al. (2011) reported dominantly sinistral slip indicators. In any case it must have considerable vertical displacement because high-pressure granulites to the north are emplaced over amphibolite-facies rocks with medium-pressure granulite boudins to the south. D5 includes regional-scale open folds that lack any axial planar fabrics, and are largely responsible for the basin and dome interference pattern of the Hengshan (Zhang et al., 2007). This stage of deformation is also associated with a series of low-angle detachment faults, leading Zhang et al. (2007) to suggest that this last phase of deformation was related to exhumation of the complex. Support for this interpretation comes from the near-isothermal decompressional symplectites and coronas that surround embayed garnet grains that formed during this late exhumation stage of the Hengshan. Zhao et al. (2007) presented evidence that the entire sequence of events from the high-grade metamorphism during D2 to the exhumation during D5 lasted from 1880 Ma to 1820 Ma. It is not known when the M1 metamorphism occurred, so we do not relate it to the same single tectonic event and PT-t path as Zhao et al. (2007), but rather, we just say it predates the circa 1880-1820 Ma event.

Trap et al. (2011) presented a comprehensive structural analysis of the entire exposed part of the High Pressure Belt, focusing on the role of partial melting interacting with the deformation. They divided the complex into units of diatexite and metatexite (sensu Sawyer, 2008). They show that the overall geometry of the HPB is that of a 400 km long (ENE) and 100 km wide antiform with a gentle north-dipping northern limb bound by the newly-defined Datong-Chengde shear zone, and a southern limb that dips steeply south, bound by the Zhujifang shear zone (Figs. 7, 17, 25, 26). The antiformal hinge curves from E-W to NE-SW, and plunges W in the W, and E in the E. Based on their analysis Trap et al. (2011) defined four main stages of deformation related to the establishment of this geometry.

D1 is an amphibolite-facies gneissic foliation preserved in paleosomes with an associated L1 mineral lineation, which becomes mingled with S2 in metatexites. Outside the zone of partial melting (PMZ) S1 remains the dominant fabric as an E-W to NE-SW gneissic foliation with a NW/SE-trending sillimanite, biotite or amphibole mineral lineation. Top-to-the-SE shear parallel to L1 is indicated by sigma-type porphyroclasts (Trap et al., 2011). Kröner et al. (2005a, 2006) and Guo et al. (2005) obtained SHRIMP U-Pb ages of 1881 +/- 8 Ma and 1872 +/- 16 Ma in migmatites and high-pressure granulites, which Trap et al. (2007, 2011) interpreted as a phase of crustal thickening during the D1 event leading to the major partial melting and crustal anatectic event at circa 1850 Ma.

The most significant structure within the PMZ is D2, which formed during amphibolite to granulite facies metamorphism accompanied by in situ partial melting (Trap et al., 2011). Numerous conventional multigrain and SHRIMP U-Pb ages from migmatites and HP granulites date this event rather precisely at 1850 +/- 10 Ma (Zhao et al., 2002, 2005, 2006, Guo et al., 2006; Faure et al., 2007; Wang J. et al., 2010). The S2 foliation is defined by leucocratic material in the veins that is parallel to S1, forming a composite S1-S2 fabric. Trap et al., 2011 used a range of syn-kinematic structures involving the locally-derived melt to demonstrate melt-enhanced orogenic flow of the PMZ, including zones of SW/NE- and E/W -trending coaxial flow, westward non-coaxial flow, sinistral strike-slip shearing in the presence of melt, and north-verging syn-anatectic folding.

Fig 26. Near here- cross sections at 1.93 and 1.80 Ga

The consistent E-W to NE-SW orogenic flow (see Fig 7a) is remarkably similar to that of modern orogens, such as the Tethysides, where orogenic flow parallel to the orogenic strike at mid-to-lower crustal levels is widely thought to partly accommodate orogenic escape and collapse of orogenic highlands. The near- parallelism of the Zhujifang and Datong-Chengde Shear Zones, which are at the heart of the zone of partial melting within the northern margin of the craton is geometrically analogous to the flow to the east away from the extant India - Asia collision (e.g. Tapponier and Molnar, 1976; Molnar, 1988; Molnar and Tapponnier, 1975). Thus, we relate this exposed Paleoproterozoic mid-lower crustal flow at circa 1.85 Ga to the proposed 1.85 Ga continent-continent collision on the northern margin of the craton, a few hundred km to the north. Such orogen-parallel flow during continent-continent collision is common (England and McKenzie, 1982; Houseman and England, 1993; Royden et al., 1997; Klemperer, 2006; Clark and Royden, 2000) and matches the geometry of the NCC system, so we so do not call on oroclinal bending of a supposed NS-striking TNCO to explain this phenomena (c.f. Trap et al., 2011), but instead interpret the flow in terms of the present geometry of the orogen (Figs. 7, 17, 23, 26).

D3 was a subsolidus deformation developed at the granulite-amphibolite facies transition, but the E-W flow is still recognized by subsolidus structures such as pressure shadows and porphyroclast systems, indicating co-axial flow (Trap et al., 2011). The main Datong-Chengde Shear Zone formed during D3 as a km-scale ductile normal-sense shear zone. S3 is a mylonitic foliation that shows top-to-the- NW senses of movement, such that the DCSZ has a normal-sinistral sense of movement (present coordinates).

D4 is represented by the formation of the late Zhujiafang strike-slip shear zones. The ZSZ has a sub-vertical to steep south-dipping mylonitic to ultramylonitic foliation that shows sinistral kinematics (Trap et al., 2007; Wang, 2010), although Kröner (2005b) reported dextral shear in places. Early vertical motion may be explained by low-strain zones that still preserve a steep lineation (Trap et al., 2007).

The P-T evolution of the HP rocks in the Hengshan has been the subject of considerable research and the near-isothermal decompressional part of the PT-t path is well established. The "peak" high-pressure granulite assemblages (M1 of Trap et al., 2011, M2 of Zhang et al. (2007) consist of garnet + clinopyroxene +/- quartz, and locally an eclogite facies assemblage of garnet + quartz + omphacite pseudomorphs (Zhao et al., 2001 a, Zhang et al., 2006). This assemblage is succeeded by a medium-pressure assemblage of garnet + plagioclase + clinopyroxene + orthopyroxene +/- quartz, a low-pressure (M3) granulite facies assemblage of orthopyroxene + clinopyroxene _ plagioclase +/- quartz, then finally an amphibolite-facies assemblage of hornblende + plagioclase (Trap et al., 2011). M1 (M2 of Zhang et al., 2007) took place at conditions of 800-850 C – 14-16 kbar, M2 under conditions of 800-825 – 10 kbar, M3 at 800 C – 7 kbar, and M4 at 650 C – 5 kbar (Zhang et al., 2007; Zhao et al., 2000, 2001a; O'Brien et al., 2005). These data are consistent with an isothermal decompression path from HP granulite facies to LP granulite facies conditions, followed by slow cooling through the amphibolite facies. Big questions remain, however, about the early prograde path. Are the M1 qtz-rutile assemblages reported by Zhang et al. (2007) part of the same PT path, or related to an earlier tectonothermal event? Is the PT path truly clockwise as widely reported, or, as the data suggests, do we only have sufficient data to constrain the near-isothermal decompression path? Should all of the data from the early pre-granulite events be included in the same PT path, or, as the structural data suggest, might there be an earlier tectonothermal event that is much older than the circa 1.85 Ga granulite facies event, which the above data are recording?

There has been much discussion of the origin of the circa 1.85 Ga metamorphism that formed the granulitic-eclogitic assemblages (now retrogressed) in the mafic boudins of the Hengshan Complex, with most workers suggesting that these demonstrate that the Eastern and Western Blocks collided at circa 1.85 Ga and that the high-grade metamorphism is related to this hypothetical continent-continent collision (Zhao et al., 2002a,b,c, 1999, 1999c, 2005, 2012; Kröner et al., 2005 a,b, 2006; O'Brien et al., 2005). However, this is not necessarily the case. The eclogitic metamorphism simply tells the time at which the mafic rocks were at the appropriate PT conditions to transform into eclogite. The regional structural patterns suggest a different origin for the high-grade metamorphism. The eclogites and HP granulites are all located north of the

EW-striking Zhujiafang ductile shear zone, and rocks to the south of this major tectonic structure are all medium-grade granulites. It is interesting, and no coincidence, that the EW-striking Zhujiafang shear zone and the Datong-Chengde shear zone are parallel to the EW-striking Northern Hebei Orogen on the northern margin of the Craton, and that the Zhujiafang shear zone marks a major crustal boundary, which placed high-pressure granulites over medium-pressure granulites at circa 1.85 Ga. That is one reason why Kusky and Li (2003), Kusky et al (2007a, b), Kusky and Santosh (2009), and Kusky (2011) related the formation of these granulites to a continent- continent collision along the northern margin of the craton at circa 1.85 Ga, when the NCC joined the Columbia/Nuna Continent, and formed a Tibetan-scale plateau that occupied most of the present area of the NCC, with metamorphic grades in the finally exhumed crust increasing to the north toward the collision zone. The high-grade metamorphism at 1.85 Ga has in our opinion nothing to do with a NS-striking Paleoproterozoic orogen named the TNCO, which we think did not, and does not, exist.

4.4.3 Post collisional extension. Recent studies have demonstrated that the continent – continent collision was likely terminated by 1750 Ma. Yu J.H. et al. (1993, 1996), Ramo et al. (1995), Xie G.H. (2005) and Zhang, S.H. et al. (2007) identified a suite of anorthosite, mangerite, charnockite, and alkali-feldspar granites (AMCG suite) in an ENE-striking belt across the northern margin of the craton, which indicate that convergent tectonism had ended by then. Liu J.F. et al. (2015) showed that rocks of this suite from the Longhua and Jianping areas are 1753-1673 Ma in age, and that they are alkaline and enriched in LREE and LILEs, and depleted in heavy REEs and HFSEs. Their geochemical signatures suggest that these rocks were derived from early Precambrian, lower crust of the NCC and that they formed from noritic magmas through fractional crystallization near the base of the crust. Other granites and rapakivi granites of this age have the characteristics of A-type granites and may have originated through partial melting of the middle or upper crust. Liu J.F. et al. (2015) synthesized data on the AMCG suite, and suggested that they intruded in a post-orogenic extensional setting during post-collisional collapse of the orogen that was followed by the formation of rift and graben structures and mafic dike swarms that propagated across the whole craton, such as the 1780 Ma Taihang dyke swarm that emanates from the Xiong'er plume centre of the >0.1 M km^2 Large Igneous Province (Peng et al., 2015b).Eventually this led to the break-out of the NCC from the Columbia/Nuna Continent, and the beginning of a stable phase of evolution of the NCC that would last until the Phanerozoic (Li, Q.L. et al., 2007; Kusky et al., 2007a; Jiang N. et al., 2011; Wang W. et al., 2013).

5. Discussion: Growth of the NCC by Progressive Accretion of arcs, microcontinents, and oceanic plateaus, and comparison with other Precambrian and younger tectonic provinces as a test of Archean tectonic style

5.1 Assessment of Precambrian tectonic stylesin the North China Craton

Suture zones and orogens are defined by using a combination of structural, stratigraphic, geochronologic, metamorphic, paleontologic, paleomagnetic, and paleoclimatic data. In old high-grade Precambrian terranes such as the NCC some of these tools are not available, but sutures between different tectonic units must still be defined using a multi-disciplinary tectonic analysis. Suturing of different small tectonic units or large cratons is not a simple process whereby different terranes just “amalgamate” or "dock" or instantaneously bang into each other and stop, but involves complex and protracted geological processes (structural, metamorphic, magmatic, geochemical, temporal, erosional, depositional and others). An integrated or holistic assessment of these processes in the NCC to search for evidence of the operation of the Wilson Cycle, and hence plate tectonics in the Precambrian is presented in this work.

From 2.5 Ga to 1.8 Ga, the NCC grew by outward accretion of island arcs, accretionary wedges, oceanic plateaus, and ribbon micro-continents, progressively from the Eastern Block, to younger orogens to the west, northwest, then north (Fig. 17). The Eastern Block has been proposed to have formed by amalgamation of 'microblocks" between 3.8 Ga and ~ 2.6 Ga, with a peak between 2.6 and 2.7 Ga (Zhai M.G. et al., 2005, 2010, 2014; Zhai M.G. and Santosh, 2011), but the exact timing and nature of these proposed suturing events remain elusive, so are not discussed in detail in this paper. The oldest known rocks in the Eastern Block include the Tiejashan trondhjemitic and granitic gneisses NE of Beijing with zircon populations of 3.8 and 3.3 Ga, and the Caozhuang meta-sedimentary and meta-volcanic rocks of Eastern Hebei with ages of 3.3 Ga and detrital zircons of 3.7 Ga (Wu F.Y. et al., 2005). Old detrital zircons in Paleozoic rocks surrounding the NCC, especially in the Qinling orogen on the southern margin of the NCC have yielded detrital zircons of up to 4.1 Ga with cores that possibly reach back to 4.45 Ga (Diwu C.R. et al., 2010, 2013) suggesting that there may yet be other regions of very ancient crust to be discovered in the NCC. While recognizing these older different components of the Eastern NCC, they do not represent volumetrically significant components of the NCC, so we start our analysis from the time at which the western margin of the Eastern Block can be shown to have had an extensive passive margin developed on it (>2.5 Ga), and examine events from that point to when the craton became stable when it broke out of the Columbia (Nuna) Continent at circa 1750 Ma.

What does this evolution tell us about the style of Neoarchean tectonics in the NCC and perhaps globally? Before 2.6 Ga there was accretion of micro-cratons, arcs or arc-type archipelagos that were dismembered into smaller blocks during accretion or younger tectonism, whereas after 2.5 Ga there was a progressive accretion of continental shelves, arcs, microcontinents, and oceanic plateaus in orogens around older continental nuclei. This includes the first appearance of true ophiolites, ophiolitic mélanges, and linear orogenic belts with strike lengths of ~ 1,300 km; these contrast with the proposed boundaries between micro-blocks in the Eastern Block, which are only hundreds of kilometers long. Whether this distinction holds up or not depends on further detailed structural and tectonic analysis of the older plate boundaries within the Eastern Block, to determine whether the short strike-lengths are original, parts of a complex anastomosing accreted archipelago, or perhaps modified by syn- to post-accretion strike-slip or other events.

Another pertinent question is: ‘was the apparent change in style of accretionary tectonics at 2.5 Ga in the NCC a reflection of local changes in ambient tectonic conditions, or was it representative of a global phenomenon, as originally suggested by Burke et al. (1976)? Dewey (2007) suggested that the style of tectonics on Earth changed at about 3.0 Ga, from a “plume-dominated system” to a “plate-dominated system.” While our observations about the apparent change in tectonic style between 3.0 and 2.5 Ga in the NCC are consistent with this hypothesis, the style of pre-3.0 Ga tectonics in the NCC has yet to be rigorously tested, and remains a matter of discussion between the authors (e.g., see Dewey, 2007; Kusky et al., 2013a, b).

The style of accretion in the NCC is similar to that of the Superior Province (e.g., Card, 1990; Percival et al., 2006, 2012), in which progressively younger arcs, accretionary prisms, and microcontinents were added to the outboard portions of a core microcontinent (in a general sense), to form a large craton at the end of the Archean. This in turn has led some to propose the existence of a large end-Archean supercontinent, Kenorland (e.g., Hoffman, 1991; Aspler and Chiarenzelli, 1998; Bleeker, 2003; Santosh et al., 2009). Without any paleontological or rigorous paleomagnetic data it is difficult to test such a hypothesis, but the global data from Archean cratons do suggest a major amalgamation event at the end of the Archean. In the case of the North China Craton, the evidence does suggest that the style of accretion changed from small arc-like landmasses between 3.8 and 2-7-2.6 Ga, to accretion of larger arc terranes to an amalgamated continental landmass at the end of the Archean, followed by progressive addition of arcs and reworking of existing crust until the record terminated at circa 1.7 Ga. This style of tectonism is also consistent with modern orogens such as the Carpathians in which the slab hinge converges relative to the upper plate (e.g., Doglioni et al., 2007).

5.2 Orogenic styles in Archean vs. Phanerozoic orogens as inferred from map patterns

One of the common ideas about Archean orogens is that they have fundamentally different characteristics and map patterns from Phanerozoic orogens, but we have shown that this is not the case for the late Archean of the NCC. Some geologists and geodynamic modelers claim that Phanerozoic orogens exhibit linear patterns, whereas Archean orogens are characterized by basins and domes. They then use this statement to claim that the crustal and geothermal gradients in the Archean were higher, and that the Archean tectonic style was dominated by vertical, rather than horizontal, movements (e.g., Choukroune et al., 1995; Hamilton, 2003, 2007; Rey et al., 2003; Van Kranendonk et al., 2004; Bedard, 2006; Cagnard et al., 2006; Rey and Houseman, 2006; Gapais et al., 2009; Bedard et al., 2013; Debaille et al., 2013; Lin et al., 2013). In spite of the fact it is possible to construct numerical geodynamic models in the laboratory to explain this scenario, the basic observations and interpretations of such a fundamental difference between Archean and Phanerozoic orogens are mostly invalid (e.g., Polat et al., 2014) (for reviews of differences of opinion about Early Archean tectonics, see Van Kranendonk et al. 2004; Dewey, 2007; Kusky et al., 2013). In the NCC it is possible to find both “basin and dome” map patterns (e.g., the Taipingzhai gneiss terrane in Fig. 8) and linear map patterns (e.g., the 1,300 km long COB in Fig. 17). Thus, we briefly compare other terranes of Archean and younger ages globally to see if these different map patterns reflect a secular change in tectonic pattern, or just different tectonic environments.

Fig. 27a-b compares geological maps of the Harrison Lake area of the Mesozoic Coast Range Plutonic Complex in Canada with the famous “basin-and-dome” early Archean granite-greenstone terrane of the Pilbara craton, Western Australia. Note that the scale and style of deformation are remarkably similar, as are the types and relative abundances of rock types. There are many other examples of younger basin and dome map patterns from numerous Phanerozoic orogens around the world (e.g., see maps of Newfoundland and parts of the Sierra Nevada, figures 3 and 4 in Burke et al., 1976) and in the accretionary orogen of Japan. Thus, domal granitoids intruding a mixed volcano-plutonic and sedimentary succession are not a characteristic unique to the Archean.

Fig. 27 near here

Likewise, some workers claim that linear tectonic belts that characterize Phanerozoic orogens are absent from the Archean record (e.g., Hamilton, 2007). This is also untrue, especially for the Neoarchean, as exemplified by examples from the NCC in this paper. Fig. 28-a-b compares the map pattern in the Paleozoic Appalachians of Newfoundland with that of the Archean Yilgarn Craton. Note again that the styles and scales of the linear tectonic belts as well as their constituent rock types are similar in these two orogens of contrasting age. Fig. 28 c-d compares the Paleozoic Altaids or Central Asian Orogenic Belt (CAOB), with the Archean Superior Province of Canada. Clearly both orogens are characterized by elongate linear belts of metasedimentary lithotectonic assemblages, metavolcanic/plutonic terrains, older gneissic ribbon continents, and by granitoid belts that extend for up to several thousand kilometers in linear to curvilinear belts (see Percival et al., 2012; Sengör et al., 2014). In fact, comparison of the two figures shows that the older Superior craton, the largest surviving fragment of an Archean craton on the planet, exhibits greater linearity than the equivalent Paleozoic CAOB. There are differences, however, in that the Superior Craton shows a fairly regular outward growth from the oldest "core" of the craton in the north (Percival et al., 2012), whereas the CAOB shows progressive outward growth of accretionary orogens to the south (present coordinates) from the Siberian Craton, and to the north (present coordinates) from the North China Craton, with the two orogens separated by a giant shear zone (see review by Xiao et al., 2015). Thus, the notion that Archean belts are dominantly characterized by dome-and-basin shaped outcrop patterns, and that Phanerozoic orogens are all characterized by linear outcrop patterns is a myth and should be dismissed. There is as much variation in Archean terranes, especially in the Neoarchean, as there is in young orogens, and similar map patterns can be found in both in different environments. Thus, this notion cannot be used to suggest that Archean tectonic styles were different from those in the Phanerozoic, and should not be used as input for numerical models.

In summary, we emphasize this fundamental point about orogenic style, because failure to appreciate the importance of the correct interpretation of map patterns can lead to erroneous interpretations of the geology, geochemistry, geochronology, metamorphic patterns, and eventually to wrong conclusions about the role of plate tectonics in the early Earth. For example, the long-misunderstood interpretation and theoretical modelling (sagduction and diapirism) of the dome-and-basin map pattern of East Pilbara (Fig. 27b) is resolved by field-based evidence that the so-called 12 km-thick intact volcanic pile is actually broken into 5 units by at least 4 thin, but major, thrusts along which the mafic-ultramafic lavas of each unit are capped by cherts and marked by shear fabrics, and this scenario is constrained and confirmed by multiple U-Pb zircon dates that increase upwards in the volcanic pile (see Fig.29, based on data from Kitajima et al., 2008).

Figs. 28, 29 near here

Thus, comparison of map patterns between Phanerozoic and Archean terranes reveals that there is no fundamental difference between the two. Linear belts with 1,000's of km of strike length occur in both, and dome-basin map patterns of comparable scale can be found in orogenic belts of both ages. The map patterns depend on tectonic setting, not age. Methods of tectonic analysis to search for sutures in other Archean terranes are likely to be successful, as we have shown for the North China Craton.

6. Conclusions

The North China Craton (NCC) consists of a number of discrete tectonic units that can be interpreted coherently using the paradigm of plate tectonics from at least 2.7 Ga into younger times, and from understanding the geological effects of those plate tectonic processes in the preserved geology. From that perspective, we reach the following conclusions:

1. At about 2.5 Ga the tectonic style in the NCC underwent an *apparent* change from accretion of microcontinents and arc-type archipelagos (characteristic during the interval 3.8-2.7/2.6 Ga; Burke et al., 1976), to accretion of long linear orogenic units (Fig. 30). Whether this reflects a true change in the length-scale of accreted tectonic elements, or dismemberment of a larger arc

system as in the extant Timor-Australia collision zone, remains to be tested. Crustal growth progressively moved from the Eastern Block in a clockwise direction first to the west, then NW, and north together with development of a series of sutures from 2.7 Ga, 2.5 Ga, 2.43 Ga, 2.3 Ga, to 1.9 Ga (and followed by sutures of the Central Asian orogenic belt in the Paleozoic; Fig. 30). This type of progressive accretion away from an older nucleus is similar to that of the Superior Province of North America (Fig. 25), reflecting the amalgamation of smaller tectonic units into larger continental landmasses at the end of the Archean (perhaps leading to the formation of the Kenorland Continent) and into the Paleoproterozoic with the formation of the Columbia (Nuna) Continent.

2. A circa 2.5 Ga suture zone can be traced for ~1,300 km from north to south through a series of exposed Archean massifs in the North China Craton (Fig. 30). The suture separates the late Archean Wutai/Fuping arc in the Central Orogenic Belt on the west from the Eastern Block in the east. The subduction zone dipped to the west under the arc, and several accretionary prism fragments with fore-arc ophiolites and ophiolitic mélanges were obducted over the Eastern Block during the collision (Fig. 18). The Eastern Block consists of a series of smaller "microblocks" that may represent a tectonic collage of microcontinents and a SW-Pacific arc-like archipelago that contains small relicts of ancient crust up to 3.8 Ga old, and underwent a major accretion and crustal growth event at 2.7-2.6 Ga. A thick passive margin of shelf sediments, which formed on the western edge of this Eastern Block by 2.5 Ga, was involved in and imbricated with the arc and fore-arc ophiolitic mélanges in the Central Orogenic Belt during its collision with the Eastern Block at 2.5 Ga.

Fig. 30 near here

3. After collision of the Wutai/Fuping arc in the Central Orogenic Belt with the Eastern Block, subduction polarity reversed so that an oceanic slab dipped beneath the Eastern Block (Fig. 18), and generated a suite of mafic dikes and granites, with associated regional metamorphism, from underplated mafic magmas. This period of eastward subduction ended about 70 Ma later, at 2.43 Ga, when the Western Block collided with the arc-modified margin of the composite Eastern Block, shutting off that subduction system (Fig. 20).

4. Soon after this second collision, the composite North China Craton underwent rifting, and a fragment drifted off its northern margin, leaving a failed rift arm striking through the center of the Craton. Passive margin sediments were deposited over the rift facies sediments, and were affected by the collision of an arc along the northern margin of the craton, which took place at circa 2.3 Ga (Fig. 30). This arc was built on older basement, and soon after this collision the northern margin of the craton was modified to become an Andean-style arc (possibly through reversal of subduction polarity), and the entire craton was affected by Andean-type tectonics from 2.3 Ga to 1.9 Ga (Fig. 26). Features related to this significant interval in the development of the NCC include suites of continental-margin arc magmatic rocks that form a swath several hundred km wide that strikes E-W across the craton. Along the northern margin there was UHT metamorphism related to a ridge subduction event, deposition of volcanic and volcaniclastic rocks in retro-arc foreland basins several hundred km from the active margin front, and deposition of thick clastic sediments in an apron adjacent to the arc. The scale of these tectonic units is the same as that in the present-day Andes.

5. From about 1.88-1.79 Ga, the entire NCC underwent a high–grade granulite facies event with high-P granulites and eclogites from this event now exposed in the north, and medium-P granulites now exposed in the center and south parts of the craton. Crustal anataxis is locally associated with this metamorphic event and large-scale lower-crustal flow accommodated escape parallel to the orogen. This craton-wide event was not associated with the addition of any new juvenile crust, just the re-working of older crust, and we relate this to continent-continent collision along the northern margin of the craton (Figs. 26, 30), when the Andean margin collided with another continental mass, most likely the Columbia/Nuna Continent. The length-scale of this deformation, metamorphism and crustal anataxis is similar to that associated with the extant India-Asia collision, and the time-scale of the on-going Alpine-Himalaya collision is similar to the circa 100 Ma duration of this event in the North China Craton.

6. Following this collisional history, a suite of anorthosite, mangerite, charnockite, and alkali-feldspar granites (AMCG suite) intruded the northern margin of the craton in the ~1.75-1.67 Ga interval, along with the N-S swarm of compositionally-similar Taihang mafic dikes that transect the whole craton. Subsequent formation of rifts led to the break-away of the NCC from the Columbia/Nuna Continent, deposition of shelf sediments on the new passive northern continental margin, and a long period of stability for the NCC followed until the Paleozoic, when new orogenic material was added to its northern and southern margins.

7. A re-assessment of the validity of the so-called “Trans-North China Orogen” (TNCO), supposedly formed at 1.9-1.85 Ga as a collision zone between the Western and Eastern Blocks of the craton after 700 Ma of west-dipping subduction, reveals that it does not exist as a Paleoproterozoic orogen. The metamorphic data used to define its existence are not unique to the

belt, its boundaries are not defined by necessary, coeval shear zones, and there is no juvenile material in the orogen of that age (juvenile crust was generated at 2.8-2.7, and 2.5 Ga in the NCC: Wang W. et al., 2012, Geng Y.S. et al., 2012, Nutman et al., 2011; Peng P. et al., 2014). There are no Paleoproterozoic ophiolites, and no accreted sediments and arc rocks in the purported orogen, but these would be expected if the model of 700 Ma of subduction beneath this belt were correct. We suggest that the notion of a Paleoproterozoic "TNCO" in the NCC should be abandoned.

8. The NCC provides a good example of late Archean terranes that are not fundamentally different in their map geometry and components from those of equivalent parts of younger orogens, including the Phanerozoic. Linear belts with 1,000's of km of strike-length occur in both, and pluton-centered dome-basin map patterns of comparable scale can be found in orogenic belts of both late Archean and Phanerozoic age.

9. Rigorous application of the multidisciplinary tools of plate tectonics to the study of the NCC reveals the operation of the Wilson Cycle, and thus plate tectonics, at least as far back as the Neoarchean.

Acknowledgments

This work was supported by National Natural Science Foundation of China (No. 41572203) awarded to Tim Kusky, and NSERC Discovery Grant (No. 250926) awarded to Ali Polat. We thank various colleagues for fruitful discussions and field trips throughout the North China Craton over the years, including Alfred Kröner, Simon Wilde, Li Jianghai, Peng Peng, M.

Santosh, M.G. Zhai, Chunming Wu, Wei Lin, and many others. Y. Huang, B. Huang, B.Y. Lan, Z.C. Wang, and Y. J. Zhang are thanked for diligent help in drafting figures.

References

Aspler, L. B., and Chiarenzelli, J.R., 1998. Protracted breakup of Kenorland, a Neoarchean supercontinent? Geochronologic, tectonostratigraphic and sedimentologic evidence from the Paleoproterozoic, Sedimentary Geology 120, 7.

Bai, J., 1986. The Precambrian crustal evolution of the Wutaishan area. In: Bai, J. (Ed.), The Early Precambrian Geology of Wutaishan. Tianjin Science and Technology Press, Tianjin, pp. 376–383 (in Chinese with English abstract).

Bai, J., Huang, X.G., Wang, H., 1996. The Precambrian Crustal Evolution of China, second edition. Geological Publishing House, Beijing, pp. 80–90.

Bedard, J.H., 2006. A catalytic delamination-driven model for coupled genesis of Archaean crust and sub-continental lithospheric mantle, Geochemica et Cosmochemica Acta 70, 1188-1214.

Bedard, J.H., Harris, L.B., and Thurston, P.C., 2013. The hunting of the Snark, Precambrian Research 229, 20-48.

Bird, J.M., and Dewey, J.F., 1970. Lithosphere plate-continental margin tectonics and the evolution of the Appalachian orogeny, Geological Society of America Bulletin, 81, 1031-1060.

Bleeker, W., 2003. The late Archean record: a puzzle in ca. 35 pieces, *Lithos* 71.2, 99-134.

Bosworth, W., and Kidd, W.S.F., 1985. Thrusts, melanges, folded thrusts, and duplexes in the Taconic Foreland. pp. 117-146 in Lindemann, R.H., (editor) Field Trip Guidebook, 57th Annual Meeting, New York State Geological Association, 27-29 September 1985, Skidmore College, Saratoga Springs, NY.

Bradley, D.C., 1983. Tectonics of the Acadian orogeny in New England and adjacent Canada, Journal of Geology 91, 381-400.

Bradley, D. C., and T. M. Kusky, 1986. Geologic methods of estimating convergence rates during arc-continent collision; Journal of Geology, 94, pp. 667-681

Bradley, D.C., Kusky, T.M., Haeussler, P., Rowley, D.C., Goldfarb, R., and Nelson, S., 2003,Geologic signature of early ridge subduction in the accretionary wedge, forearc basin, and magmatic arc of south-central Alaska, *in* Sisson, V.B., Roeske, S., and Pavlis, T.L. (eds.), Geology of a Transpressional Orogen Developed During a Ridge - Trench Interaction Along the North Pacific Margin, Geological Society of America Special Paper 371, pp. 19-50.

Burchfiel, B.C., Chen, Z.L., Liu, Y.P., Royden, L. 1995. Tectonics of the Longmenshan and adjacent regions, Central China, International Geology Review, 37, 661-735.

Burke K, Dewey J F, Kidd W S F. 1976, Dominance of horizontal movements, arc and microcontinental collisions during the later permobile regime, in: The Early History of the Earth, B.F. Windley (ed.) The early history of the Earth, Wiley, 113: 129.

Burke, K., Dewey, J.F., and Kidd, W.S.F., 1977, World distribution of sutures- the sites of former oceanics, Tectonophysics 40, 69-99.

Cagnard, F., Durrieu, N., Gapais, D., Brun, J.-P., Ehlers, C., 2006. Crustal thickening and lateral flow during compression of hot lithospheres, with particular reference to Precambrian times. Terra Nova 18, 72-78.

Card, K.D., 1990. A review of the Superior Province of the Canadian Shield, a product of Archean accretion, Precambrian Research 48, 99-156.

Casey, J.F., and Dewey, J.F., 1984. Initiation of subduction zones along transform and accreting plate boundaries, triple junction evolution, and fore-arc spreading centres-implications for ophiolitic geology and obduction, Geological Society of London Special Publications 13, 269-290.

Castonguay, S., Kim, J., Thompson, P.J., Gale, M.H., Joyce, N., Laird, J., and Doolan, B.L., 2012. Timing of tectono-metamorphism across the Green Mountain anticlinorium, northern Vermont Appalachians: $^{40}Ar/^{39}Ar$ data and correlations with southern Quebec Geological Society of America Bulletin, v. 124, no. 3-4, p. 352-367

Chen, L., 2007. Geochronology and Geochemistry of the Guyang Greenstone Belt. Post-Doctorate Report. Institute of Geology and Geophysics, Chinese Academy of Sciences, Beijing, pp. 1–40 (in Chinese).

Cheng, Y.Q., Wan, Y.S., Gao, J.F., Ma, R., 2001. Petrographic characteristics of three anatectically transformed metamorphic rock types of the Fuping Group- Complex of the Xiaojue Region, Pingshan, Hebei. Geol. Rev. 47, 1–8 (in Chinese with English abstract).

Choukroune, P., Bouhallier, H., Arndt, N.T., 1995. Soft lithosphere during periods of Archaean crustal growth or crustal reworking. In: Coward, M.P., Ries, A. (Eds.), Early Precambrian Processes, 95. Geol. Soc. London Spec. Publ., pp. 67-86.

Chung, S.L., Liu, D.Y., Ji, J.Q., Chu, M.F., Lee, H.Y., Wen, D.J., Lo, C.H., Lee, T.Y., Qian, Q., and Zhang, Q., 2003. Adakites from continental collision zones: Melting of thickened lower crust in southern Tibet, Geology 31, 1021-1024.

Clark, M.K., and Royden, L.H., 2000. Topographic ooze: Building the eastern margin of Tibet by lower crustal flow, Geology 28, 703-706.

Clift, P.D., Schouten, H., and Draut, A.E., 2003. A general model of arc-continent collision and subduction polarity reversal from Taiwan and the Irish Caledonides. Geological Society of London, Special Publication, 219: 81-98.

Collet, L.W., 1927. The structure of the Alps, 2nd edition (1935) published by E. Arnold, London, 304 pp.

Collins, A.S., Razakamanana, T., Windley, B.F., 2000. Neoproterozoic crustal-scale extensional detachment in Central Madagascar: implications for extensional collapse of the East African Orogen. Geology Magazine 137, 39–51.

Condie, K.C., Boryta, M.D., Liu, J.Z., Qian, X.L., 1992. The origin of khondalites geochemical evidence from the Archean to early Proterozoic granulite belt in the North China Craton. Precambrian Research 59, 207–223.

Cooper, P.A., Taylor, B., 1987. Seismotectonics of New-Guinea: A model for arc reversal following arc-continent collision. Tectonics 6, 53-67.

Debaille, V., O'Neill, C., Brandon, A.D., Haenecour, P., Yin, Q.Z., Matielli, N., and Treiman, A.H., 2013. Stagnant-lid tectonics on early Earth revealed by 142^{Nd} variations in late Archean rocks, Earth and Planetary Science Letters 373, 83-92.

Deng, H., Kusky, T.M., Polat, A., Wang, L., Wang, J.P., and Wang, S.J., 2013. Geochemistry of Neoarchean mafic volcanic rocks and late mafic dikes/sills in the Zanhuang Complex, Central Orogenic Belt, North China Craton: Implications for Geodynamic Setting, Lithos, 175-176, p. 193-212.

Deng, H., Kusky, T.M., Polat, A., Wang, J.P., Wang, L., Fu, J.M., Wang, Z.S., and Yuan, Y, 2014. Geochronology, mantle source composition and geodynamic constraints on the origin of Neoarchean mafic dikes in the Zanhuang Complex, Central Orogenic Belt, North China Craton, Lithos 205, 350-378.

Deng, H., Kusky, T., Polat, A., Wang, L., Li, Yunxiu, Wang, J.P, 2016. A 2.5 Ga fore-arc subduction-accretion complex in the Dengfeng Granite-Greenstone Belt, Southern North China Craton. Precambrian Research, 275, 241-264.

De Souza, S., Tremblay, A., and Ruffet, G., 2014, Taconian orogenesis, sedimentation and magmatism in the southern Quebec-northern Vermont Appalachians: Stratigraphic and detrital mineral record of Iapetan suturing, American Journal of Science 314, p. 1065-1103.

Dewey, J.F., 1969. Evolution of the Appalachian/Caledonian orogen. Nature, 222: 124-129.

Dewey, J.F., 1977, Suture zone complexities: A review, Tectonophysics. 40, 53-67.

Dewey, J.F., 2005, Orogeny can be very short, Proceedings of the National Academy of Sciences 102, 15286–15293.

Dewey, J.F., 2007, The secular evolution of plate tectonics and the continental crust: An outline, in Hatcher, R.D., Carlson, M.P., McBride, J.H., and Martinez Catalan, J., 4-D Framework of Continental Crust, Memoir of the Geological Society of America, v. 200, p. 1-7.

Dewey, J.F., Bird, J.M., 1970. Mountain belts and the new global tectonics. Journal of Geophysical Research 75, 2625-2647.

Dewey, J.F., and Burke, K.C., 1973, Tibetan, Variscan, and Precambrian basement reactivation: Products of continental collision, The Journal of Geology 81, 683-692.

Dewey, J.F., and Lamb, S.H., 1992, Active tectonics of the Andes, Tectonophysics 205, 79-95.

Dewey, J.F., Pitman, W.C., Ryans, W.B., and Bonnin, J., 1973, Plate tectonics and the evolution of the Alpine system, Geological Society of America Bulletin, 84, 3137-3180.

Ding, L., Kapp, P., and Wan, X.Q., 2005, Paleocene-Eocene record of ophiolite obduction and initial India-Asia collision, south-central Tibet, Tectonics 24, TC3001, doi:10.1029/2004TC001729.

Diwu, C.R., Sun, Y., Guo, H.L., and Liu, X.M., 2011, Crustal growth in the North China Craton at ~ 2.5 Ga: Evidence from in situ zircon U-Pb ages, Hf isotopes and whole-rock geochemistry of the Dengfeng Complex, Gondwana Research 20, 149-170.

Diwu, C.R., Sun, Y., Wilde, S.A., Wang, H.L., Dong, Z.C., Zhang, H., and Wang, Q., 2013, New evidence for ~ 4.45 Ga terrestrial crust from zircon xenocrysts in Ordovician ignimbrite in the North Qingling Orogenic Belt, China, Gondwana Research 23, 1484-1490.

Diwu, C.R., Sun, Y., Dong, Z.C., Chen, D.L., Chen, L., Zhang, H., 2010. In situ U–Pb geochronology of Hadean zircon xenocryst (4.1 3.9 Ga) from the western of the Northern Qinling orogenic belt. Acta Petrologica Sinica 26, 1171–1174 (in Chinese with English abstract).

Doglioni, C., Carminati, E., Cuffaro, M., and Srocca, D., 2007, Subduction kinematics and dynamic constraints, Earth Science Reviews 83, 125-175. doi.org/10.1016/j.earscirev.2007.04.001

Dong, C.Y., Wan, Y.S., Xu, Z.Y., Liu, D.Y., Yang, Z.S., Ma, M.Z., Xie, H.Q., 2011. Kondalites of the late Paleoproterozoic in the Daqingshan area, North China Craton: SHRIMPzircon U–Pb dating. Science China-Earth Sciences 54, 1034–1042.

Dong, C. Y., Wan, Y. S., Xu, Z. Y., Liu, D. Y., Yang, Z. S., Ma, M. Z., and Xie, H. Q., 2013, SHRIMP zircon U-Pb dating of Late Paleoproterozoic kondalites in the Daqing Mountains area, North China Craton, Science China Earth Sciences, v. 56, 115-125.

Dong, C. Y., Wan, Y. S., Wilde, S. A., Xu, Z. Y., Ma, M. Z., Xie, H. Q., and Liu, D. Y., 2013, Earliest Paleoproterozoic supracrustal rocks in the North China Craton recognized from the

Daqingshan area of the Khondalite Belt: Constraints on craton evolution: Gondwana Research 25, 1535-1553.

Dong, X.J., Xu, Z.Y., Liu, Z.H., Sha, Q., 2012. Zircon U–Pb geochronology of Archean high grade metamorphic from Xi Ulanbulang area, central Inner Mongolia. Science in China Series D: Earth Sciences 55, 204–212.

Draper, G., Gutiérrez, G., Lewis, J.F., 1996. Thrust emplacement of the Hispaniola peridotite belt: Orogenic expression of the mid-Cretaceous Caribbean arc polarity reversal? Geology 24, 1143-1146.

Du, L.-L., Yang, C.-H., Guo, J.-H., Wang, W., Ren, L.-D., Wan, Y.-S., Geng, Y.-S., 2010. The age of the base of the Paleoproterozoic Hutuo Group in the Wutai Mountains area, North China Craton: SHRIMP zircon U–Pb dating of basaltic andesite. Chinese Science Bulletin 55, 1782–1789.

Du, L.-L., Yang, C.H., Wang, W., Ren, L.-D., Wan, Y.-S., Song, H.-X., Geng, Y.-S., Hou, K.-J., 2011. The re-examination of the age and stratigraphic subdivision of the Hutuo Group in the Wutai Mountains area, North China Craton: evidences from geologyand zircon U–Pb geochronology. Acta Petrologica Sinica 27, 1037–1055.

England, P., and D. McKenzie, 1982, A thin viscous sheet model for continental deformation, Geophys. J. R. Astron. Soc., 70, 295–321.

Faure, M., Trap, P., Lin, W., Monie, P., Bruguier, O., 2007. Polyorogenic evolution of the Paleoproterozoic Trans-North China Belt, new insights from the Lüliangshan–Hengshan–Wutaishan and Fuping massifs. Episodes 30, 1–12.

Festa, A., Dilek, Y., Pini, G.A., Codegone, G., Ogata, K., 2012. Mechanisms and processes ofstratal disruption and mixing in the development of mélanges and broken formations:redefining and classifying mélanges. Tectonophysics 568–569, 7–24.

Fujisaki, W., Asanuma, H., Sauzuki, K., Sawaki, Y., Sakata, S., Hirata, T., Maruyama, S., Windley, B.F., 2015. Ordovician ocean plate stratigraphy and thrust duplexes of the Ballantrae Complex, SW Scotland: implications for the pelagic deposition rate and forearc accretion in the closing Iapetus Ocean. Tectonophysics 662, 312-327.

Galliard, F., Scaillet, B., and Pichavant, M., 2004, Evidence for present-day leucogranite pluton growth in Tibet, Geology 32, 801-804, doi: 10.1130/G20577.1

Gapais, D., Cagnard, F., Gueydan, F., Barbey P., Ballèvre, M., 2009. Mountain building and exhumation processes through time: inferences from nature and models. Terra Nova, 21, 188-194.

Geng, Y.-S., Wan, Y.-S., Shen, Q.-H., Li, H.-M., Zhang, R.-X., 2000. Chronological framework of the Early Precambrian important events in the Lvliang area, Shanxi province. Acta Geologica Sinica 74, 216–223 (in Chinese with English Abstract).

Geng, Y.S., Liu, F.L., Yang, C.H., 2006. Magmatic event at the end of the Archean in eastern Hebei Province and its geological implication. Acta Geologica Sinica (EnglishEdition) 80, 819–833.

Geng, Y.S., Shen, Q.H., Ren, L.D., 2010. Late Neoarchean to Early Paleoproterozoic magmatic events and tectonothermal systems in the North China Craton. Acta Petrologica Sinica 26, 1945–1966.

Geng, Y.S., Du, D.L., Ren, L.D., 2012. Growth and reworking of the early Precambrian continental crust in the North China Craton: constraints from zircon Hf isotopes. Gondwana Research. http://dx.doi.org/10.1016/j.gr.2011.07.006.

Geological Survey of Western Australia, 1990, Geology and Mineral Resources of Western Australia, Memoir 3, Geological Map of Western Australia (1988), scale 1:2,500,000, Department of Mines, Western Australia.

Gong, J.H., Zhang, J.X., Yu, S.Y., 2011. The origin of Longshoushan Group and asso-ciated rocks in the Southern part of the Alxa Block: constraint from LA-ICP-MSU–Pb zircon dating. Acta Petrologica et Mineralogica 30, 795–818 (In Chinese with English abstract).

Grant, M.L., Wilde, S.A., Wu, F.Y., Yang, J.H., 2009. The application of zircon cathodoluminescence imaging, Th–U–Pb chemistry and U–Pb ages in interpreting discrete magmatic and high-grade metamorphic events in the North China Craton at the Archean/Proterozoic boundary. Chemical Geology 261,155–171.

Griffin, W.L., Zhang, A., O'Reilly, S.Y., Ryan, C.G., 1998. Phanerozoic evolution of thelithosphere beneath the Sino-Korean craton: mantle dynamics and plate interactionsin East Asia. Geodynamics 27, 107–126.

Guo, J. H., Shi, X., Bian, A. G., Xu, R. H., Zhai, M.G. & Li, Y. G. 1999. Pb isotopic compositions of feldspar and U–Pb ages of zircons from early Proterozoic granites in the Sanggan area, North China Craton: metamorphism, crustal melting, and tectonothermal events. Acta Petrological Sinica, 15, 199–207.

Guo, J.H., Chen, Y., Liu, F., 2006. Ultra-high temperature (UHT) metamorphism of sapphirine-bearing granulite with ~1.8 Ga age in Daqingshan, Inner Mongolia. Abstract Volume of 2006 National Symposium of Petrology and Geodynamics. Nanjing University, Nanjing. 215–218 pp.

Guo, S.-S., Li, S.-G., 2009. SHRIMP zircon U–Pb ages for the Paleoproterozoic metamorphic–magmatic events in the southeast margin of the North China Craton. Science in China, Series D: Earth Sciences 52, 1039–1045.

Guo, J.H., Peng, P., Chen, Y., Jiao, S.J., and Windley, B.F., 2012, UHT sapphirine granulite metamorphism at 1.93-1.92 Ga caused by gabbronorite intrusions: Implications for tectonic evolution of the northern margin of the North China Craton, Precambrian Research 222-223, 124-142.

Hamilton, W.B., 2003. An alternative earth. GSA Today 13, 4-12.

Hamilton, W. B., 2007. Earth's first two billion years—the era of internally mobile crust. Geol. Soc. Am. Mem. 200, 233-296.

Harrison, T.M., Copeland, P., Kidd, W.S.F., and Yin, A., 1992, Raising Tibet, Science 255, 1663-1670, DOI: 10.1126/science.255.5052.1663

Harte, B., and Dempster, T.J., 1987, Regional metamorphic zones: tectonic controls, in: Oxburgh, E.R., Yardley, B.W.D., and England, P.C., (eds.), Tectonic Settings of Regional Metamorphism, Phil. Trans. R. Soc. Lond., A 321, 105-127.

Hildebrand, R.S., 2013, Mesozoic Assembly of the North American Cordillera, Geological Society of America Special Paper 495, 178 pp.

Hodges, K., 2000, Tectonics of the Himalaya and southern Tibet from two perspectives, Geological Society of America Bulletin 112, 324-350.

Hoffman, P.F., 1991, Did the breakout of Laurentia turn Gondwanaland inside-out? Science 252, 1409-1412.

Houseman, G., and P. England, (1993, Crustal thickening versus lateral expulsion in the Indian-Asian continental collision, J. Geophys. Res., 98, 12,233–12,249.

Hsu, K., 1991, Exhumation of high-pressure metamorphic rocks, Geology 19, 107-110.

Huang, X.N., Li, Z.H., Kusky, T.M., and Chen, Z., 2004, Microstructures of the Zunhua 2.50 Ga podiform chromite, North China Craton and implications for the deformation and rheology of the Archean oceanic lithospheric mantle, Chapter 10, in Kusky, T.M., Precambrian Ophiolites and Related Rocks, Developments in Precambrian Geology 13, Elsevier, Amsterdam, pp. 321-337.

Hubbard, J., and Shaw, J.W., 2009, Uplift of the Longmen Shan and Tibetan plateau, and the 2008 Wenchuan (M = 7.9) earthquake, Nature 458, 194-197. doi:10.1038/nature07837

Ishwar-Kumar, C., Sajeev, K., Windley, B.F., Kusky, T.M., Feng, P., Ratheesh-Kumar, R.T., Huang, Y., Zhang, Y., Razakamanana, T., Yagi, K., and Itaya, T., 2015, Evolution of high-pressure mafic granulites and pelitic gneisses from NE Madagascar: Tectonic implications, In: Kusky, T.M., and Xiao, W.J., (eds.),“Comparative tectonic and dynamic analysis of cratons, orogens, basins, and metallogeny: A Special Volume to honor the career of Brian F. Windley”,Tectonophysics, v. 662, p. 219-242. doi: 10.1016/j.tecto.2015.07.019.

Jahn, B.M., Zhang, Z.Q., 1984. Archean granulite gneisses from eastern Hebei Province, China: rare earth geochemistry and tectonic implications. Contributions to Mineralogy and Petrology 85, 224–243.

Jahn, B.M., Auvray, Q.H., Shen, Q.H., Liu, D.Y., Zhang, Z.Q., Dong, Y.J., Ye, X.J., Zhang, Q.Z., Cornichet, J., and Mace, J., 1988, Archean crustal evolution in China: The Taishan complex, and evidence for juvenile crustal addition form long-term depleted mantle, Precambrian Research 38, 381-403.

Jahn, B.M., Liu, D.Y., Wan, Y.S., Song, B., Wu, J.S., 2008. Archean crustal evolution of the Jiaodong Peninsula, China, as revealed by zircon SHRIMP geochronology, elemental and Nd-isotope geochemistry. American Journal of Science 308, 232–269.

Jian, P., Kröner, A., Windley, B.F., Zhang, Q., Zhang, W., Zhang, L., 2012. Episodic mantle melting-crustal reworking in the late Neoarchean of the northwestern North China Craton: zircon ages of magmatic and metamorphic rocks from the Yinshan Block. Precambrian Res. 222, 230–254.

Jian, P., Zhang, Q., Liu, D.Y., Jin, W.J., Jia, X.Q., Qian, Q., 2005. SHRIMP datingand geological significance of Late Achaean high-Mg diorite (sanukite) andhornblende–granite at Guyang of Inner Monglia. Acta Petrol. Sin. 21, 151–157(in Chinese with English abstract).

Jiang, C.C., 1987. Precambrian Geology of Eastern Part of Liaoning and Jilin. Liaoning Science and Technology Publishing House, Shenyang.

Jiang, N., Guo, J.H., Zhai, M.G., 2011. Nature and origin of the Wenquan granite: Implications for the provenance of Proterozoic A-type granites in the North China craton. Journal of Asian Earth Sciences 42 (1), 76–82.

Johnston, S.T., 2008, The Cordilleran Ribbon Continentent of North America, Annual Reviews of Earth and Planetary Sciences 36, 495-530.

Kay, S.M., and Rapela, C.W., 1990, Plutonism from Antartica to Alaska, Geological Society of America Special Paper 241, 263 pp.

Kay, S.M., Kay, Kay, R.W., Citron, G.P., 1982, Tectonic controls on tholeiitic and calc-alkaline magmatism in the Aleutian arc, Journal of Geophysical Research 87, 4051-4072.

Kidd, W.S.F., Plesch, A., and Vollmer, F.W., 1995. Lithofacies and Structure of the Taconic Flysch, Melange, and Allochthon, in the New York Capital District. pp. 57-80 in Garver, J.I. and Smith, J.A. (eds), Field Trip Guide for the 67th Annual Meeting of the New York State Geological Association, Union College, Schenectady, N.Y

Kirby, E., Whipple, K.X., Tang, W.Q., and Chen, Z.L., 2003, Distribution of active rock uplift along the eastern margin of the Tibetan Plateau: Inferences from bedrock channel longitudinal profiles, Journal of Geophysical Research 108, 2217,

Kitajima, K., Hirata, T., Maruyama, S., and Yamanashi, T., 2008, U-Pb zircon geochronology using LA-ICP-MS in the North Pole Dome, Pilbara Craton, Western Australia: a new tectonic model for the Archean chert-/greenstone succession. International Geology Review 50, 1-14.

Klemperer, S., 2006, Crustal flow in Tibet: geophysical evidence for the physical state of Tibetan lithosphere, and inferred patterns of active flow, in: Law, R.D., Searle, M.P., and Godin, L., eds.), Channel Flow, ductile Extrusion, and Exhumation in Continental Collision Zones, Geological Society of London 268, 39-70.

Kröner, A., Cui, W.Y., Wang, S.Q., Wang, C.Q., Nemchin, A.A., 1998. Single zircon ages from high-grade rocks of the Jianping Complex, Liaoning Province, NE China. Journal of Asian Earth Science 16, 519–532.

Kröner, A., Hegner, E., Collins, A.S., Windley, B.F., Brewer, T.S., Razakamanana, T., Pidgeon, R.T., 2000. Age and magmatic history of the Antananarivo Block, Central Madagascar, as derived from zircon geochronology and Nd isotopic systematics. American Journal of Science 300, 251–288.

Kröner, A., Wilde, S.A., Li, J.H., Wang, K.Y., 2005a. Age and evolution of a late Archean to Paleoproterozoic upper to lower crustal section in the Wutais-han/Hengshan/Fuping terrain of northern China. J. Asian Earth Sci. 24, 577–595.

Kröner, A., Wilde, S.A., O'Brien, P.J., Li, J.H., Passchier, C.W., Walte, N.P., Liu, D.Y., 2005b. Field relationships, geochemistry, zircon ages and evolution of a late Archaean to Palaeoproterozoic lower crustal section in the Hengshan Terrain of northern China. Acta Geol. Sin. 79, 605–632.

Kröner, A., Wilde, S.A., Zhao, G.C., O'Brien, P.J., Sun, M., Liu, D.Y., Wan, Y.S., Liu, S.W., Guo, J.H., 2006. Zircon geochronology and metamorphic evolution of mafic dykes in the Hengshan Complex of northern China: evidence for late Palaeoprotero-zoic extension and subsequent high-pressure metamorphism in the North China Craton. Precambrian Res. 146, 45–67.

Kusky, T. M., 2011a. Geophysical and geological tests of tectonic models of the North China Craton. Gondwana Research 20, 26-35.

Kusky, T.M., 2011b, Comparison of results of recent seismic profiles with tectonic models of the North China craton. Journal of Earth Science 22(2):250-259.

Kusky, T.M., and Li, J., 2003, Paleoproterozoic tectonic evolution of the North China craton: Journal of Asian Earth Sciences, v. 22, p. 383–397.

Kusky, T.M., and Li, J.H., 2008, Discussion of “U-Pb zircon age constraints on the Dongwanzi ultramafic-mafic body, North China, confirm it is not an Archean ophiolite”, Earth and Planetary Science Letters, 273, 227-230.

Kusky T.M., Li, J.H., 2010, Origin and Emplacement of Archean Ophiolites of the Central Orogenic Belt, North China Craton. Journal of Earth Science 21(5):744-781.

Kusky, T.M., and Mooney, W., 2015, Is the Ordos Basin floored by a trapped oceanic plateau? Earth and Planetary Science Letters, 429, 197-204.

Kusky, T.M., and Santosh, M., 2009, The Columbia Connection in North China, in Reddy, S.M., Mazumder, R., Evans, D., and Collins, A.S., Paleoproterozoic Supercontinents and Global Evolution, Geological Society of London Special Publication 323, 49-71.

Kusky, T.M., Zhai, M.G., 2012, The Neoarchean ophiolite in the North China Craton: Early Precambrian plate tectonics and scientific debate, Journal of Earth Sciences, vol. 23, no. 3, p. 277-284.

Kusky, T.M., Li, Jianghai, and Tucker, R.T., 2001, The Archean Dongwanzi ophiolite complex, North China Craton: 2.505 Billion Year Old Oceanic Crust and Mantle, Science, 292, 1142-1145.

Kusky, T.M., Li, Z.H., Glass, A., and Huang, H., A., 2004, Origin and Emplacement of Archean Ophiolites of the Central Orogenic Belt, North China Craton Chapter 7, in Kusky, T.M., Precambrian Ophiolites and Related Rocks, Developments in Precambrian Geology 13, Elsevier, Amsterdam, pp. 223-274.

Kusky, T.M., Stern, R.J., and Dewey, J.F., (editors), 2013, Secular Changes in Geologic and Tectonic Processes, Special Issue of Gondwana Research, 24, p. 451-547.

Kusky, T.M., Windley, B.F., and Zhai, M.G., 2007a, Tectonic Evolution of the North China Block: from Orogen to Craton to Orogen, in Zhai. M.G., Windley, B.F., Kusky, T.M., and Meng, Q.R., Mesozoic Sub-Continental Lithospheric Thinning Under Eastern Asia, Geological Society of London Special Publication 280, p. 1-34.

Kusky, T., Li, J.H., and Santosh, M., 2007b, The Paleoproterozoic North Hebei Orogen: North China Craton's Collisional Suture with Columbia Supercontinent, In; Zhai, M.G., Xiao, W.J., Kusky, T.M., and Santosh, M., Tectonic Evolution of China and Adjacent Crustal Fragments, Special Issue of Gondwana Research, v. 12, no. 1-2, p. 4-28.

Kusky, T.M., Zhi, X.C., Li, J.H., Xia, Q.X., Raharimahefa, T., and Huang, X.N., 2007c, Chondritic Osmium isotopic composition of Archean ophiolitic mantle. In; Zhai, M.G., Xiao, W.J., Kusky, T.M., and Santosh, M., Tectonic Evolution of China and Adjacent Crustal Fragments, Special Issue of Gondwana Research. V. 12, no. 1-2, p. 67-76.

Kusky, T.M., Lu Wang, Junpeng Wang, Hao Deng, 2012, AGU meeting,San Francisco, USA. A late Archean tectonic mélange belt in the Central Orogenic Belt, North China Craton, Abstracts with Programs.

Kusky, T.M., Li, X.Y., Wang, Z.S., Fu, J.M., Ze, L., and Zhu, P.M., 2013a, Are Wilson Cycles preserved in Archean cratons? A comparison of the North China and Slave cratons, in Polat, A., (editor) 2014, John Tuzo Wilson: a Canadian who revolutionized Earth Sciences, Special Issue of Canadian Journal of Earth Sciences 51, 297-311.

Kusky, T.M., Windley, B.F., Safonova, I., Wakita, K., Wakabashi, J., Polat, A., and Santosh, M., 2013b, Recognition of Ocean plate stratigraphy in accretionary orogens through Earth history: A record of 3.8 billion years of sea floor spreading, subduction, and accretion, GR Focus review paper, in Kusky, T.M., Stern, R.J., and Dewey, J.F., Secular Changes in Geologic and Tectonic Processes, Special Issue of Gondwana Research, v. 42, p. 501-547.

Lebron, M.C., Perfit, M.R., 1993. Stratigraphic and petrochemical data support subduction polarity reversal of the Cretaceous Caribbean island arc. The Journal of Geology 101, 389-396.

Le Fort, P., Cuney, M., Deniel, C., France-Lanord, C., Sheppard, S.M.F., Upreti, B.N., and Vidl, P., 1987, Crustal generation of the Himalayan leucogranites, Tectonophysics 134, 39-57.

Li, J.H., and Kusky, T.M., 2007, A Late Archean foreland fold and thrust belt in the North China Craton: Implications for early collisional tectonics, In; Zhai, M.G., Xiao, W.J., Kusky, T.M., and Santosh, M., Tectonic Evolution of China and Adjacent Crustal Fragments, Special Issue of Gondwana Research, 12, no. 1-2, p. 47-66.

Li, J.H., and Qian, X.L., 1991, A study of Longquanguan shear zone in the northern part of the Taihang Mountain: Shanxi Geology, v. 6, p. 17–29.

Li, J.H., Qian, X.L., Hou, G.T., 2000a. New interpretation of the "Luliang Movement". Earth Science 25 (1), 15–20 (in Chinese with English abstract).

Li, J.H., Kroener, A., Qian, X.L., O'Brien, P., 2000b. The tectonic evolution of early high-pressure granulite belt, North China Craton (NCC). Acta Geological Sinica 247 (2), 246–256.

Li, J.H., Qian, X.L., Huang, X.N., Liu, S.W., 2000c. The tectonic framework of the basement of North China Craton and its implication for the early Precambrian cratonization. Acta Petrologica Sinica 16 (1), 1–10.

Li, J.H., Kusky, T.M., and Huang, X., 2002a, Neoarchean podiform chromitites and harzburgite tectonite in ophiolitic melange, North China Craton, Remnants of Archean oceanic mantle, GSA Today, July, volume 12, number 7, p. 4-11, plus cover.

Li, J.H., Niu, X.L., Chen, Z., Feng, J., and Huang, X.N., 2002b, The discovery of podiform chromite in west Liaoning and its implications for plate tectonics, Acta Petrologica Sinica 18 (2), 187-192 (in Chinese with English abstract).

Li, J.H., Kusky, T.M., Niu, X.L., and Feng, J., 2004, NeoArchean massive sulfide of Wutai Mountain, North China: a black smoker chimney and mound complex within 2.50 Ga-old oceanic crust, Chapter 11, in Kusky, T.M., Precambrian Ophiolites and Related Rocks, Developments in Precambrian Geology 13, Elsevier, Amsterdam, pp. 339-361.

Li, N., Chen, Y.J., McNaughton, N.J., Ling, X.X., Deng, X.H., Yao, J.M., and Wu, Y.S., 2015, Formation and tectonic evolution of the khondalite series at the southern margin of the North China Craton: Geochronological constraints from a 1.85 Ga Mo deposit in the Xiong'ershan area, Precambrian Research 269, 1-17.

Li, Q.L., Chen, F.K., Guo, J.H., Li, X.H., Yang,Y.Hh., and Siebel, W., 2007, Zircon ages and Nd-Hf isotopic composition of the Zhaertai Group (Inner Mongolia): Evidence for early

Proterozoic evolution of the northern North China Craton, Journal of Asian Earth Sciences 30, 573-590.

Li, S.S., Santosh, M., Cen, K., Teng, X.M., and He, X.F., 2015, Neoarchean convergent margin tectonics associated with microblock amalgamation in the North China Craton: Evidence from the Yishui Complex, Gondwana Research, http://dx.doi.org/10.1016/j.gr.2015.11.004

Li, S.Z., Zhao, G.C., Sun, M., Han, Z.Z., Zhao, G.T., Hao, D., 2006. Are the south and north Liaohe Groups of North China craton different exotic terranes? Nd isotope constraints. Gondwana Research 9, 198–208.

Li, S.Z., Zhao, G.C., 2007. SHRIMP U–Pb zircon geochronology of the Liaojigranitoids: constraints on the evolution of the Paleoproterozoic Jiao-Liao-Jibelt in the Eastern Block of the North China Craton. Precambrian Research158, 1–16.

Li, S.Z., Zhao, G.C., Wilde, S.A., Zhang, J., Sun, M., Zhang, G.W., and Dai, L.M., 2010, Deformation history of the Hengshan-Wutai-Fuping Complexes: Implications for the evolution of the Trans-North China Orogen, Gondwana Research 18, 611-631.

Li, S.Z., Zhao, G.C., Santosh, M., Liu, X., and Dai, L.M., 2011, Paleoproterozoic tectonothermal evolution and deep crustal processes in the Jiao-Liao-Ji Belt, North China craton: A review, Geological Journal 46, 525-543, DOI: 10.1002/gj.1282.

Li, S.-Z., Zhao, G.-C., Santosh, M., Liu, X., Dai, L.-M., Suo, Y.-H., Tam, P.-Y., Song, M.-C., Wang, P.-C., 2012. Paleoproterozoic structural evolution of the southern segment of the Jiao–Liao-Ji Belt, North China Craton. Precambrian Research 200–203, 59–73.

Li, T.S., Zhai, M.G., Peng, P., Chen, L., Guo, J.H., 2010b. Ca. 2.5 billion year old coeval ultramafic–mafic and syenitic dykes in Eastern Hebei: implications for cratonization of the North China Craton. Precambrian Research 180, 143–155.

Li, X.-P., Yang, Z. Y., Zhao, G. C., Grapes, G., and Guo, J. H., 2010, Geochronology of khondalite series rocks of the Jining Complex: confirmation of depositional age and tectonometamorphic evolution of the North China Craton: International Geology Review, v. 53, n. 10, p. 1194–1211.

Li, Y.H., Hou, K.J., Wan, D.F., Zhang, Z.J., and Yue, G.L., 2014, Precambrian banded iron formations in the North China Craton: Silicon and oxygen isotopes and genetic implications, Ore Geology Reviews 57, 299-307.

Lim, C., Kidd, W.S.F., and Howe, S., 2005. Late shortening and extensional structures and veins in the western margin of the Taconic Orogen (NY-VT). J. Geol., 113, 419-438

Lin, B.Q., Cui, W.Y., Wang, S.Q., Shen, E.S., 1997. The Archean Geology and Gold Deposits in western Liaoning Province. Seismological Press, Beijing, pp. 1–130 (in Chinese).

Lin, S., Parks, J., Heaman, L.M., Simonetti, A., Corkery, T., 2013. Diapirism and sagduction as a mechanism for deposition and burial of "Timiskaming-type" sedimentary sequences, Superior Provice: Evidence from detrital zircon geochronology and implications for the Borden Lake conglomerate in the exposed middle to lower crust in the Kapuskasing uplift.Precambrian Research, v. 238, p. 148-157.

Liu, C.H., Zhao, G.C., Sun, M., Wu, F.Y., Yang, J.H., Yin, C.Q., Leung, Y.H., 2011a. U Pb and Hf isotopic study of detrital zircons from the Yejishan Group of the Lüliang Complex: constraints on the timing of collision between the Eastern and Western Blocks, North China Craton. Sedimentary Geology 236, 129–140.

Liu, C.H., Zhao, G.C., Sun, M., Zhang, J., Yin, C.Q., Wu, F.Y., Yang, J.H., 2011b. U–Pb and Hf isotopic study of detrital zircons from the Hutuo Group of the Wutai Complex: constraints on the timing of collision between the Eastern and Western Blocks, North China Craton. Gondwana Research 20, 106–121.

Liu, J.-f., Li, J.-y., Qu, J.-f., Hu, Z.-c., Feng, Q.-w.,Guo, C.-l., 2015, Late Paleoproterozoic tectonic setting of the northern margin of the North China Craton: Constraints from the geochronology and geochemistry of the mangerites in the Longhua and Jianping areas, Precambrian Research, http://dx.doi.org/10.1016/j.precamres.2015.10.022

Liu, J.G., Rudnick, R., Walker, R.J., Gao, S., Wu, F.Y., Piccoli, P.M., Yuan, H.L., Xu, W.L., and Xu, Y.G., 2011, Mapping lithospheric boundaries using Os isotopes of mantle xenoliths: an example from the North China Craton, Geochemica et Cosmochimica Acta 75, 3881-3902.

Liu, S. J., Dong, C. Y., Xu, Z. Y., Santosh, M., Ma, M. Z., Xie, H. Q., Liu, D. Y., and Wan, Y. S., 2012, Paleoproterozoic episodic magmatism and high-grade metamorphism in the North China Craton: Evidence from SHRIMP zircon dating of magmatic suites from the Daqingshan area: Geological Journal, http://dx.doi.org/10.1002/gj.2453

Liu, S., Pan, Y., Xie, Q., Zhang, J., and Li, Q., 2004, Archean geodynamics in the central zone, North China craton: Constraints from geochemistry of two contrasting series of granitoids in the Fuping and Wutai Complexes: Precambrian Research, v. 130, p. 229–249, doi: 10.1016/j.precamres.2003.12.001.

Liu, S.W., Liang, H.H., 1997. Metamorphism of Al-rich gneisses from the Fuping Complex, Taihang Mountain, China. Acta Petrologica Sinica 13, 303–312 (in Chinese with English abstract).

Liu, S.-W., Li, Q.-G., Liu, C.-H., Lü, Y.-J., Zhang, F., 2009b. Guandishan granitoids of the Paleoproterozoic Luliang metamorphic complex in the Trans-North China Orogen: SHRIMP zircon ages, petrogenesis and tectonic implications. Acta Geologica Sinica — English Edition 83 (3), 580–602.

Liu, S.W., Santosh, M., Wang, W., Bai, X., Yang, P.T., 2011a. Zircon U–Pb chronology of the Jianping Complex: implications for the Precambrian crustal evolution history of the northern margin of North China Craton. Gondwana Research 20, 48–63.

Lu, S.N., Zhao, G.C., Wang, H.C., Hao, G., 2008b. Precambrian metamorphic basementand sedimentary cover of the North China Craton: A review. PrecambrianResearch 160, 77–93.

Liu, S.-W., Zhang, J., Li, Q.-G., Zhang, L.-F., Wang, W., Yang, P.-T., 2012. Geochemistry and U–Pb zircon ages of metamorphic volcanic rocks of the Paleoproterozoic Lvliang Complex and constraints on the evolution of the Trans-North China Orogen, North China Craton. Precambrian Research. http://dx.doi.org/10.1016/j.precamres.2011.07.006.

Luo, Y., Sun, M., Zhao, G.C., Li, S.Z., Xu, P., Ye, K., Xia, X.P.,2004. LA-ICP-MS U–Pb zircon ages of the Liaohe Group in theEastern Block of the North China Craton: constraints on the evolutionof the Jiao-Liao-Ji Orogen. Precambrian Res. 134, 349–371.

Lu, X.-P., Wu, F.-Y., Lin, J.-Q., Sun, D.-Y., Zhang, Y.-B., Guo, C.-L., 2004a. Geochronological successions of the Early Precambrian granitic magmatism in southern Liaoning Peninsula and its constraints on tectonic evolution of the North China Craton. Chinese Journal of Geology (Scientia Geologica Sinica) 39, 123–139 (in Chinese with English abstract).

Lu, X.-P., Wu, F.-Y., Zhang, Y.-B., Zhao, C.-B., Guo, C.-L., 2004b. Emplacement age and tectonic setting of the Paleoproterozoic Liaoji granites in Tonghua area, southern Jilin Province. Acta Petrologica Sinica 20, 381–392 (in Chinese with English abstract).

Lu, X.-P., Wu, F.-Y., Guo, J.-H., Wilde, S.A., Yang, J.-H., Liu, X.-M., Zhang, X.-O., 2006. Zircon U–Pb geochronological constraints on the Paleoproterozoic crustal evolution of the Eastern Block in the North China Craton. Precambrian Research 146, 138–164.

Lv, B., Zhai, M.G., Li, T.S., and Peng, P., 2012, Zircon U-Pb ages and geochemistry of the Qinglong volcano-sedimentary rock series in Eastern Hebei: Implications for ~2500 Ma intra-continental rifting in the North China Cratons, Precambrian Research 208-211, 145-160.

Ma, M. Z., Wan, Y. S., Xu, Z. Y., Liu, S. J., Xie, H. Q., Dong, C. Y., and Liu, D. Y., 2012a, Late Paleoproterozoic K-feldspar pegmatite vein in the Daqingshan area, North China Craton: SHRIMP age and Hf composition of zircons: Geological Bulletin of China, v. 31, p. 825–833 (in Chinese with English abstract).

Ma, M. Z., Wan, Y. S., Santosh, M., Xu, Z. Y., Xie, H. Q., Dong, C. Y., and Liu, D. Y., 2012b, Decoding multiple tectonothermal events in zircons from single rock samples: SHRIMP zircon U-Pb data from the late Neoarchean rocks of Daqingshan, North China Craton: Gondwana Research, v. 22, n. 3–4, p. 810–827.

Ma, M.Z., Xu, Z.Y., Zhang, L.C., Dong, C.Y., Dong, X.J., Liu, S.J., Liu, D.Y., Wan, Y.S., 2013. SHRIMP dating and Hf isotope analysis of zircons from the Early Precambrian basement in the Xi Ulanbulang area, Wuchuan, Inner Mongolia. Acta Petrologica Sinica 29, 501–516.

Ma, X., Fan, H.-R., Santosh, M., Guo, J., 2015. Petrology andgeochemistry of the Guyang hornblendite complex in the Yinshan block, North ChinaCraton: Implications for the melting of subduction-modified mantle, PrecambrianResearch(in press), http://dx.doi.org/10.1016/j.precamres.2015.12.001.

Ma, X., Guo, J., Liu, F., Qian, Q., Fan, H., 2013a. Zircon U–Pb ages, trace elements andNd–Hf isotopic geochemistry of Guyang sanukitoids and related rocks: Implica-tions for the Archean crustal evolution of the Yinshan Block, North China Craton.Precambrian Res. 230, 61–78.

Ma, X., Fan, H., Santosh, M., Guo, J., 2013b. Geochemistry and zircon U–Pb chronology of charnockites in the Yinshan Block, North China Craton: tectonic evolution involving Neoarchaean ridge subduction. Int. Geol. Rev. 55, 1688–1704.

Martin, H., Moyen, J-F., Rapp, R. 2010. The sanukitoid series: magmatism at the Archean-Proterozoic transition. Transactions of Royal Society of Edinburgh: Earth and Environmental Science, 100, 15-33.

Menzies, M., Fan, W.-M. and Zhang, M. 1993. Paleozoicand Cenozoic lithoprobes and loss of 120 kmof Archaean lithosphere, Sino-Korean craton, China.In: Prichard, H. M., Alabaser, T., Harris,N. B. W. & Neary, C. R. (eds) Magmatic Processesand Plate Tectonics. Geological Society, London,Special Publications, 76, 71–81.

Molnar, P. (1988), Continental tectonics in the aftermath of plate tectonics, Nature, 335, 131–137.

Molnar, P., and P. Tapponnier (1975), Cenozoic tectonics of Asia: Effects of a continental collision, Science, 189(4201), 419–426.

Nelson, K.D., Zhao, W.J., Brown, L.D., Kuo, J., Che, J.K., Liu, X.W., Klemperer, S.L., Makovsky, Y., Meissner, R., Mechie, J., Kind, R., Wenzel, F., Ni, J., Nabelek, J., Leshou, C.,Tan, H.D., Wei, W.B., Jones, A.G., Booker, J., Unsworth, M., Kidd, W.S.F., Hauck, M., Alsdorf, D., Ross, A., Cogan, M., Wu, C.D., Sandvol, E., and Edward, M., 1996, Partially Molten middle crust beneath southern Tibet: Synthesis of project INDEPTH results, Science 274, 1684-1688. DOI: 10.1126/science.274.5293.1684

Nutman, A.P., Friend, C.R.L., 2007. Adjacent terranes with ca. 2715 and 2650 Ma high-pressure metamorphic assemblages in the Nuuk region of the North Atlantic Craton, southern West Greenland: Complexities of Neoarchaean collisional orogeny. Precambrian Research 155, 159–203.

Nutman, A.P., Wan, Y.S., Du, L.L., Friend, C.R.L., Dong, C.Y., Xie, H.Q., Wang, W., Sun, H.Y., and Liu, D.Y., 2011, Multistage late Neoarchean crustal evolution of the North China Craton, eastern Hebei, Precambrian Research 189, 43-65.

Ohta, H., Maruyama, S., Takahashi, E., Watanabe, Y., and Kato, Y., 1996, Field occurrence, geochemistry and petrogenesis of the Archean Mid-Oceanic Ridge Basalts (AMORBs) of the Clearville area, Pilbara Craton, Western Australia, Lithos 37, 199-221.

O'Brien, P.J., Walte, N., Li, J.H., 2005. The petrology of two distinct granulite types in the Hengshan Mts, China, and tectonic implications. J. Asian Earth Sci. 24, 615–627.

Pearce, J.A., Harris, N.B.W., and Tindle, A.G., 1984, Trace element discrimination diagrams for the tectonic interpretation of granitic rocks, Journal of Petrology 25, 956-983.

Peng, C., Xue, L.F., Zhu, M., Chai, Y., Liu, W.Y., 2015, The location and evolution of the tectonic boundary between the Paleoproterozoic Jiao-Liao-Ji Belt and the Longgang Block, northeast China, PrecambrianResearch, http://dx.doi.org/10.1016/j.precamres.2015.10.016

Peng, P., Guo, J.-H., Zhai, M.-G., Bleeker, W., 2010. Paleoproterozoic gabbronoritic and granitic magmatism in the northern margin of the North China Craton: evidence of crust–mantle interaction. Precambrian Research 183, 635–659.

Peng, P., Guo, J.H., Windley, B.F., and Li, X.H., 2011, Halaqin volcano-sedimentary succession in the central-northern margin of the North China Craton: Products of Late Paleoproterozoic ridge subduction, Precambrian Research 187, 165-180.

Peng, P., Guo, J., Windley, B.F., Liu, F., Chu, Z., Zhai, M., 2012a. Petrogenesis of Late Paleoproterozoic Liangcheng charnockites and S-type granites in the central northern margin of the North China Craton: implications for ridge subduction. Precambrian Research 222-223, 107-123, http://dx.doi.org/10.1016/j.precamres.2011.06.002.

Peng, P., Guo, J.H., ZHai, M.G., Windley, B.F., Li, T.S., and Liu, F., 2012b, Genesis of the Hengling magmatic belt in the North China Crton: Implications for Paleoproterozoic tectonics, Lithos 148, 27-44.

Peng, P., Wang, X.P., Lai, Y., Wang, C., Windley, B.F., 2015b. Large-scale liquid immiscibility and fractional crystallization in the 1780 Ma Taihang dyke swarm: implications for genesis of the bimodal Xiong'er volcanic province. Lithos 236-237, 106-122.

Peng, P., Wang, X.P., Windley, B.F., Guo, J.H., Zhai, M.G., and Li, Y., 2014, Spatial distribution of ~ 1950-1800 Ma metamorphic events in the North China Craton: Implications for tectonic subdivision of the craton, Lithos 202-203, p. 250-266.

Peng, P., Wang, C., Wang, X.P., and Yang, S.Y., 2015, Qingyuan high-grade granite-greenstone terrain in the Eastern North China Craton: Root of a Neoarchean arc, Tectonophysics 662, 7-21.

Percival, J., Sanborn-Barrie, M., Skulski, T., Stott, G.M., Helmstaedt, H., and White, D.J., 2006, Tectonic evolution of the western Superior Province from NATMAP and Lithoprobe studies, Canadian Journal of Earth Sciences 43, 1085-1117.

Percival, J.A., Skulski, T., Sanborn-Barrie, M., Stott, G.M., Leclair, A.D., Corkery, M.T., Boily, M., 2012. Geology and Tectonic Evolution of the Superior Province, Canada in: Percival, J.A., Cook, F.A., Clowes, R.M., (Eds.), Tectonic Styles in Canada: The LITHOPROBE Perspective. Geological Association of Canada Special Paper 49, pp. 321–378.

Pidgeon, R.T., 1980. Isotopic ages of the zircons from the Archean granulite facies rocks,Eastern Hebei, China. Geological Review 26, 198–207.

Polat, A., Kusky, T.M., Li, J.H., Fryer, B., Kerrich, R., and Patrick, K., 2005, Geochemistry of the Neoarchean (ca. 2.55-2.50 Ga) volcanic and ophiolitic rocks in the Wutaishan greenstone belt, central orogenic belt, North China craton: implications for geodynamic setting and continental growth, Geol. Soc. Amer. Bull. 117, 1387-1399.

Polat, A., Herzberg, C., Munker, C., Rodgers, R., Kusky, T., Li, J.H., Fryer, B., and Delany, J., 2006, Geochemical and petrological evidence for a suprasubduction zone origin of Neoarchean (ca. 2.5 Ga) peridotites, central orogenic belt, North China craton, Bulletin of the Geological Society of America, v. 118, no. 7, p. 771-784.

Polat, A., (editor) 2014, John Tuzo Wilson: a Canadian who revolutionized Earth Sciences, Special Issue of Canadian Journal of Earth Sciences 51, v-viii, 10.1139/cjes-2014-0007

Pubellier, M., Bader, A.G., Rangin, C., Deffontaines, B., Quebral, R., 1999, Upper plate deformation induced by subduction of a volcanic arc: the Snellius Plateau (Molucca Sea, Indonesia and Mindanao, Philippines). Tectonophysics 304, 345-368.

Qi, H.L., Hao, X.H., Zhang, X.D., Nie, W.D., 1999. The geological features of granite–greenstone belts in Qinglong area, Eastern Hebei. Progress in Precambrian Research 22 (4), 1–17.

Qian, X.L., Li, J.H., 1999. Discovery of Neoarchean unconformity and its implication for continental cratonization of North China craton. Science in China 42 (4), 399–407.

Raharimahefa, T., and Kusky, T.M., 2006, Structural and remote sensing studies of the Southern Betsisimarka suture, Madagascar, Gondwana Research, Volume 10, Issues 1-2, August 2006, Pages 186-19710.1016/j.gr.2005.11.022

Raharimahefa, T., and Kusky, T.M., 2009, Structural and remote sensing analysis of the Betsisimarka suture in northeastern Madagascar, Gondwana Research, Volume 15, Issue 1, February 2009, Pages 14-27

Rämö, O.T., Haapala, I., Vaasjoki, M., Yu, J.H., Fu, H.Q., 1995. 1700 Ma Shachang complex, northeast China: Proterozoic rapakivi granite not associated with Paleoproterozoic orogenic crust. Geology 23 (9): 815–818.

Ramos, V.A., and Folguera, A., 2011, Payenia volcanic province in Southern Andes: an appraisal of an exceptional Quaternary tectonic setting, Journal of Volcanology and Geothermal Research, 201, 53–64.

Ramos, V.A., and Kay, S.M., 2006, Overview of the tectonic evolution of the southern Central Andes of Mendoza and Neuquén (35°–39°S latitude), in: V.A. Ramos (Eds.), Evolution of an Andean Margin: A Tectonic and Magmatic View from the Andes to the Neuquén Basin (35°–39°S Latitude), Geological Society of America, 1–18.

Ramos, V., Litvak, V.D., Folguera, A., and Spangnuoldo, M., 2014, An Andean tectonic cycle: From crustal thickening to extension in a thin crust (34-37 SL), Geoscience Frontiers 5, 351-367.

Reed, D.L., Meyer, A.W., Silver, E.A., and Prasetyo, H., 1987, Contourite sedimentation in an intracoeanic forearc system: Eastern Sunda Arc, Indonesia, Marine Geology 76, 223-241.

Rey, P., Houseman, G., 2006. Lithospheric scale gravitational flow: the impact of body forces on orogenic processes from Archaean to Phanerozoic. In: Buiter, S.J.H., Schreurs, G. (Eds.), Analogue and Numerical Modeling of Crustal-Scale Processes, Geol. Soc. Spec. Publ., vol. 253, pp. 153–167.

Rey, P.F., Philippot, P., Thébaud, N., 2003. Contribution of mantle plumes, crustal thickening and greenstone blanketing to the 2.75-2.65 Ga global crisis. Precambrian Res. 127, 43-60.

Rogers, W.B., Isachsen, Y.W., Mock, T.D., and Nyahay, R.E., 1999, Overview of New York Geology, New York State Museum, Educational Leaflet 33.

Rowley, D.B., 1982, A new method for estimating displacements of large thrust faults affecting Atlantic-type shelf sequences: with an application to the Champlain Thrust, Vermont. Tectonics, v. 1, p. 369-388.

Rowley, D. B. , 1996, Age of initiation of collision between India and Asia: A review of stratigraphic data, Earth Planet. Sci. Lett., 145, 1–13.

Rowley, D.B., and W.S.F. Kidd, 1981, Stratigraphic relationships and detrital composition of the medial Ordovician flysch of western New England: implications for the tectonic evolution of the Taconic Orogeny. Journal of Geology, v. 89, p.199-218.

Royden, L.H., Burchfiel, B.C., King, R. W., Wang, E., Chen, Z.L., Shen, F., and Liu, Y.P., 1997, Surface deformation and lower crustal flow in eastern Tibet, Science 276, 788-790.

Rutherford, E., Burke, K., and Lytwyn, J., 2001, Tectonic history of Sumba Island, Indonesia, since the Late Cretaceous and its rapid escape into the forearc in the Miocene, Journal of Asian Earth Sciences 19, 453-479.

Santosh, M., 2010. Assembling North China Craton within the Columbia supercontinent: the role of double-sided subduction. Precambrian Research 178, 149–167.

Santosh, M., Kusky, T., 2010. Origin of paired high pressure–ultrahigh-temperature orogens: a ridge subduction and slab window model. Terra Nova 22, 35–42.

Santosh, M., Maruyama, S., and Yamamoto, S., 2009, "The making and breaking of supercontinents: some speculations based on superplumes, super downwelling and the role of tectosphere." Gondwana Research 15.3, 324-341.

Santosh, M., Sajeev, K., Li, J.H., 2006. Extreme crustal metamorphism during Columbia supercontinent assembly: evidence from North China Craton. Gondwana Research 10, 256–266.

Santosh, M., Teng, X.M., He, X.F., Tang, L., and Yang, Q.Y., 2015, Discovery of Neoarchean suprasubduction zone ophiolite suite from Yishui Complex in the North China Craton, *Gondwana Research* (2015), doi: 10.1016/j.gr.2015.10.017

Santosh, M., Tsunogaeb, T., Li, J.H., Liu, S.J., 2007a. Discovery of sapphirine-bearing Mg–Al granulites in the North China Craton: implications for Paleoproterozoic ultrahigh temperature metamorphism. Gondwana Research 11, 263–285.

Santosh, M., Wilde, S. A., and Li, J. H., 2007b, Timing of Palaeoproterozoic ultrahigh-temperature metamorphism in the North China Craton: evidence from SHRIMP U–Pb zircon geochronology: Precambrian Research, v. 159, n. 3–4, p. 178–196,

Santosh, M., Wan, Y. S., Liu, D. Y., Dong, C. Y., and Li, J. H., 2009, Anatomy of zircons from an ultrahot orogen: the amalgamation of the North China Craton within the Columbia supercontinent: Journal of Geology, v. 117, n. 4, p. 429–443,

Sengör, A.M.C., and Natal'in, B., 2004,, Ribbon continents: A marginal affair of central importance, Geological Society of America, Abstracts with Programs 36, p. 534.

Şengör, A.M.C., Natal'in, B. A., 2004. Phanerozoic analogues of Archaean oceanic basement fragments: Altaid ophiolites and ophirags. In: Kusky T.M. (Ed.), Precambrian Ophiolites and Related Rocks, Developments in Precambrian Geology, Vol. 13 (K.C. Condie, Series Editor), Elsevier B.V., Amsterdam, pp. 675-726.

Şengör, A.M.C., Natal'in, B.A., Sunal, G., van der Voo, R., 2014. A new look at the Altaids: A superorogenic complex in Northern and Central Asia as a factory of continental crust. Part I: Geological data compilation (exclusive of palaeomagnetic observations). Austrian Journal of Earth Sciences 107, 169–232.

Shi, Y.R., Wilde, S.A., Zhao, X.T., Ma, Y.S., Du, L.L., and Liu, D.Y., 2012, Late Neoarchean magmatic and subsequent metamorphic events in the northern North China Craton: SHRIMP zircon dating and Hf isotopes of Archean rocks from Yunmengshan Geopark, Miyun, Beijing, Gondwana Research 21, 785-800.

Stern, R.J., 2004. Subduction initiation: spontaneous and induced. Earth and Planetary Science Letters, 226: 275-292.

Tapponnier, P., and P. Molnar (1976), Slip-line field theory and large-scale continental tectonics, Nature, 264, 319–324.

Tian, Y.Q., 1991. Geology and Gold Mineralization of Wutai–Hengshan Greenstone Belt. Shanxi Science and Technology Press, Taiyuan, pp. 1–25 (in Chinese).

Trap, P., Faure, M., Lin, W., Monié, P., 2007. Late Paleoproterozoic (1900–1800 Ma) nappe-stacking and polyphase deformation in the Hengshan–Wutaishan area: implications for the understanding of the Trans-North-China Belt, North China Craton. Precambrian Res. 156, 85–106.

Trap, P., Faure, M., Lin, W., Bruguier, O., Monié, P., 2008. Contrasted tectonic styles for the Paleoproterozoic evolution of the North China Craton. Evidence for a ∼2.1 Ga thermal and tectonic event in the Fuping Massif. J. Struct. Geol. 30, 1109–1125.

Trap, P., Faure, M., Lin, W.,Monié, P., Meffre, S., Melleton, J., 2009a. The Zanhuang Massif, the second and eastern suture zone of the Paleoproterozoic Trans-North China Orogen. Precambrian Research 172, 80-98.

Trap, P., Faure, M., Lin, W., Monié, P., Meffre, S., 2009b. The Lüliang Massif: a key area for the understanding of the Palaeoproterozoic. In: Evans, D., Reddy, S., Collins, A. (Eds.), Palaeoproterozoic Supercontinents and Global Evolution. Geol. Soc. London Spec. Publ. 323. , pp. 99–125.

Trap, P., Faure, M., Lin, W., Breton, N.L., Monié, P., 2012. Paleoproterozoic tectonic evolution of the Trans-North China Orogen: Toward a comprehensive model. Precambrian Research 222-223, 191-211.

Tremblay, A., Ruffet, G., and Castonguay, S., 2000, Acadian metamorphism in the Dunnage zone of southern Quebec, northern Appalachians: 40Ar/39Ar evidence for collision diachronism, Geological Society of America Bulletin 112, p. 136-146.

Van Kranendonk, M.J., Collins, W.J., Hickman, A.H., Pawley, M.J., 2004. Critical tests of vertical vs. horizontal tectonic models for the Archean East Pilbara granite-greenstone terrane, Pilbara Craton, Western Australia. Precambrian Research 131, 173-211.

Van Staal, C., Barr, S.M., and Murphy, J.B., 2012, Provenance and tectonic evolution of Ganderia: constraints on the evolution of the Iapetus and Rheic oceans, Geology 40, 987-990.

Wakita, K., Pubellier, M., Windley, B.F., 20013.Tectonic processes from rifting to collision via subduction in SE Asia and thewestern Pacific: a key to understanding the architecture of the Central Asian Orogenic Belt. Lithosphere 5, 265-276.

Wan, B., Windley, B.F., Xiao, W.J., Feng, J.Y., and Zhang, J., 2015, Paleoproterozoic high-pressure metamorphism in the northern North China Craton and implications for the Nuna supercontinent, Nature Communications, DOI: 10.1038/ncomms9344

Wan, Y.S., Song, B., Liu, D.Y., Li, H.M., Yang, C., Zhang, Q.D., Yang, C.H., Geng, Y.S.,Shen, Q.H., 2001. Geochronology and geochemistry of 3.8–2.5 Ga Archaean rock belt in Dongshan Scenic Park, Anshan area. Acta Geologica Sinica 75, 363–370(In Chinese with English abstract).

Wan, Y.S., Liu, D.Y., Song, B., Wu, J.S., Yang, C.H., Zhang, Z.Q., Geng, Y.S., 2005. Geochemical and Nd isotopic compositions of 3.8 Ga meta-quartz dioritic and trondhjemitic rocks from the Anshan area and their geological significance. Journal of Asian Earth Sciences 4, 563–575.

Wan, Y.-S., Wilde, S., Liu, D.-Y., Yang, C.-X., Song, B., Yin, X.-Y., 2006a. Further evidence for 1.85 Ga metamorphism in the Central Zone of the North China Craton: SHRIMP U–Pb dating of zircon from metamorphic rocks in the Lushan area, Henan Province. Gondwana Research 9, 189–197.

Wan, Y. S., Song, B., Liu, D. Y., Wilde, S. A., Wu, J. S., Shi, Y. R., Yin, X. Y., and Zhou, H. Y., 2006b, SHRIMP U-Pb zircon geochronology of Palaeoproterozoic metasedimentary rocks in the North China Craton: Evidence for a major Late Palaeoproterozoic tectonothermal event: Precambrian Research, v. 149, n. 3–4, p. 249–271,

Wan, Y. S., Liu, D. Y., Xu, Z. Y., Dong, C. Y., Wang, Z. J., Zhou, H. Y., Yang, Z. S., Liu, Z. H., and Wu, J. S., 2008, Paleoproterozoic crustally derived carbonate-rich magmatic rocks from the Daqinshan area, North China Craton: Geological, petrographical, geochronological and geochemical (Hf, Nd, O and C) evidence: American Journal of Science, v. 308, n. 3, p. 351–378.

Wan, Y. S., Liu, D. Y., Dong, C. Y., Xu, Z. Y., Wang, Z. J., Wilde, S. A., Yang, Y. H., Liu, Z. H., and Zhou, H. Y., 2009, The Precambrian Khondalite Belt in the Daqingshan area, North China Craton: evidence for multiple metamorphic events in the Palaeoproterozoic, *in* Reddy, S. M., Mazumder, R., Evans, D. A. D.,and Collins, A. S., editors, Palaeoproterozoic

Supercontinents and Global Evolution: Geological Society, London, Special Publications, v. 323, p. 73–97.

Wan, Yusheng and Xie, Hangqiang and Yang, Hua and Wang, Zejiu and Liu, Dunyi and Kroener, Alfred and Wilde, Simon A. and Geng, Yuansheng and Sun, Liuyi and Ma, Mingzhu and Liu, Shoujie and Dong, Chunyan and Du, Lilin. 2013. Is the Ordos Block Archean or Paleoproterozoic in Age? Implications for the Precambrian Evolution of the North China Craton. American Journal of Science. 313 (7): pp. 683-711.

Wang, D., Guo, J.H., Huang, G.Y, and Scheltens, M., 2015, The Neoarchean ultramafic-mafic complex in the Yinshan Block, North China Craton: Magmatic monitor of development of Archean lithospheric mantle, Precambrian Research 270, 80-99.

Wang, J.P., Kusky, T.M., Polat, A., Wang, L., Deng, H., Wang, S.J., 2013. A late Archean tectonic mélange belt in the Central Orogenic Belt, North China Craton. Tectonophysics 608, 929-946.

Wang, J.P., Kusky, T.M., Wang, L., Polat, A., and Deng, H., 2015, A Neoarchean subduction polarity reversal event in the North China craton, Lithos, 220-223, p. 133-146.

Wang, J.P., Kusky, T.M., Wang, L., Polat, A., Wang, S.J., and Deng, H., 2016, Structural relationships along a Neoarchean arc-continent collision zone,, North China Craton, Geological Society of America Bulletin, doi: 10.1130/B31479.1

Wang, J.P., Kusky, T.M., Wang, L., Polat, A., Deng, H., Fu, J.M., and Wang, S.J., in review, Petrogenesis and geochemistry of circa 2.5 Ga granitoids in the western Zanhuan Massif: Implications for the Precambrian tectonic evolution of the North China Craton, Lithos.

Wang, K.Y., Li, J.L., Hao, J., Li, J.H., and Zhao, S.P., 1996, The Wutaishan orogenic belt within the Shanxi province, northern China: A record of Archean collision tectonics: Precambrian Research, v. 78, p. 95–103.

Wang, K.-Y., Wilde, S.-A., 2002. Precise SHRIMP U–Pb ages of Dawaliang granite in Wutaishan area, Shanxi Province. Acta Petrologica et Mineralogica 21, 407–411 (in Chinese with English abstract).

Wang, K., Li, J.L., Hao, J., 1997. Late Arhean mafic-ultramafic rocks from the Wutaishan, Shanxi Province; a possible ophiolitic melange. Acta Petrologica Sinica 13 (2), 139–151.

Wang, L., Kusky, T.M., Polat, A., Wang, S.J., Jiang, X.F., Zong, K.Q., Wang, J.P., Deng, H., and Fu, J.M., 2014, Partial melting of deeply subducted eclogite from the Sulu orogen in China, Nature Communications, DOI: 10.1038/ncomms6604.

Wang, W., Liu, S.W., Santosh, M., Wang, G.H., Bai, X., and Guo, R.R., 2015, Neoarchean intra-oceanic arc system in the Western Liaoning Province: Implications for Early Precambrian crustal evolution in the Eastern Block of the North China Craton, Earth Science Reviews 150, 329-364.

Wang, W., Liu, X.S., Hu, J.M., Li, Z.H., Zhao, Y., Zhai, M.G., Liu, X.C., Clarke, G., Zhang, S.H., and Qu, H.J., 2014, Late Paleoproterozoic medium-P high grade metamorphism of basement rocks beneath the northern margin of the Ordos basin, NW China: Petrology, phase equilibrium modelling and U-Pb geochronology, Precambrian Research 25, 181-196.

Wang, W., Liu, S.W., Bai, X., Li, Q.G., Yang, P.T., Zhao, Y., Zhang, S.H., Guo, R.R., 2013. Geochemistry and zircon U–Pb–Hf isotopes of the late Paleoproterozoic Jianping diorite–monzonite–syenite suite of the North China Craton: Implications for petrogenesis and geodynamic setting. Lithos 162-163, 175-194.

Wang, W., Liu, S.W., Wilde, S.A., Li, Q.G., Zhang, J., Bai, X., Yang, P.T., Guo, R.R., 2012, Petrogenesis and geochronology of Precambrian granitoid gneisses in Western Liaoning Province: constraints on Neoarchean to early Paleoproterozoic crustal evolution of the North China Craton. Precambrian Research 222, 290–311.

Wang, Y. J., Fan, W. M., Zhang, Y. H., 2004. Geochemical, 40Ar/39Ar geochronological and Sr–Nd isotopic constraints on the origin of Paleoproterozoic mafic dikes from the southern Taihang Mountains and implications for the 1800 Ma event of the North China Craton. Precambrian Research. 135 (1-2): 55–79.

Wang Z. H., 2009. Tectonic evolution of the Hengshan-Wutai-Fuping complexes and its implication for the Trans-North China Orogen. Precambrian Research, 170: 73-87.

Wang Z. H., Wilde S. A. and Wan J. L., 2010a. Tectonic setting and significance of 2. 3 ~ 2. 1

Ga magmatic events in the Trans-North China Orogen: New constraints from the Yanmenguan mafic-ultramafic intrusion in the Hengshan-Wutai-Fuping area. Precambrian Research, 178: 27-42.

Wang, Z.T., Zhou, H.R., Wang, X.L., and Jing, X.C., 2015, Characteristics of the crystalline basement beneath the Ordos Basin: Constraint from aeromagnetic data, Geoscience Frontiers 6, 1-13. http://dx.doi.org/10.1016/j.gsf.2014.02.004

Wang, D., Guo, J.H., Huang, G.Y., and Scheltens, M., 2015, The Neoarchean ultramafic-mafic complex in the Yinshan Block, North China Craton: Magmatic monitor of development of Archean lithospheric mantle, Precambrian Research 220, 80-99.

Wilde, S.A., 1998. SHRIMP U–Pb zircon dating of granites and gneisses in the Taihangshan–Wutaishan area: implications for the timing of crustal growth in the North China Craton. Chinese Science Bulletin 43, 144.

Wilde, S.A., Zhao, G.-C., Sun, M., 2002. Development of the North China Craton during the Late Archean and its final amalgamation at 1.8 Ga: some speculation on its position within a global Paleoproterozoic supercontinent. Gondwana Research 5, 85–94.

Wilde, S.A., Zhao, G.-C., Wang, K.-Y., Sun, M., 2003. SHRIMP zircon U–Pb age of the Hutuo Group in Wutai Mts.: new evidence for the Paleoproterozoic amalgamation of the North China Craton. Chinese Science Bulletin 48, 2180–2186 (in Chinese).

Wilde, S.A., and Zhao, G.C., 2005, Late Archean to Paleoproterozoic evolution of the North China Craton, Journal of Asian Earth Sciences, 24, 577-595.

Wilde, S.A., Zhao, G.C., and Wang, K.Y., 2004, First SHRIMP zircon U-Pb ages for Hutuo Group in Wutaishan: Further evidence for Palaeoproterozoic amalgamation of North China Craton, Chinese Science Bulletin 49, 83-90.

Wilde, S.A., Cawood, P.A., Wang, K.Y., Nemchin, A.A., 2005a. Granitoid evolution in the late Archean Wutai Complex, North China Craton. J. Asian Earth Sci. 24, 597–613, doi:10.1016/j.jseaes.2003.11.006.

Wilde, S.A., and Zhao, G.C., 2005b, Late Archean to Paleoproterozoic evolution of the North China Craton, Journal of Asian Earth Sciences, 24, 577-595.

Windley, B.F., 1995, The Evolving Continents, Third Edition, John Wiley and Sons, Chichester, 526 pp.

Windley, B.F, Garde, A.A., 2009. Arc-generated blocks with crustal sections in the North Atlantic craton of West Greenland: new mechanism of crustal growth in the Archean with modern analogues. Earth Science Reviews 93, 1–30.

Windley, B.F., Maruyama, S., Xiao, W.J., 2010. Delamination/thinning of sub-continental lithospheric mantle under Eastern China: the role of water and multiple subduction. American Journal of Science 310, 1250-1293.

Wu, C.H., Zhong, C.T., 1998. The Paleoproterozoic SW–NE collision model for the central North China Craton. Progress of Precambrian Research 21, 28–50.

Wu, C. H., Sun, M., Li, H. M., Zhao, G. C., and Xia, X. P., 2006, LA-ICP-MS U-Pb zircon ages of the khondalites from the Wulashan and Jining high-grade terrain in northern margin of the North China Craton: constraints on sedimentary age of the khondalite: Acta Petrologica Sinica, v. 22, n. 11, p. 2639–2654 (in Chinese with English abstract).

Wu, F.Y., Yang, J.H., Liu, X.M., Li, T.S., Xie, L.W., Yang, Y.H., 2005. Hf isotopic characteristics of 3.8 Ga zircon and time of early crust of North China Craton. Chinese Science Bulletin 50, 1996–2003.

Wu, F.-Y., Han, R.-H., Yang, J.-H., Wilde, S.A., Zhai, M.-G., Park, S.-C., 2007. Initial constraints on the timing of granitic magmatism in North Korea using U–Pb zircon geochronology. Chemical Geology 238, 232–248.

Wu, J.S., Liu, D.Y., Jin, L.G., 1986. The U–Pb zircon age of metamorphic lava within the Hutuo group, Wutai metamorphic terrain. Geological Review 32 (2), 178–183.

Wu, M.L., Zhao, G.C., Sun, M., Yin, C.Q., Li, S.Z., Tam, P.Y., 2012a. Petrology and P–Tpath of the Yishui mafic granulites: implications for tectonothermal evolution ofthe Western Shandong Complex in the Eastern Block of the North China Craton.Precambrian Research, http://dx.doi.org/10.1016/j.precamres.2011.08.008.

Xiao, L.L., Liu, F.L., and Chen, Y., 2014, Metamorphic P-T-t paths of the Zanhuang metamorphic complex: Implications for the Paleoproterozoic evolution of the Trans-North China orogeny, Precambrian Research 255, 216-235.

Xiao, W.J., Kusky, T.M., Safonova, I., Schulmann, K., and Sun, M., 2015, Tectonics of the Central Asian Orogenic Belt and its Pacific analogues, Journal of Asian Earth Sciences 113, Part 1, 1-542, ISSN 1367-9120 (no vol and page numbers yet?)

Xiao, W.J., Windley, B.F.., Sun, S., Li, J., 2015, A Tale of Amalgamation of Three Permo-Triassic Collage Systems in Central Asia: Oroclines, Sutures, and Terminal Accretion, Annual Reviews of Earth and Planetary Sciences, 43, 477-507.

Xie, G.H., 2005, Petrology and Geochemistry of the Damiao Anorthosite and the Miyun Rapakivi Granite. Sci. Press, Beijing, p. 195 (in Chinese).

Xiu, Q.Y., Yu, H.F., Li, Q., 2004. Discussion on the Petrogenic Time of Longshoushan Group, Gansu Province. Acta Gelogica Sinica 78, 366–373 (In Chinese with English Abstract).

Yamamoto, S., Senshu, H., Rino, S., Omon, S., and Maruyama, S., 2009, Granite subduction: arc subduction, tectonic erosion and sediment subduction, Gondwana Research 15, 443-453.

Yang, C.-H., Du, L.-L., Ren, L.-D., Song, H.-X., Wan, Y.-S., Xie, H.-Q., Liu, Z.-X., 2011. The age and petrogenesis of the Xuting granite in the Zanhuang Complex, Hebei Province:

constraints on the structural evolution of the Trans-North China Orogen, North China. Acta Petrologica Sinica 27, 1003–1016 (in Chinese with English abstract).

Yang , C.H., Du, L.L. Ren, L.D., Song, H.X., Wan, Y.S., Xie, H.Q., and Geng, Y.S., 2013, Delineation of the ca. 2.7 GA TTG gneisses in the Zanhuang Complex, North China Craton and its geological implications, Journal of Asian Earth Sciences 72, 178-189.

Yang, D.-B., Xu, W.-L., Pei, F.-P., Wang, Q.-H., 2009. Petrogenesis of the Paleoproterozoic K-feldspar granites in Bengbu Uplift: constraints from petrogeochemistry, zircon U–Pb dating and Hf isotope. Earth Science — Journal of China University of Geosciences 34, 148–164 (in Chinese with English abstract).

Yang, J.H., Wu, F.Y., Wilde, S.A., Zhao, G.C., 2008. Petrogenesis and geodynamics of Late Archean magmatism in eastern Hebei, eastern North China Craton: Geochronological, geochemical and Nd–Hf isotopic evidence. Precambrian Research 167, 125–149.

Yang, Q.Y., and Santosh, M., 2015, Paleoproterozoic arc magmatism in the North China Craton: No Siderian global tectonic shutdown, Gondwana Research 28, p. 82-105.

Yang, Q.Y., Santosh, M., Collins, A. S., Teng, X.M., 2015, Microblock amalgamation in the North China Craton: Evidence from Neoarchaean magmatic suite in the western margin of the Jiaoliao Block, Gondwana Research, doi: 10.1016/j.gr.2015.04.002

Yang, T., Wu, J.P., Fang, L.H., et al., 2012. 3-D S-wave velocity of crust and upper mantle beneath North China. Progress in Geophysics 27, 0441e0454. http://dx.doi.org/10.6038/j.issn.1004-2903.2012.02.07 (in Chinese with English abstract).

Yang, Y.T., Li, W., Ma, L., 2005, Tectonic and stratigraphic controls of hydrocarbon systems in the Ordos Basin: a multicycle cratonic basin in central China. AAPG Bulletin 89, 255e269.

Yin, A., and Harrison, T.M., 2000, Geologic evolution of the Himalayan-Tibetan orogeny, Annual Review of Earth and Planetary Sciences, 28, 211-280, DOI: 10.1146/annurev.earth.28.1.211

Yin, C.Q., Zhao, G.C., Sun, M., Xia, X.P., Wei, C.J., Zhou, X.W., and Leung, W.H. 2009, LA_ICP-MS U-Pb zircon ages of the Qianlishan Complex: Constraints on the evolution of the Khondalite Belt in the Western Block of the North China Craton, Precambrian Research 174, 78-94.

Yin, C.Q., Zhao, G.C., Guo, J.H., Xia, X.W., Zhou, X.W., and Liu, C.H., 2011, U-Pb and Hf isotopic study of zircons of the Helanshan Complex: Constraints on the evolution of the Khondalite Belt in the Western Block of the North China Craton, Lithos 122, 25-38.

Yu, J.H., Fu, H.Q., Zhang, F.L., Wan, F.X., 1993. The plutonism and volcanism of Proterozoic rapakivi suite near Beijing, I: Anorogenic magmatism and rifting. Beijing Geology 5, 4–20 (in Chinese with English abstract).

Yu, J.H., Fu, H.Q., Haapala, I., Rämö, O.T., Vaasjoki, M., Mortensen, J.K., 1996. A 1.70 Ga Anorogenic Rapakivi Granite Suite in the Northern Part of North China Craton. Journal of Geology and Mineral Research of North China 11(3),342-350 (in English with Chinese abstract).

Yu, J.-H., Wang, D.-Z., Wang, C.-Y., Li, H.-M., 1997. Ages of the Lvliang Group and its main metamorphism in the Lvliang Mountains, Shanxi: evidence from single grain zircon U–Pb ages. Geological Review 43, 403–408 (in Chinese with English abstract).

Zhai, M.G., 2004. Precambrian geological events in the North China Craton. In: Malpas,J., Fletcher, C.J.N., Ali, J.R., Aitchison, J.C. (Eds.), Tectonic Evolution of China:Geological Society of London Special Publication, 226, pp. 57–72.

Zhai, M.G., 2011, Cratonization and the Ancient North China Continent: A summary and Review, Science China Earth Sciences, 54, 1110-1120.

Zhai, M.G., 2014. Multi-stage crustal growth and cratonization of the North China Craton. Geoscience Frontiers 5, 457-469.

Zhai, M., and Liu, W.J., 2003. Paleoproterozoic tectonic history of the North China craton: a review. Precam. Res. 122, 183-199.

Zhai, M.G., Peng, P., 2007. Paleoproterozoic events in North China Craton. Acta Petrol. Sinica 23, 2665–2687 (in Chinese with English abstract).

Zhai, M.G., and Santosh, M., 2011, The early Precambrian odyssey of the North China craton: A synoptic overview, Gondwana Research 20, 6-25.

Zhai, M.-G., Santosh, M., 2013. Metallogeny of the North China Craton: link with secular changes in the evolving Earth. Gondwana Research 24, 275–297.

Zhai, M.G., Windley, B.F. 1989. Banded iron formation in high-grade gneisses in northern China and implications for early crustal growth. Transactions of Institute of Mining and Metallurgy. 98, Section B, 32-34.

Zhai, M.G., Bian, A.G., Zhao, T.P., 2000. The amalgamation of thesupercontinent of North China craton at the end of the neoarchean andits break up during late Proterozoic and Mesoproterozoic. Science inChina (D) 43, 219–232.

Zhai, M.G., Windley, B.F., Kusky, T.M., and Meng, Q.R., 2007, Mesozoic Sub-Continental Lithospheric Thinning Under Eastern Asia, Geological Society of London Special Publication 280, 352 pp., ISBN 978-1-86239-225-0

Zhai, M.G., Guo, J.H., and Liu, W.J., 2005, Neoarchean to Paleoproterozoic continental evolution and tectonic history of the North China Craton, Journal of Asian Earth Sciences 24, 547-561.

Zhai, M.G., Li, T.S., Peng, P., Hu, B., Liu, F., Zhang, Y.B., Guo, J.H., 2010. Precambrian key tectonic events and evolution of the North China Craton. In: Kusky, T.M., Zhai, M.G., Xiao, W.J. (Eds.), The Evolving Continents: Geological Society of London Special Publications, 338, pp. 235–262.

Zhang, C.H., Li, C.M., Deng, H.L., Liu, Y., Wei, B., Li, H.B., and Ziu, Z., 2011, Mesozoic contraction deformation in the Yanshan and northern Taihang mountains and its implications to the destruction of the North China Craton, Science China, Earth Sciences 54, 798-822.

Zhang, C.L., Diwu, C.R., Kroner, A., Sun, Y., Luo, J.L., Li, Q.L., Gou, L.L., Lin, H.B., Wei, X.S., and Zhao, J., 2015, Archean-Paleoproterozoic crustal evolution of the Ordos Block in the North China Craton: Constraints from zircon U-Pb geochronology and Hf isotopes for gneissic granitoids of the basement, Precambrian Research 267, 121-136.

Zhang, H., Yuan, L.L., Xue, F.H., and Zhai, M.G., 2014, Neoarchean metagabbro and charnockite in the Yinshan Block, western North China Craton: Petrogenesis and tectonic implications, Precambrian Research 255, 563-582.

Zhang, J., Zhao, G.C., Li, S.Z., Sun, M., Liu, S.W., Wilde, S.A., Kröner, A., Yin, C.Q., 2007. Deformation history of the Hengshan Complex: implications for the tectonic evolution of the Trans-North China Orogen. J. Struct. Geol. 29, 933–949, doi:10.1016/j.jsg.2007.02.013.

Zhang, J., Zhao, G.C., Li, S.Z., Sun, M., Wilde, S.A., Liu, S.W., Yin, C.Q., 2009. Polyphase deformation of the Fuping Complex, Trans-North China Orogen: structures, SHRIMP U–Pb zircon ages and tectonic implications. J. Struct. Geol. 31, 177–193, doi:10.1016/j.jsg.2008.11.008.

Zhang, J., Zhao, G.C., Li, S.Z., Sun, M., Chan, L.S., Shen, W.L., and Liu, S.W., 2012, Structural pattern of the Wutai Complex and its constraints on the tectonic framework of the Trans-North China Orogen, Precambrian Research 222-223, 212-229.

Zhang, J.X., Gong, J.H., Yu, S.Y., Li, H.K., Hou, K.J., 2013. Neoarchean–Paleoproterozoic multiple tectonothermal events in the western Alxa block, NorthChina Craton and their geological implication: evidence from zircon U–Pb agesand Hf isotopic composition. Precambrian Res. 235, 36–57.

Zhang, L.C., Zhai, M.G., Zhang, X.J., Xiang, P., Dai, Y.P., Wang, C.L., Pirajno, F., 2012c. Formation age and tectonic setting of the Shirengou Neoarchean banded iron deposit in eastern Hebei Province: constraints from geochemistry and SIMS zircon U–Pb dating. Precambrian Research, http://dx.doi.org/10.1016/j.precamres.2011.09.007.

Zhang, Q., Ni, Z.Y., Zhai, M.G., 2003. Comments on the Archean ophiolites in Eastern Hebei. Earth Science Frontiers 10, 429–437. (in Chinese with English abstract).

Zhang, Q., Wang, Y., Zhou, G.Q., Qian, Q., Robinson, P.T., 2004. Ophiolites in China: their distribution, ages and tectonic settings, in: Y. Dilek, P.T. Robinson (Eds.), Ophiolites in Earth History, Geol. Soc. Spec. Publ. (London), vol. 218, 2004, pp. 541–566.

Zhang, S.H., Liu, S.W., Zhao, Y., Yang, J.H., Song, B., Liu, X.M., 2007. The 1.75–1.68 Ga anorthosite-mangerite-alkali granitoid-rapakivi granite suite from the northern North China Craton: magmatism related to a Paleoproterozoic orogen. Precambrian Research 155, 287–312.

Zhang, S.H., Gao, R., Li, H.Y., Hou, H.S., Wu, H.C., Li, Q.S., Yang, K., Li, C, Li W.H., Zhang, JS., Yang, T.S., Keller, G.R., and Liu, M., 2014, Crustal structures revealed from a deep seismic reflection profile across the Solonker suture zone of the Central Asian orogenic belt, northern China: An integrated interpretation, Tectonophysics 612-613, 26-39.

Zhang, X.H., Yuan, L.L., Xue, F.H., and Zhai, M.G., 2014, Neoarchean metagabbro and charnockite in the Yinshan Block, western North China Craton: Petrogenesis and tectonic implications, Precambrian Research 255, 563-582.

Zhang, X.J., Zhang, L.C., Xiang, P., Wan, B.O., Pirajno, F., 2011. Zircon U–Pb age, Hf isotopes and geochemistry of Shuichang Algoma-type banded iron-formation, North China Craton: constraints on the ore-forming age and tectonic setting. GondwanaResearch 20, 137–148.

Zhang, Y.-F., Liu, J.-T., Xiao, R.-G., Wang, S.-Z., Wang, J., Bao, D.-J., 2010. The hyalotourmalites of Houxianyu borate deposit in eastern Liaoning: zircon features and

SHRIMP dating. Earth Science — Journal of China University of Geosciences 35, 985–999 (in Chinese with English abstract).

Zhang, Y.Q., Ma, Y.S., Yang, N., Shi, W., and Dong, S., 2003, Cenozoic extensional stress evolution in North China, Journal of Geodynamics 36, 591-613.

Zhao, G.C., 2001. Paleoproterozoic assembly of the North China Craton. Geological Magazine 138, 87-91.

Zhao, G.-C., Wilde, S.A., Cawood, P.A., Sun, M., 2002a. SHRIMP U–Pb zircon ages of the Fuping Complex: implications for Late Archean to Paleoproterozoic accretion and assembly of the North China Craton. American Journal of Science 302, 191–226.

Zhao, G.-C., Cao, L., Wilde, S.A., Sun, M., Choe, W.-J., Li, S.-Z., 2006. Implications based on the first SHRIMP U–Pb zircon dating on Precambrian granitoid rocks in North Korea. Earth and Planetary Science Letters 251, 365–379.

Zhao, G.-C., Wilde, S.A., Sun, M., Guo, J.-H., Kröner, A., Li, S.-Z., Li, X.-P., Zhang, J., 2008a. SHRIMP U–Pb zircon geochronology of the Huai'an Complex: constrains on Late Archean to Paleoproterozoic magmatic and metamorphic events in the Trans-North China Orogen. American Journal of Science 308, 270–303.

Zhao, G.C., Kro¨ner, A., Wilde, S.A., Sun, M., Li, S.Z., Li, X.P., Zhang, J., Xia, X.P., He, Y.H.,2007. Lithotectonic elements and geological events in the Hengshan–Wutai–Fuping belt: a synthesis and implications for the evolution of the Trans-NorthChina Orogen. Geological Magazine 144, 753–775.

Zhao, G.-C., Wilde, S.A., Sun, M., Li, S.-Z., Li, X.-P., Zhang, J., 2008b. SHRIMP U–Pb zircon ages of granitoid rocks in the Lvliang Complex: implications for the accretion and evolution of the Trans-North China Orogen. Precambrian Research 160, 213–226.

Zhao, G.C., and Cawood, P.A., 2012, Precambrian Geology of China, Precambrian Research 222-223, 13-54.

Zhao, G.C., Guo, J.H., 2012. Precambrian Geology of China: Preface. Precambrian Research 222-223, 1-12.

Zhao, G., and Kröner, A., 2002a, Introduction, in Kröner, A., Zhao, G.C., Wilde, S.A., Zhai, M.G., Passchier, C.W., Sun, M., Guo, J.H., O'Brien, P.J., and Walter, N., eds., Late Archean to Paleoproterozoic lower to upper crustal section in the Hengshan-Wutaishan area of North China: Guidebook for Penrose Conference Field Trip, p. 1–2.

Zhao, G.C., and Wilde, S.A., 2002, Features of tectonic units of the North China Craton Basement, and amalgamation during early Proterozoic,Science in China (Series D), v. 32, 7, p. 538-548.

Zhao, G.C., Zhai, M.G., 2013. Lithotectonic elements of Precambrian basement in the North China Craton: review and tectonic implications. Gondwana Research 23, 1207-1240.

Zhao, G.C., Wilde, S.A., Cawood, P.A., Lu, L.Z., 1999. Thermal evolution of two textural types of mafic granulites in the North China Craton: evidence for both mantle plume and collisional tectonics. Geological Magazine 136, 223-240.

Zhao, G.C., Cawood, P.A., Lu, L.Z., 1999c. Petrology and P–T history of the Wutai amphibolites: implications for tectonic evolution of the Wutai Complex, China. Precambrian Res. 93, 181–199.

Zhao G.C., Wilde, S.A., Cawood, P.A., Sun, M., 2001a. Archean blocks and their boundaries in the North China Craton: Lithological, geochemical, structural and P-T path constraints and tectonic evolution. Precambrian Research 107, 45-73.

Zhao, G.C., Cawood, P.A., Wilde, S.A., Lu, L.Z., 2001b. High-pressure granulites (retrograded eclogites) from the Hengshan Complex, North ChinaCraton: petrology and Tectonic implications. Journal of Petrology 42,1141e1170.

Zhao, G.C, Wilde, S.A., Cawood, PA. and Sun, M. (2001c, SH RIMP U-Pb zircon ages of the Fuping Complex: implications for late Archean to Palaeoproterozoic accretion and assembly of the North China Craton. Amer. J. Sci., 302, 191-226.

Zhao, G.C., Wilde, S.A., Cawood, P.A., Sun, M., 2002b. SHRIMP U–Pb zircon ages of the Fuping Complex: implications for accretion and assembly of the North China Craton. Am. J. Sci. 302, 191–226.

Zhao, G., Sun, M., and Wilde, S.A., 2002c, SHRIMP U-Pb zircon ages of the Fuping Complex, in Kröner, A., Zhao, G.C., Wilde, S.A., Zhai, M.G., Passchier, C.W., Sun, M., Guo, J.H., O'Brien, P.J., and Walte, N., eds., Late Archean to Paleoproterozoic lower to upper crustal section in the Hengshan-Wutaishan area of North China: Guidebook for Penrose Conference Field Trip, p. 34–36.

Zhao, G.C., Sun, M., Wilde, S.A., Li, S.Z., 2005. Late Archean to Paleoproterozoic evolution of the North China Craton: Key issues revisited. Precambrian Research 136, 177-202.

Zhao, G. C., Wilde, S. A., Li, S. Z., et al., 2007. U-Pb Zircon Age Constraints on the Dongwanzi Ultramafic-Mafic Body, North China, Confirm It Is not an Archean Ophiolite. Earth and Planetary Science Letters, 255(1–2): 85–93, doi:10.1016/j.epsl.2006.12.007

Zhao, G.C., 2009. Metamorphic evolution of major tectonic units in the basement of the North China Craton: Key issues and discussion. Acta Petrologica Sinica 25, 1772-1792.

Zhao, G. C., Wilde, S. A., Guo, J. H., Cawood, P. A., Sun, M., and Li, X. P., 2010, Single zircon grains record two Paleoproterozoic collisional events in the North China Craton: Precambrian Research, v. 177, n. 3–4, p. 266–276, http://dx.doi.org/10.1016/j.precamres.2009.12.007

Zhao, G.C., Cawood, P.A., Wilde, S.A., Sun, M., Zhang, J., He, Y.H., Yin, C.Q., 2012. Amalgamation of the North China Craton: key issues and discussion. Precambrian Research 222-223, 55-76.

Zhao, R.-F., Guo, J.-H., Peng, P., Liu, F., 2011. 2.1 Ga crustal remelting event in Hengshan Complex: evidence from zircon U–Pb dating and Hf–Nd isotopic study on potassic granites. Acta Petrologica Sinica 27, 1607–1623 (in Chinese with English abstract).

Zheng, T.Y., Zhao, L., Zhu, R.X., 2009, New evidence from seismic imaging for subduction during assembly of the North China Craton, Geology 37, 395-398.

Zhong, C. T., Deng, J. F., Wan, Y. S., Mao, D. B., and Li, H. M., 2007, Magma recording of Paleoproterozoic orogeny in central segment of northern margin of North China Craton: Geochemical characteristics and zircon SHRIMP dating of S-type granitoids: Geochimica, v. 36, p. 633–637 (in Chinese with English abstract).

Zhou, R.J., Li, Y., Densmore, A.L., Ellis, M.A., He, Y.L., Li, Y.Z., and Li, X.G., 2007, Active tectonics of the Longmen Shan region on the eastern margin of the Tibetan Plateau, Acta Geological Sinica 81, 593-604, DOI: 10.1111/j.1755-6724.2007.tb00983.x

Zhu, R. Xu, Y.G., Zhu, G., Zhang, H.F., Xia, Q.K., Zheng, T.Y., 2012. Destruction of the North China Craton. Sci. China 55, 1565.

Figure Captions

Fig. 1. Map of the NCC showing Archean division into the Eastern Block, Central Orogenic Belt (COB), Western Block (modified from Kusky, 2011) and Inner Mongolia-Northern Hebei Orogen (which includes the Yinshan Block and the northern part of the khondalite belt). Note that the northern part of the COB is strongly overprinted by tectonism related to events in the IMNHO, thus two colors are uses to express this multi-phase part of the orogens. Dashed line outlines the Ordos Basin. This section of the paper is dedicated to testing this division, and further refining the traces and ages of specific sutures. Abbreviations as follows: AL – Alashan (Alxa); BD – Beidashan; CD – Chengde; DF – Denfeng; EH – Eastern Hebei; ES – Eastern Shandong; : FP – Fuping; FX – Fuxin; GY – Guyang; HA- Huai'an; HL – Helenshan; HS – Hengshan; JN – Jining; LG – Langrim; LL – Luliang; LS – Longshoushan; MY – Miyun; NH – Northern Hebei; NL – Northern Liaoning; QL – Qianlishan; SJ – Southern Jilin; SL-Southern Liaoning; TH – Taihua; WC – Wuchuan; WD – Wulushan-Daqingshan; WL – Western Liaoning; WS Western Shandong; WT – Wutai; XH – Xuanhua; ZH – Zanhuang; ZT – Zhongtiao.

Fig. 2. Idealized cross-section of an accretionary orogen that experienced an arc/continent collision and is in the process of converting to a continent-continent collisional orogen. Some orogens are temporarily "frozen" in this stage (e.g., Taconic, Acadian, Alps), others progress to hard continent-continent-collisions (e.g., Himalayan, Dabie-Sulu). Inspired by cross-sections by Collet (1927), Harte and Dempster (1987), Bradley and Kusky (1986), Rowley and Kidd (1981), among others.

Fig. 3. Simplified map of northeastern USA showing relationships between the Ordovician Taconic suture and accretionary complex, Devonian Acadian and younger Alleghenian sutures, Acadian plutons, superimposed passive margin and foreland basin sequences, and intracontinental basins and domes in the foreland. Modified after Rogers et al., 1999. An outline (in red) of the North China Craton (with N to the S) is drawn over the map for comparison. We use this orogen for comparison with the NCC in several places in the manuscript.

Fig. 4. Map of the Zanhuang massif showing the location of the suture between the Wutai/Fuping arc in the Central Orogenic Belt and the passive margin on the western edge of the Eastern Block. WZD = Western Zanhuang Domain, CZD = Central Zanhuang Domain, EZD = Eastern Zanhuang Domain. Inset shows location of the Zanhuang Massif (ZH) in the Central Orogenic Belt (COB), south of the Wutai (WT) and Fuping (FP) Complexes WB – Western Block, EB – Eastern Block. Map modified from Trap et al. (2012) and Wang et al. (2013, 2015, 2016).

Fig. 5. Structural profile of ophiolitic mélange in Zanhuang massif. Modified from Wang et al. (2016). Original mapping at 1:200 scale.

Fig 6. Field photographs of exotic blocks in the Zanhuang mélange. A: Mafic blocks that are interpreted as deformed pillow structures with epidosite lenses preserved in the altered cores, all within an amphibolitic matrix. B: Mafic blocks interpreted as relict pillows dispersed in a metapelitic matrix. C: Strongly sheared and disrupted mélange containing doleritic blocks and relict pillow fragments with epidosite cores in a metapelitic matrix. D: Ultramafic blocks in strongly deformed metapelite matrix. E: Ultramafic blocks dispersed in a metapelitic matrix. F:

Broken-apart marble layer and blocks in strongly deformed matrix of micaschist. Modified from Wang et al., 2013 (see Wang et al., 2013 for locations).

Fig. 7. (a) Map of Wutai- Fuping- Hengshan Complexes and cross-section (b) after Trap et al., 2012. The cross-section is correlated with a seismic section (e) from Zheng et al., (2009). Reflector L2 is interpreted here as aa Archean paleo-subduction zone, and L1 is interpreted to show the basement of the Western Block being thrust over the Central Orogenic Belt following its collision with the amalgamated Eastern Block and Wutai arc in the Central Orogenic Belt. Note that the Taihang suture of Trap et al. (2012) corresponds to the Zunhua-Zanhuang suture of Kusky et al. (2011).

Fig 8. Map of the eastern Hebei area, after Li et al. (2000d). Note the locations of the Shangyin ophiolitic sheet, NW Belt of Dongwanzi Ophiolite and Zunhua ophiolitic mélange. The mafic/ultramafic intrusion between the NW belt of DWO and the Shangyin Ophiolite is a Paleozoic intrusion with rafts of underlying basement. The suture between the Eastern Block and the Central Orogenic belt extends across this map from Santunyin to Qinglong and is locally offset by younger faults.

Fig 9. Map of ophiolitic mélange north of Zunhua. The mélange contains blocks of pillow lava, mafic dikes, gabbro, serpentinite, harzburgite, and podiform chromite in dunite pods enclosed in harzburgite, all in a metasedimentary matrix. Map modified after Li et al., 2002.

Fig 10. Field photographs for field relationships of rock units in the Zunhua Structural/ ophiolitic mélange belt. (a) foliated chert representing marine sediments on top of the Dongwanzi Ophiolite;

(b) relic pillow lavas in the Shangyin Ophiolitic Sheet; (c) diabase dikes cutting across the gabbro in the Dongwanzi Ophiolite; (d) layered gabbros in the the Shangyin Ophiolitic Sheet; (e) serpentinized harzburgite from the several km thick mantle section in the Shangyin Ophiolitic Sheet, which is cut by late potassic granite dikes; (f) blocks of harzburgite with podiform chromite bodies in metasedimentary matrix of the Zunhua ophiolitic mélange.

Fig. 11. Photographs of nodular and orbicular textures of podiform chromites (chromites in dunite envelopes cutting harzburgite tectonite) from the Zunhua ophiolitic mélange. Nodular and orbicular textures in podiform chromites like these illustrated are only known from ophiolites or the modern sea-floor, of any age, anywhere in the world.

Fig. 12. Model showing the evolution and age constraints of the Shangyin Ophiolitic Sheet and Zunhua podiform chromites. Initial formation of oceanic lithosphere was at anoceanic ridge (likely forearc), generating pillow lavas, dike complex, gabbro, layered gabbro, dunite, harzburgite tectonite, and podiform chromites. Gabbro from the crustal section of the ophiolite has yielded a 2505 ± 2 Ma U-Pb age (upper left panel, after Kusky et al., 2001) and peridotites from the mantle section have yielded a Lu-Hf age of 2528 ± 130 Ma (upper right panel, after Polat et al., 2005). Podiform chromites from the Zunhua peridotite have yielded a poorly-constrained Re-Os isochron of ~2.6 Ga (lower left panel after Kusky et al., 2007), and plot on the chondritic evolutionary trajectory for the convecting upper mantle (lower right panel, after Kusky et al., 2007). Together, these data show that the crustal and mantle components of the Dongwanzi ophiolite and Zunhua ophiolitic mélange formed at the same time, and are consistent with the Os isotopic composition of the mantle at circa 2.5 Ga. Figure from Kusky at al. (2011).

Fig. 13. Map of part of the Jianping Complex, Liaoning, showing the locations of podiform chromite pods in a serpentinitic matrix. Map modified after Liu, S.W., et al. (2011).

Fig. 14. Field photographs of various exotic blocks in different matrices in the Jianping Complex. A-C: Metagabbro blocks in a metapelitic matrix, northeast of Dongfangshen in the SW corner of map. D: amphibolite in deformed metagabbro, north of Dongfangshen. E: metabasaltic blocks in a paragneiss matrix, north of Dongfangshen. F: ultramafic block in deformed metagabbro, north of Dongfangshen.

Fig. 15. (a) Simple geological map of the Dengfeng Complex in the Junzhao area (modified from Diwu, C.Z., et al., 2011), showing from west to east: TTG gneisses, and volcano-sedimentary assemblages intruded by metadiorites. All units are cut by younger circa 2.5 Ga granites. Metasediments and metabasites (amphibolite grade) are in thrust contact with each other with many shear zones developed in the sequence. The volcano-sedimentary assemblages were intruded by the metadiorite pluton that split the structurally-imbricated assemblage into two parts. (b) Simplified cross section across the Denfeng complex. We interpret this region to represent the transition from the arc to the accretionary prism.

Fig. 16. Field photographs showing structural relationships of rock units in the Dengfeng Granite-Greenstone Belt. (a) basaltic amphibolites, sandstones and greywackes imbricated because of top-to-the-SE thrusting; (b) strongly sheared basaltic amphibolites with a sheared alteration zone; (c) strongly sheared metagreywacke intercalated with quartzites, with a quartzite

lense showing to-to-SE thrust kinematics (inset); (d) foliated gabbro showing relict gabbroic igneous texture; (e) strong foliated greywackes; (f) mylonitized greywackes.

Fig. 17. Map of the North China craton and surrounding orogens, showing the location of the 2.5 Ga Zanhuang-Zunhua (Z-Z) suture, the 2.4 Ga suture, the Inner Mongolia Northern Hebei Orogen. Dashed line shows the approximate southern extent of the Khondalite Belt. Boxes show places where circa 2.5 Ga metamorphism has been documented within the Central Orogenic Belt (see Supplementary Data Table 1 for details). Abbreviations as follows: AL – Alashan (Alxa); BD – Beidashan; CD – Chengde; DF – Denfeng; EH – Eastern Hebei; ES – Eastern Shandong; : FP – Fuping; FX – Fuxin; GY – Guyang; HA- Huai'an; HL – Helenshan; HS – Hengshan; JN – Jining; LL – Luliang; MY – Miyun; NH – Northern Hebei; QL – Qianlishan; SJ – Southern Jilin; TH – Taihua; WC – Wuchuan; WD – Wulushan-Daqingshan; WS Western Shandong; WT – Wutai; XH – Xuanhua; ZH – Zanhuang; ZT – Zhongtiao.

Fig 18. Cross-sections showing stages in the tectonic development of the NCC at 2.55 and 2.5 Ga. Panel a shows the early stages of the collision between the Wutai/Fuping intraoceanic arc with the Eastern Block of the NCC. This collision at circa 2.55 Ga caused the obduction of the Dongwanzi (DWO), Shangyin and other Archean ophiolite fragments, the formation of the ophiolitic melanges of the Zunhua-Zanhuang suture belt, led to the deposition of flysch in the Qinglong foreland basin, and imbrication of the underlying shelf sequence in foreland fold-thrust belts. Panel b shows later stages of this collision at 2.50 Ga in which the arc polarity has been reversed with a new slab dipping beneath the Eastern Block, bringing in the Ordos oceanic plateau to the collision zone. The slab is releasing fluids and metasomatizing the overlying mantle wedge, generating melts, which led to the intrusion of mafic dikes and plutons across the

Eastern Block at this time (Wang et al., 2015, Deng et al., 2014) and is postulated to be the cause of the widespread CCW metamorphism of rocks in the Eastern Block at circa 2.5 Ga.

Fig 19. Map of the eastern Sunda (Banda) arc colliding with Australia, with a propagating arc-polarity reversal shown by the Flores thrust marking an incipient subduction zone forming where the Timor section of the arc has already collided. The arc polarity reversal is migrating westward along the arc as the arc/continent collision progresses. Modified from Reed et al., 1987). The red line shows the outline of the NCC at the same scale as the map for comparison. Note the remarkable similarities in geology and scale to the NCC, including the seaward-dipping suture on the northern edge of Australia (analogous to the western edge of the Eastern Block of the NCC), and the arc-polarity reversal with a landward-dipping thrust, analogous to the "Trans North China Suture of the NCC, developed on the western side of the accreted Wutai/Fuping arc soon after its collision with the NCC at circa 2.5 Ga.

Fig. 20. Cross-sections showing stages in the tectonic development of the NCC at 2.43 and 2.3 Ga. Panel a at 2.43 Ga shows the accretion of the Ordos oceanic plateau to the collision-modified margin of the Eastern Block, and the initial impingement of the Yinshan Ribbon Microcontinent to the Ordos Block and the northern margin of the amalgamated Eastern and Western Blocks. Panel b shows later stages of the accretion of the Yinshan Block to the northern margin of the NCC, and the initial conversion of the NCC to an Andean-style plate margin with the active arc along the north margin of the continent.

Fig. 21. Map of Cordilleran Ribbon Continent before it accreted to North America, forming large segments of the present North American Cordilleran Orogen. Modified from Johnston

(2008). Red outlines show the southern NCC reconstructed before the proposed collision with the composite Yinshan Ribbon Microcontinent, arc, and accretionary orogen in the IMNHO, overlain on the pre-collision North American Cordillera.

Fig. 22. Comarison of the NCC with different segments of the Andes. Maps in A and B of the Andes are shown with an outline of the NCC at the same scale plotted over the Andean maps for comparison. Red triangles in (b) show locations of active volcanoes. Location of magmatic rocks in C compiled from (Peng et al., 2012, Li et al., 2007, Zhang et al., 2015, and Gong et al. 2011; see Supplementary Data Table 2 for details). Note that most magmatism and deformation is concentrated within 600 km of the active Andean margin (see “600 km front" line), but can extend as far as 1000 km (1000 km “Andean front” line). as in the present day Andes. Distribution of circa 2.3-1.88 sedimentary basins of this age is also located in the retro-arc region and the distribution, types of rocks, and associate with magmatic rocks are all similar to the modern day Andean system. Abbreviations as follows: AL – Alashan (Alxa); BD – Beidashan; DF – Denfeng; DWO – Dongwanzi Ophiolite; EH – Eastern Hebei; GY – Guyang; HS – Hengshan; LG – Langrim; LS – Longshoushan; QL – Qianlishan; SJ – Southern Jilin; WL – Western Liaoning; ZH – Zanhuang; ZUH - Zunhua.

Fig. 23. Stratigraphic section of Hutuo group, with ages of detrital zircons. Modified from Liu CH et al. (2011).

Fig. 24. NW-SE cross-section from based on residual gravity data across the Jiao-Liao-Ji Belt (modified from Peng C. et al., 2015), showing asymmetric shape of basin deepening to N, and complex thrust/normal fault system along the north margin. We interpret this as a retro-arc basin.

Fig. 25. (a) Map of Tibet with the trace of the outline of the NCC plotted over it for scale. Note in cross section (b) that the lower crust beneath Tibet is partially molten at depths similar to the present exposure level of the NCC. Thus, the formation of the many anatectic granites and high-grade metamorphism at this time (c) was analogous to processes currently going on beneath Tibet. Map (a) and cross-section (b) redrawn from Nelson et al., 1996. Metamorphic data compiled from Peng et al., 2014; Zhang et al., 2015; Wan et al., 2013, Wang et al., 2014, and Zhang et al., 2015 (Supplementary Data Table 3). Locations of anatectic melts and plutons of this age (d) are compiled from sources listed in Supplementary Data Table 4. Abbreviations as follows: BD – Beidashan; DF – Denfeng; EH – Eastern Hebei; FP – Fuping; FX – Fuxin; GY – Guyang; HS – Hengshan; JN – Jining; LS – Longshoushan; NH – Northern Hebei; ZH – Zanhuang; ZT – Zhongtiao.

Fig. 26. Cross-sections showing the tectonic development of the NCC at 1.93 and 1.8 Ga. Panel a shows the northern Andean-arc style margin of the NCC at 1.93, when the Yinshan Ribbon Microcontinent had been accreted, and the whole craton was under the influence of Andean margin style tectonics. A wide range of magmatic rocks intruded across the craton, and sedimentation in retroarc basins in Ordos, Hutuo, and Jiao Liao Ji had begun. As the ocean between the Columbia/Nuna Continent (perhaps the Siberian segment was impinging) was closing, an oceanic ridge in the ocean was subducted, causing the UHT metamorphism on the north margin of the craton at 1.92 Ga (Santosh and Kusky, 2010). Panel b shows the ultimate continent-continent collision between the Siberian segment of the Columbia/Nuna Continent with the NCC, resulting in craton-wide high-grade metamorphism, with HP granulite facies and

evidence for lower crustal flow during anatexis in the north, and medium-pressure granulite to amphibolite facies metamorphism in the center and southern parts of the craton. Widespread deformation and metamorphism during this event are the most widely recorded and preserved events from the craton.

Fig 27. Domal granitoid plutons in the Mesozoic Coast Range Complex, compared to domal granitoid plutons in the Archean Pilbara craton. The domes in Pilbara have been used to argue that plate tectonics operated fundamentally different in the Archean than in the Phanerozoic (Hamilton, 2003, 2007; Dewey, 2007; Van Kranendonk et al., 2004), but the rock types, structures, and scales are remarkably similar. We suggest that domal granitoids reflect more the specific tectonic environment rather than a global change in tectonic style. Panel a after Hildebrand (2013), panel b compiled from Geological Survey of Western Australia (1990) and Hamilton (2007).

Fig. 28. Comparison of orogens with linear tectonic styles in Neo-Archean and Paleozoic orogens. (a) the Paleozoic Newfoundland Appalachians, compared with (b) the Archean Yilgarn craton. (C) the Neoproterozoic-Paleozoic Central Asian Orogenic Belt (a.k.a. Altaids) compared to the Archean Superior craton. Note that the types of rocks and terranes, and the scales of the linear belts, are remarkably similar between the Archean and Paleozoic orogens. It cannot be argued that Neo-Archean tectonic style was fundamentally different from Phanerozoic tectonics.

Fig. 29. Stratigraphic/structural section of the North Pole area, Pilbara craton (drawn after Kitajima et al., 2008) along with U-Pb ages of units I-V showing that the 12 km thick section is comprised of five major thrust sheets each consisting of basalt capped by chert (ocean plate

stratigraphy, or OPS) that young in age downward, a relationship typical of accreted OPS in accretionary prisms of all ages (e.g., Kusky et al., 2013b). U-Pb data from Kitajima et al., 2008, and references therein. Ages of the Mount Ada Basalt are from van Kranendonk et al. (2006).

Fig. 30. Summary map of the North China craton showing the 2.5, 2.4, 2.3, and 1.9-1.85 Ga sutures discussed in text, as well as the 2.7-2.6 Ga tectonic boundaries in the Eastern Block proposed by Zhai (2011). Note that the North China craton grew by successive accretion of microblocks, arcs, oceanic plateaus, with progressively younger material added in a west to northwest direction. This style of Precambrian crustal growth is similar to that of the Superior Craton, and may signal a change from accretion of small archipelagos prior to 2.5 Ga, and addition of larger tectonic elements after that time in Earth history. Abbreviations as follows: BD – Beidashan; CD – Chengde; EH – Eastern Hebei; ES – Eastern Shandong; : FP – Fuping; HA- Huai'an; HS – Hengshan; LS – Longshoushan; MY – Miyun; NH – Northern Hebei; NL – Northern Liaoning; SJ – Southern Jilin; WC – Wuchuan; WL – Western Liaoning; WS Western Shandong; WT – Wutai; ZT – Zhongtiao.

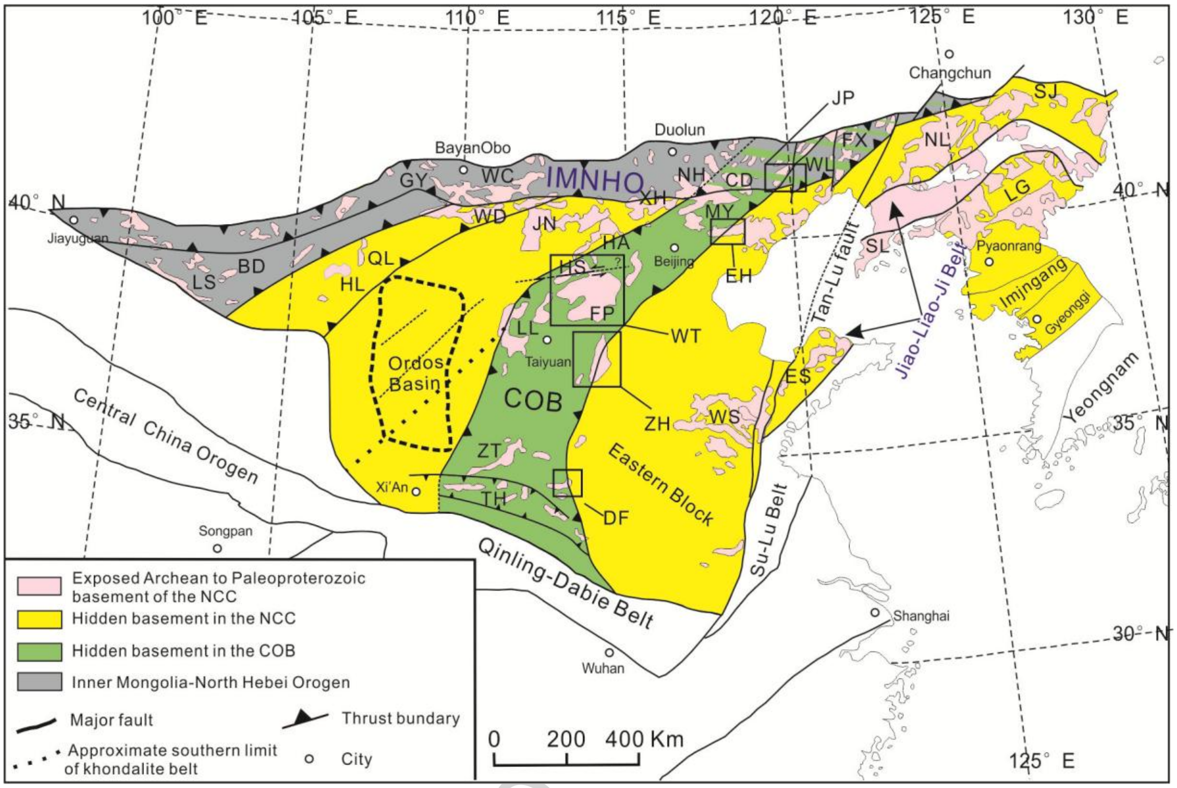

100° E
105° E
110° E
115° E
120° E
125° E
130° E
40° N
35° N
30° N
Changchun
JP
SJ
Duolun
BayanObo
FX
NL
GY
WC
IMNHO
NH
CD
WL
XH
LG
MY
Jiayuguan
WD
JN
HA
SL
Pyaonrang
LS
BD
QL
HS
Beijing
EH
Tan-Lu fault
Jiao-Liao-Ji Belt
Imjingang
HL
FP
WT
Gyeonggi
LL
Taiyuan
Ordos Basin
ES
Central China Orogen
COB
ZH
WS
Yeongnam
Eastern Block
ZT
Xi'An
TH
DF
Su-Lu Belt
Songpan
Qinling-Dabie Belt
Shanghai
Wuhan
Exposed Archean to Paleoproterozoic basement of the NCC
Hidden basement in the NCC
Hidden basement in the COB
Inner Mongolia-North Hebei Orogen
Major fault
Thrust bundary
Approximate southern limit of khondalite belt
City
0 200 400 Km
125° E

Figure 1

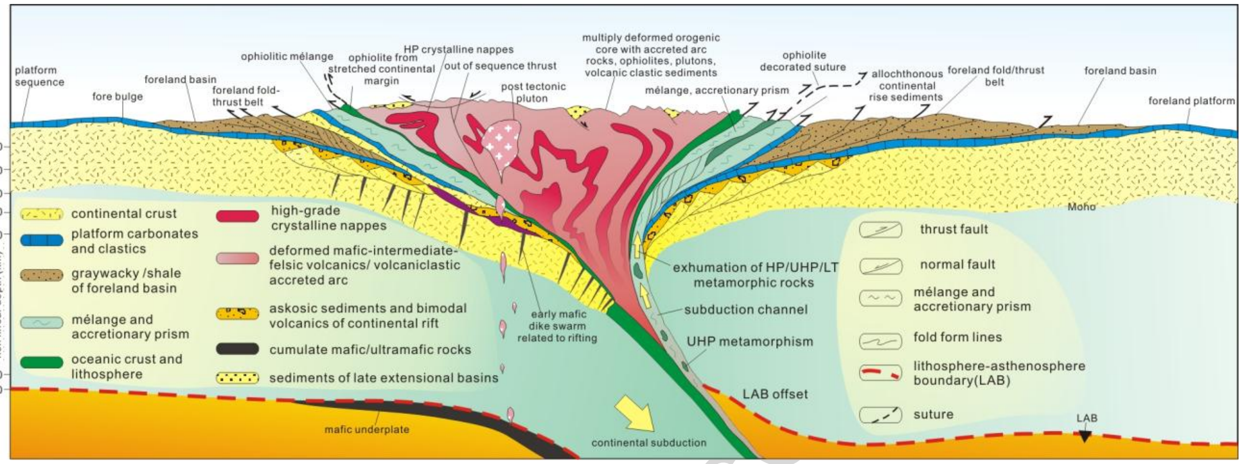
platform sequence
fore bulge
foreland basin
foreland fold-thrust belt
ophiolitic mélange
ophiolite from stretched continental margin
HP crystalline nappes
out of sequence thrust
post tectonic pluton
multiply deformed orogenic core with accreted arc rocks, ophiolites, plutons, volcanic clastic sediments
mélange, accretionary prism
ophiolite decorated suture
allochthonous continental rise sediments
foreland fold/thrust belt
foreland basin
foreland platform
Moho
10
20
30
40
50
120
300
non linear depth (km)
continental crust
platform carbonates and clastics
graywacky /shale of foreland basin
mélange and accretionary prism
oceanic crust and lithosphere
high-grade crystalline nappes
deformed mafic-intermediate-felsic volcanics/ volcaniclastic accreted arc
askosic sediments and bimodal volcanics of continental rift
cumulate mafic/ultramafic rocks
sediments of late extensional basins
early mafic dike swarm related to rifting
exhumation of HP/UHP/LT metamorphic rocks
subduction channel
UHP metamorphism
LAB offset
thrust fault
normal fault
mélange and accretionary prism
fold form lines
lithosphere-asthenosphere boundary(LAB)
suture
LAB
mafic underplate
continental subduction
Figure 2

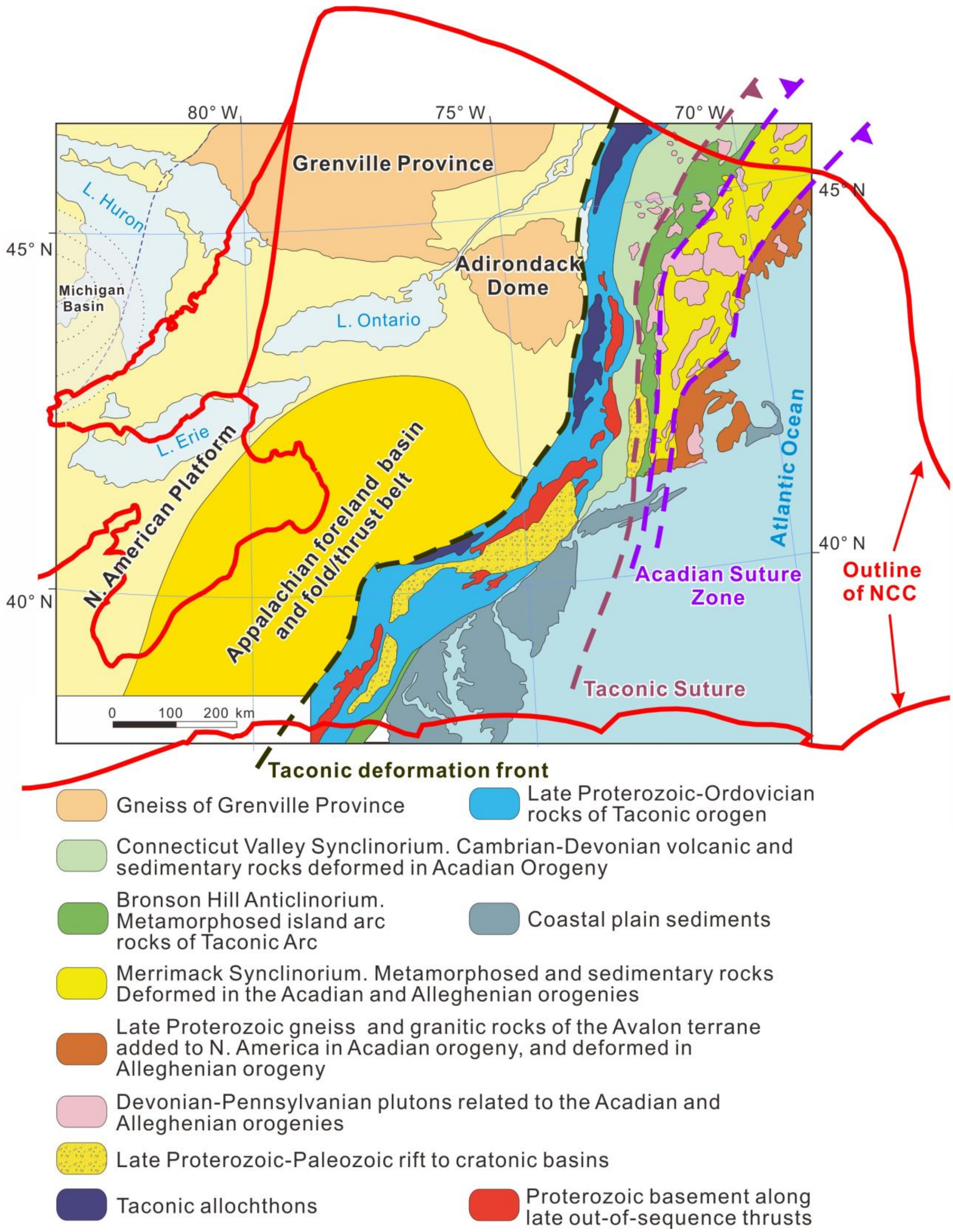
80° W
75° W
70° W
45° N
40° N
45° N
40° N
Grenville Province
L. Huron
Michigan Basin
Adirondack Dome
L. Ontario
L. Erie
N. American Platform
Appalachian foreland basin and fold/thrust belt
Atlantic Ocean
Acadian Suture Zone
Taconic Suture
Outline of NCC
0 100 200 km
Taconic deformation front
Gneiss of Grenville Province
Late Proterozoic-Ordovician rocks of Taconic orogen
Connecticut Valley Synclinorium. Cambrian-Devonian volcanic and sedimentary rocks deformed in Acadian Orogeny
Bronson Hill Anticlinorium. Metamorphosed island arc rocks of Taconic Arc
Coastal plain sediments
Merrimack Synclinorium. Metamorphosed and sedimentary rocks Deformed in the Acadian and Alleghenian orogenies
Late Proterozoic gneiss and granitic rocks of the Avalon terrane added to N. America in Acadian orogeny, and deformed in Alleghenian orogeny
Devonian-Pennsylvanian plutons related to the Acadian and Alleghenian orogenies
Late Proterozoic-Paleozoic rift to cratonic basins
Taconic allochthons
Proterozoic basement along late out-of-sequence thrusts

Figure 3

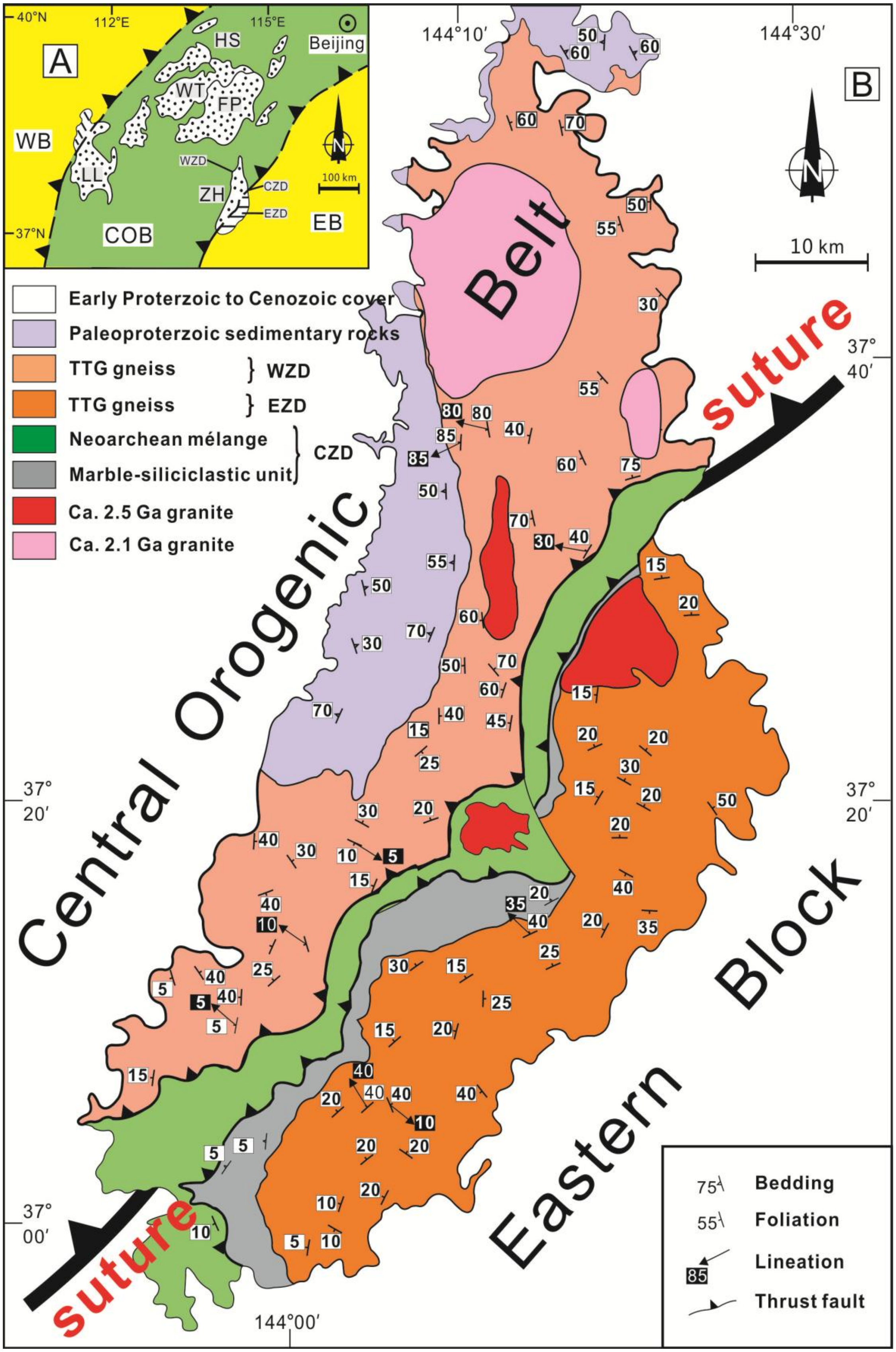

A
B
40°N
112°E
115°E
37°N
Beijing
HS
WT
FP
WB
LL
WZD
ZH
CZD
EZD
EB
COB
100 km
144°10′
144°30′
144°00′
37° 40′
37° 20′
37° 00′
10 km
Early Proterzoic to Cenozoic cover
Paleoproterzoic sedimentary rocks
TTG gneiss } WZD
TTG gneiss } EZD
Neoarchean mélange
Marble-siliciclastic unit
CZD
Ca. 2.5 Ga granite
Ca. 2.1 Ga granite
Central Orogenic Belt
Eastern Block
suture
suture
Bedding
Foliation
Lineation
Thrust fault

Figure 4

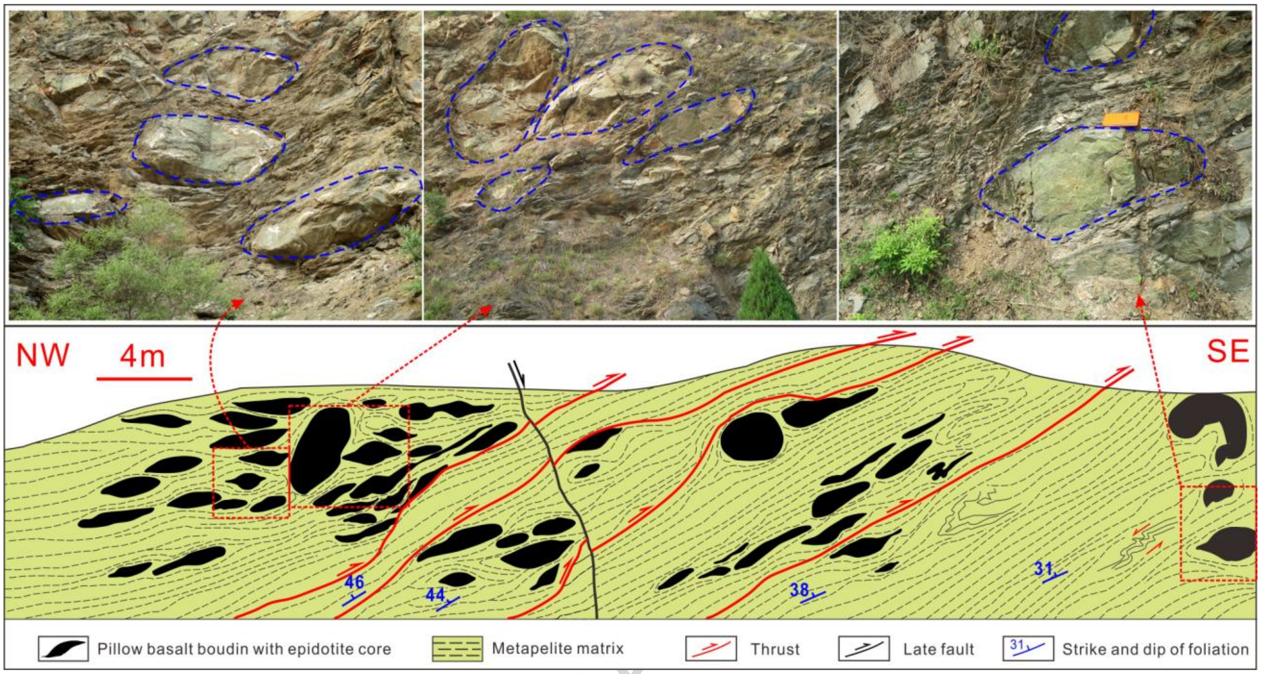
NW
4m
SE
46
44
38
31
Pillow basalt boudin with epidotite core
Metapelite matrix
Thrust
Late fault
Strike and dip of foliation

Figure 5

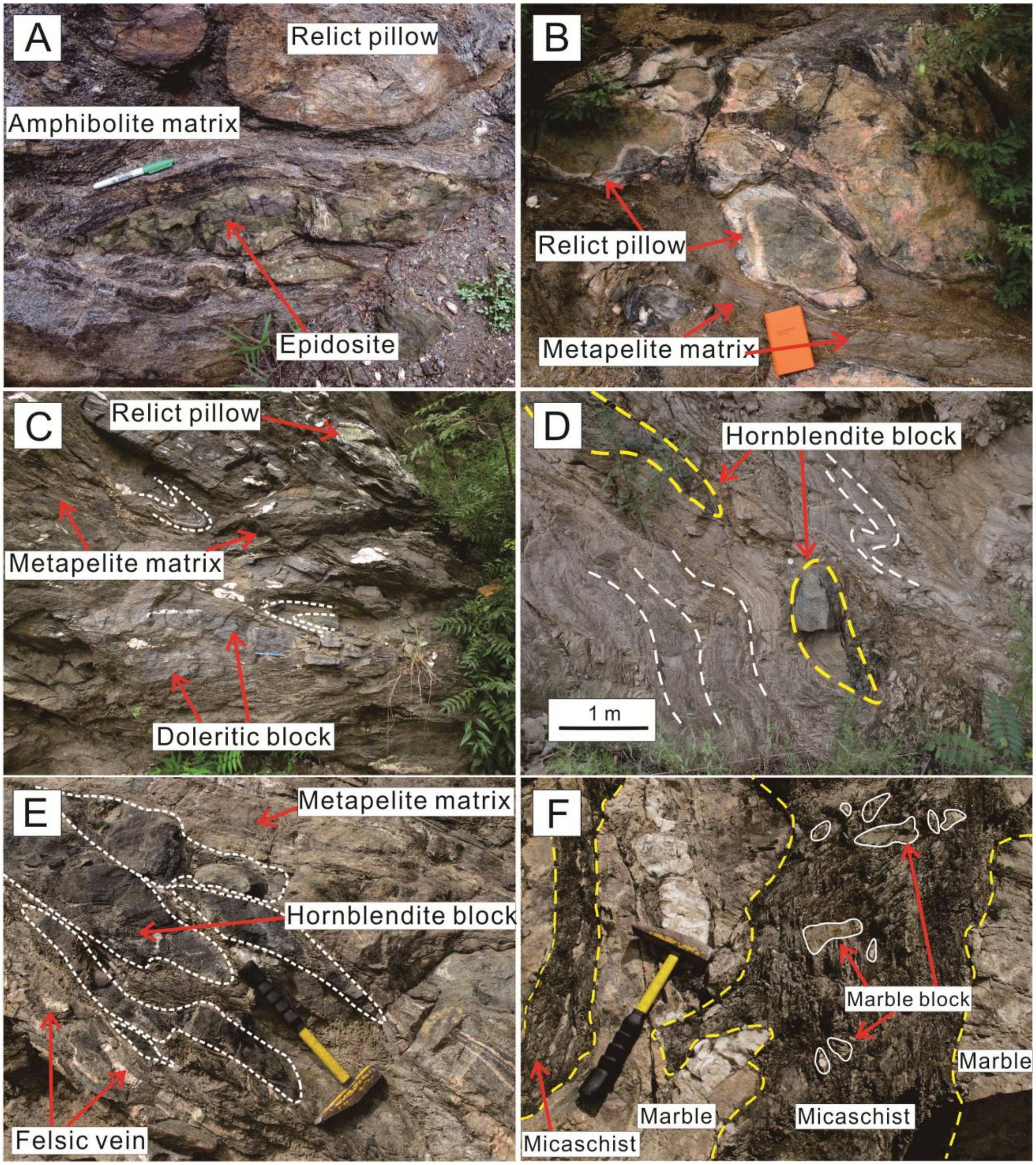
A
Relict pillow
Amphibolite matrix
Epidosite
B
Relict pillow
Metapelite matrix
C
Relict pillow
Metapelite matrix
Doleritic block
D
Hornblendite block
1 m
E
Metapelite matrix
Hornblendite block
Felsic vein
F
Marble block
Marble
Marble
Micaschist
Micaschist

Figure 6

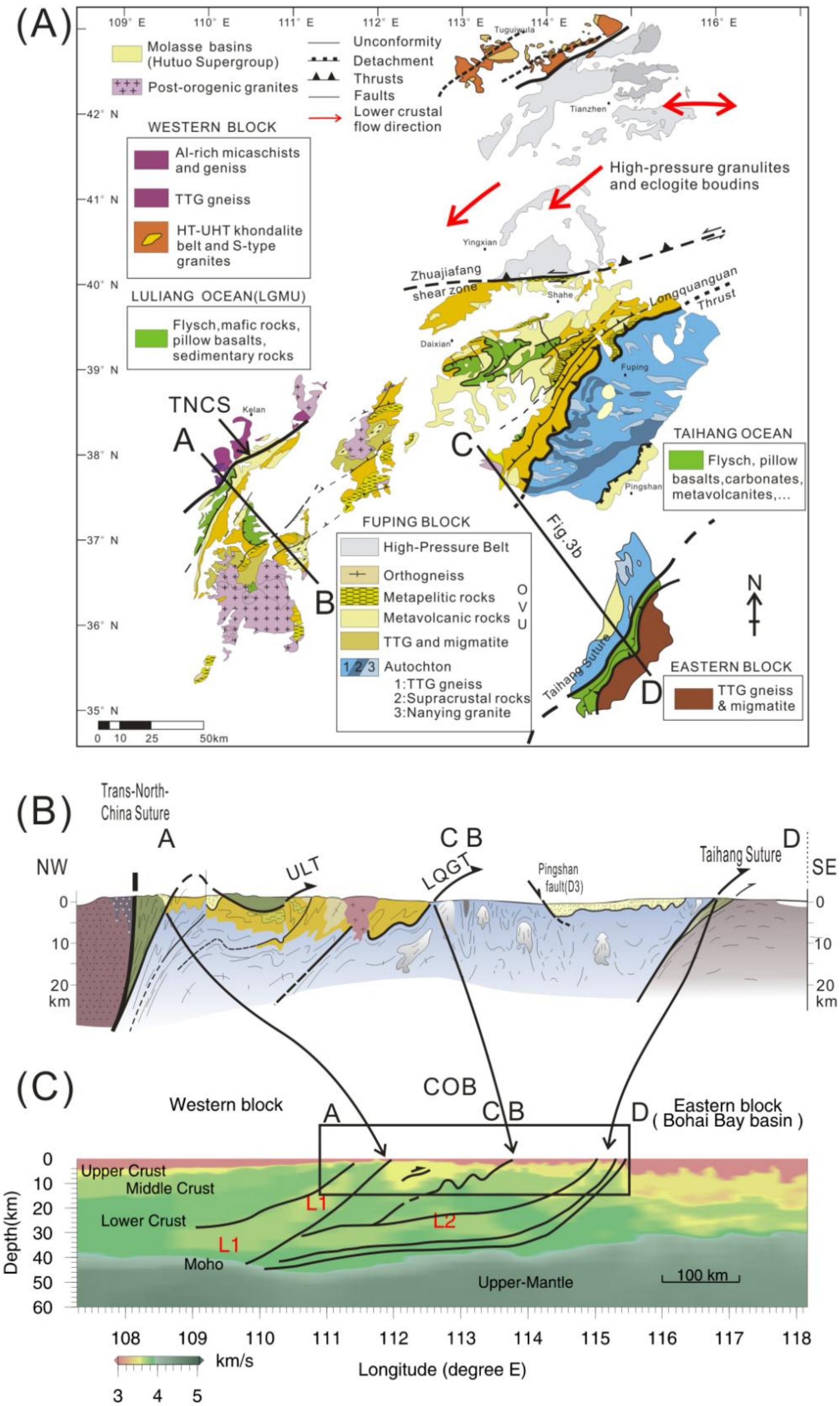

(A)
Molasse basins (Hutuo Supergroup)
Post-orogenic granites
Unconformity
Detachment
Thrusts
Faults
Lower crustal flow direction
WESTERN BLOCK
Al-rich micaschists and geniss
TTG gneiss
HT-UHT khondalite belt and S-type granites
LULIANG OCEAN(LGMU)
Flysch,mafic rocks, pillow basalts, sedimentary rocks
High-pressure granulites and eclogite boudins
Zhuajiafang shear zone
Longquanguan Thrust
TNCS
TAIHANG OCEAN
Flysch, pillow basalts,carbonates, metavolcanites,...
FUPING BLOCK
High-Pressure Belt
Orthogneiss
Metapelitic rocks
Metavolcanic rocks
TTG and migmatite
Autochton
1:TTG gneiss
2:Supracrustal rocks
3:Nanying granite
Fig.3b
Taihang Suture
EASTERN BLOCK
TTG gneiss & migmatite
(B)
Trans-North-China Suture
NW
SE
ULT
LQGT
Pingshan fault(D3)
Taihang Suture
(C)
Western block
COB
Eastern block (Bohai Bay basin)
Upper Crust
Middle Crust
Lower Crust
Moho
Upper-Mantle
Depth(km)
100 km
km/s
Longitude (degree E)

Figure 7

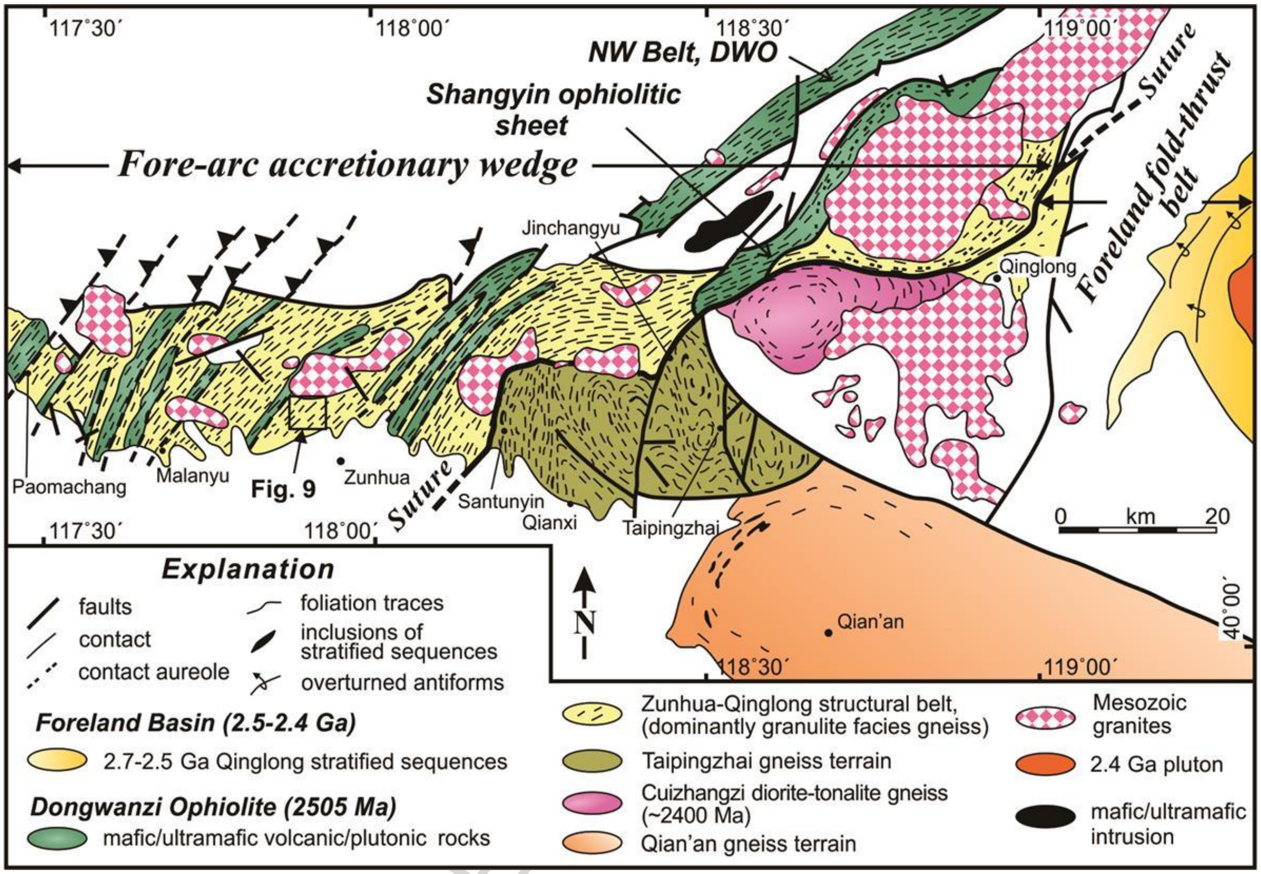
117°30´
118°00´
118°30´
119°00´
NW Belt, DWO
Shangyin ophiolitic sheet
Fore-arc accretionary wedge
Suture
Foreland fold-thrust belt
Jinchangyu
Qinglong
Paomachang
Malanyu
Fig. 9
Zunhua
Suture
Santunyin
Qianxi
Taipingzhai
0 km 20
N
Qian'an
40°00´
Explanation
faults
contact
contact aureole
foliation traces
inclusions of stratified sequences
overturned antiforms
Foreland Basin (2.5-2.4 Ga)
2.7-2.5 Ga Qinglong stratified sequences
Dongwanzi Ophiolite (2505 Ma)
mafic/ultramafic volcanic/plutonic rocks
Zunhua-Qinglong structural belt, (dominantly granulite facies gneiss)
Taipingzhai gneiss terrain
Cuizhangzi diorite-tonalite gneiss (~2400 Ma)
Qian'an gneiss terrain
Mesozoic granites
2.4 Ga pluton
mafic/ultramafic intrusion
Figure 8

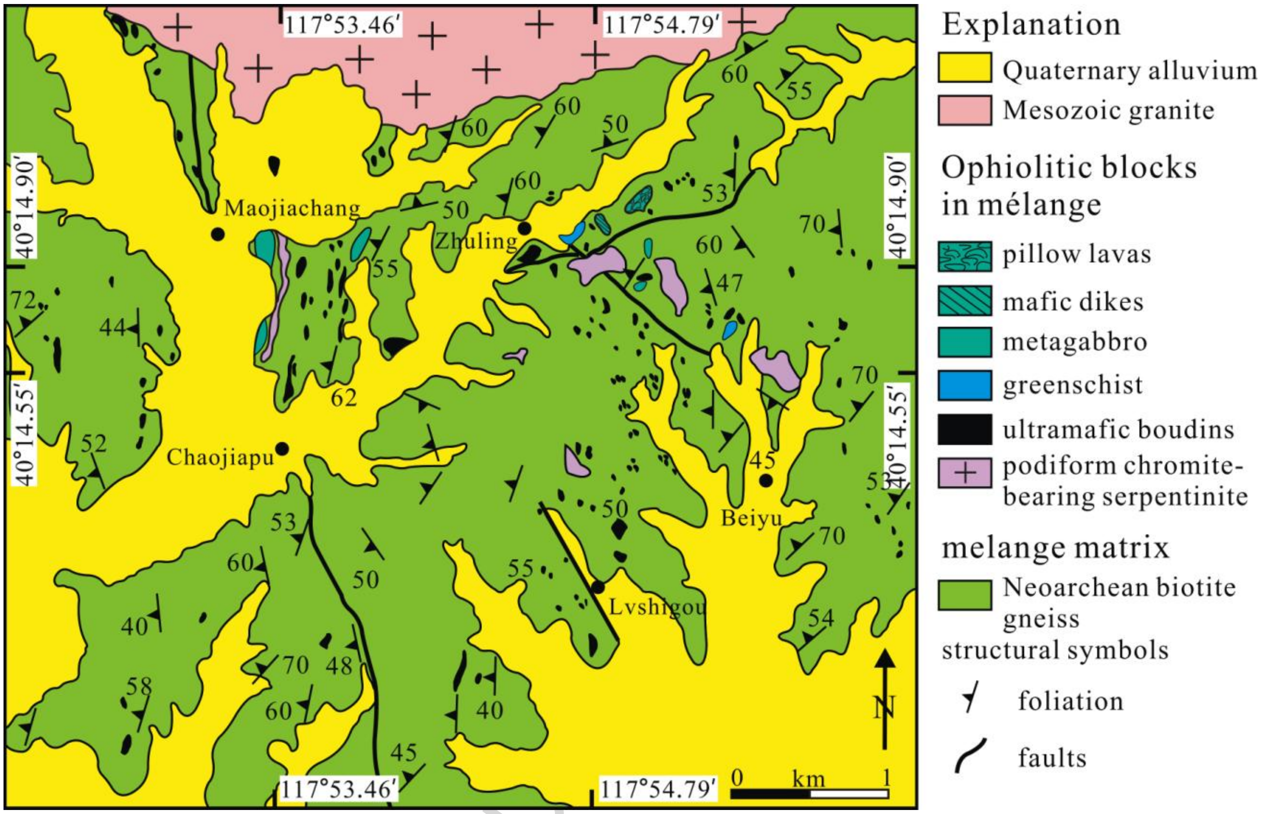
117°53.46′
117°54.79′
40°14.90′
40°14.55′
Maojiachang
Zhuling
Chaojiapu
Beiyu
Lvshigou
N
0 km 1
Explanation
Quaternary alluvium
Mesozoic granite
Ophiolitic blocks in mélange
pillow lavas
mafic dikes
metagabbro
greenschist
ultramafic boudins
podiform chromite-bearing serpentinite
melange matrix
Neoarchean biotite gneiss
structural symbols
foliation
faults

Figure 9

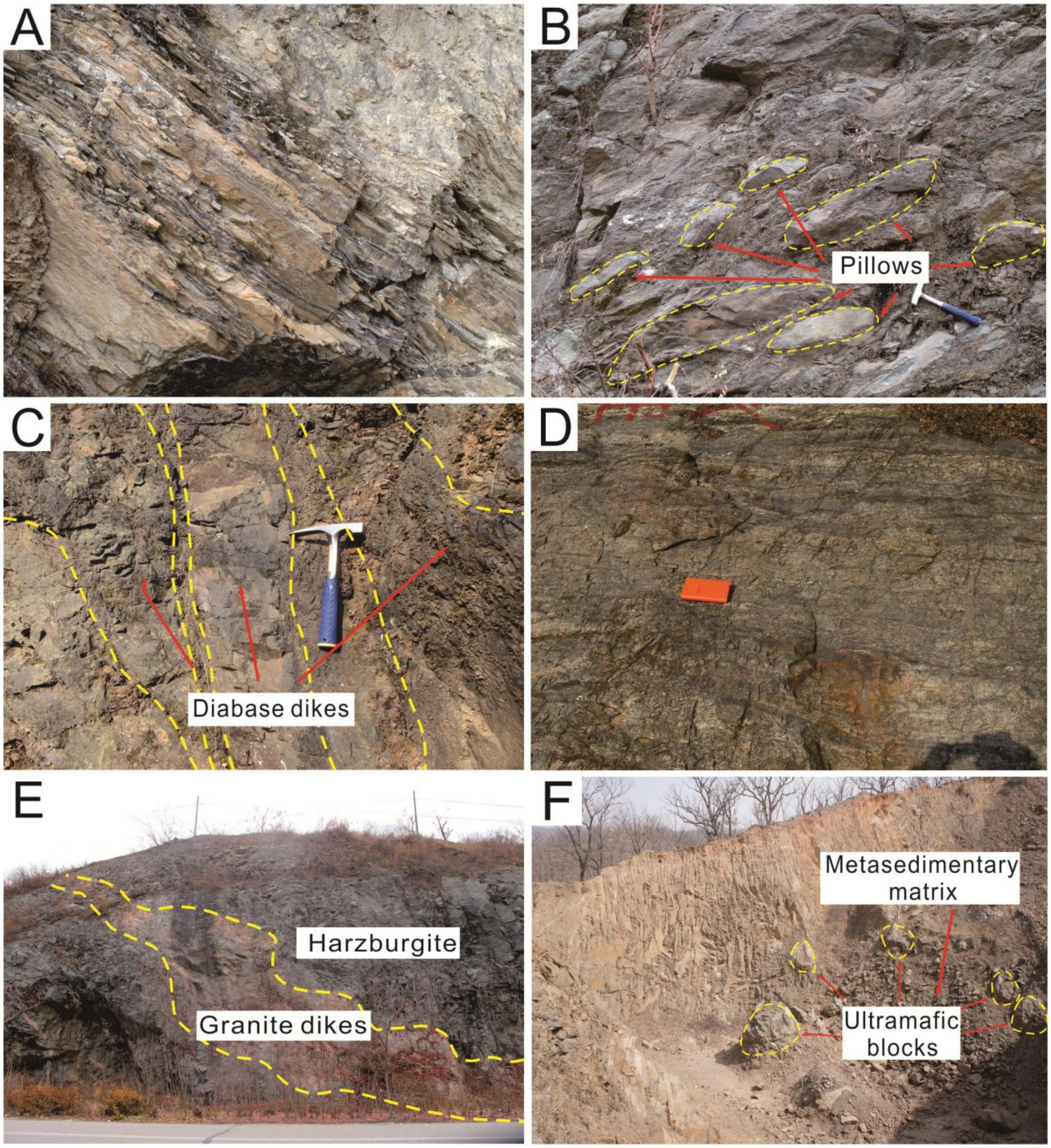
A
B
Pillows
C
Diabase dikes
D
E
Harzburgite
Granite dikes
F
Metasedimentary matrix
Ultramafic blocks

Figure 10

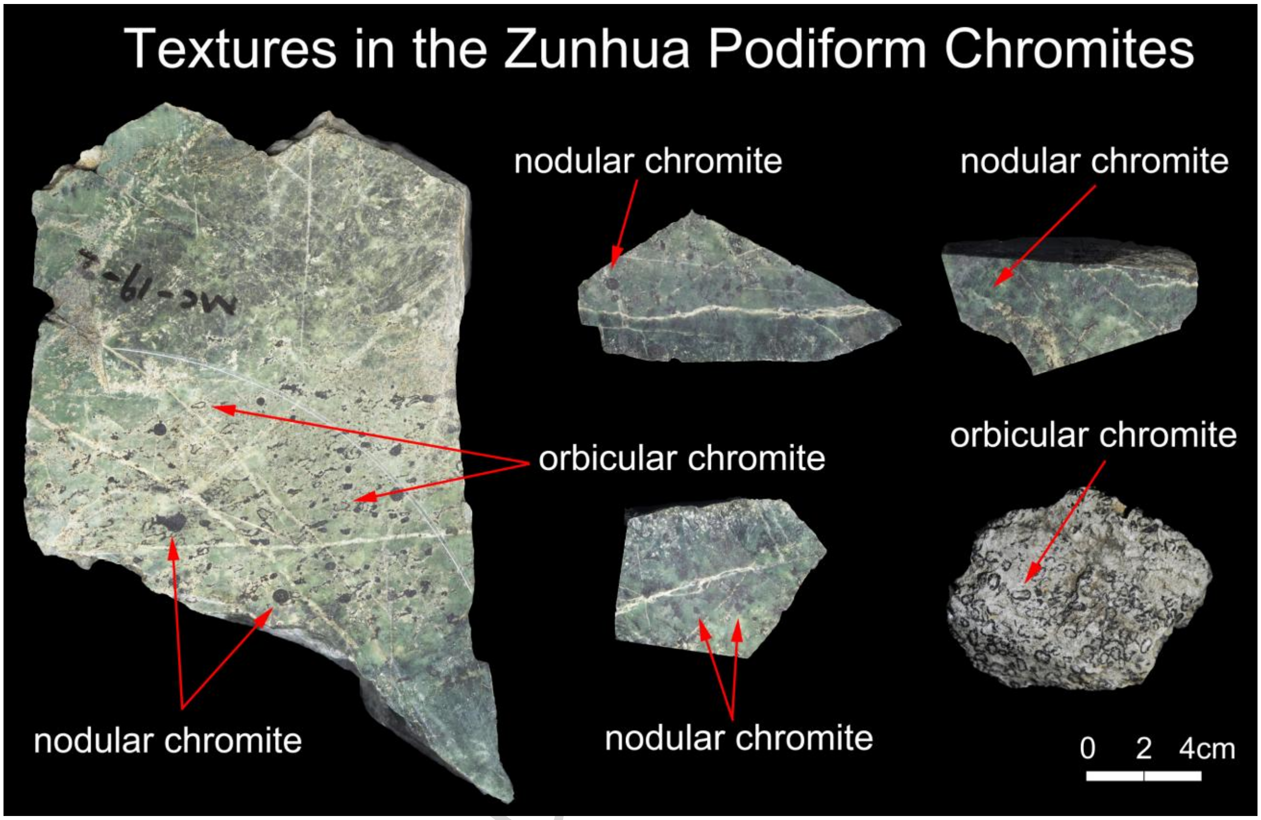
Textures in the Zunhua Podiform Chromites
MC-19-2
nodular chromite
nodular chromite
orbicular chromite
orbicular chromite
nodular chromite
nodular chromite
0 2 4cm

Figure 11

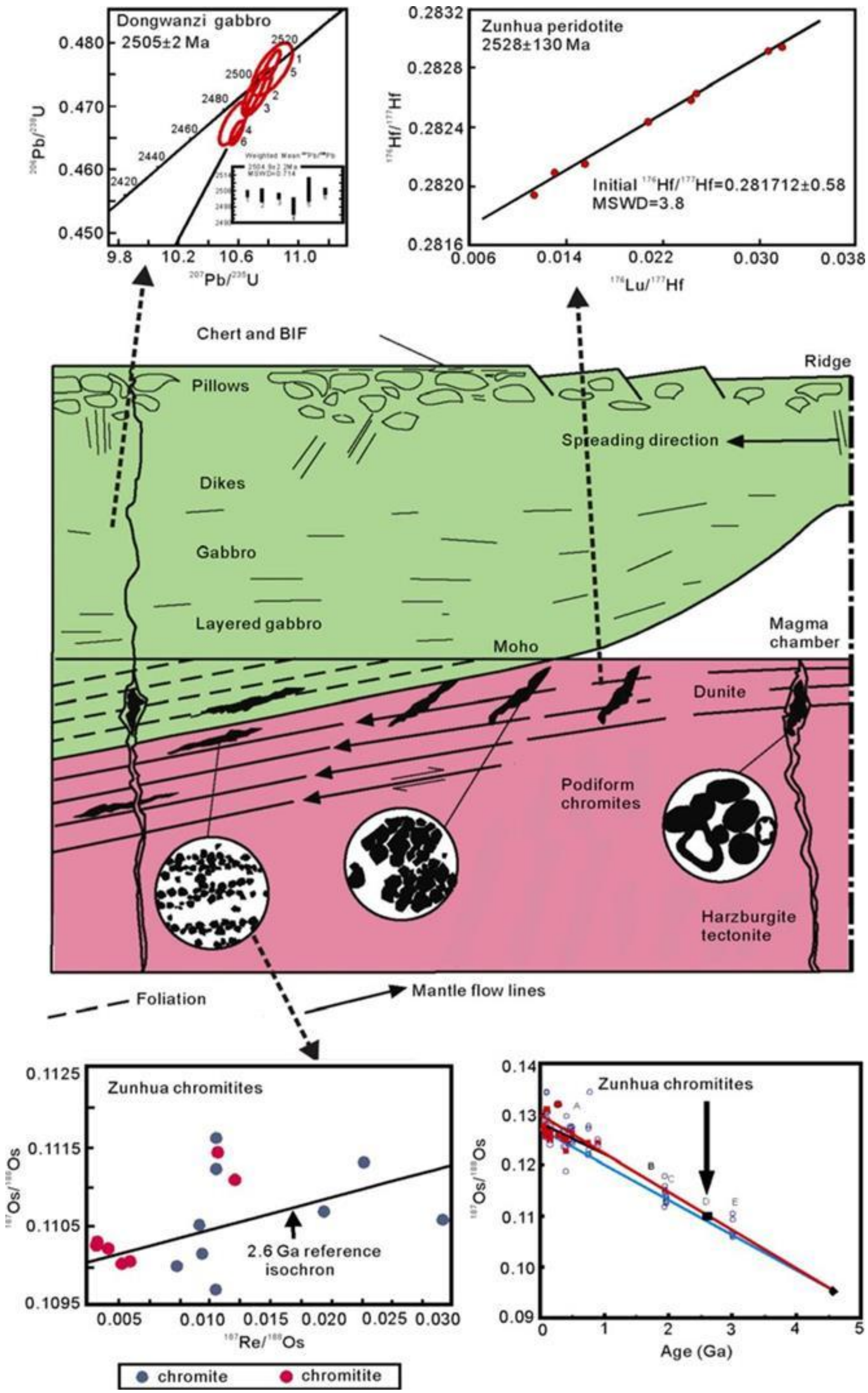

Dongwanzi gabbro
2505±2 Ma
$^{206}Pb/^{238}U$
$^{207}Pb/^{235}U$
Zunhua peridotite
2528±130 Ma
Initial $^{176}Hf/^{177}Hf$=0.281712±0.58
MSWD=3.8
$^{176}Hf/^{177}Hf$
$^{176}Lu/^{177}Hf$
Chert and BIF
Ridge
Pillows
Spreading direction
Dikes
Gabbro
Layered gabbro
Moho
Magma chamber
Dunite
Podiform chromites
Harzburgite tectonite
Foliation
Mantle flow lines
Zunhua chromitites
2.6 Ga reference isochron
$^{187}Os/^{188}Os$
$^{187}Re/^{188}Os$
Age (Ga)
chromite
chromitite

Figure 12

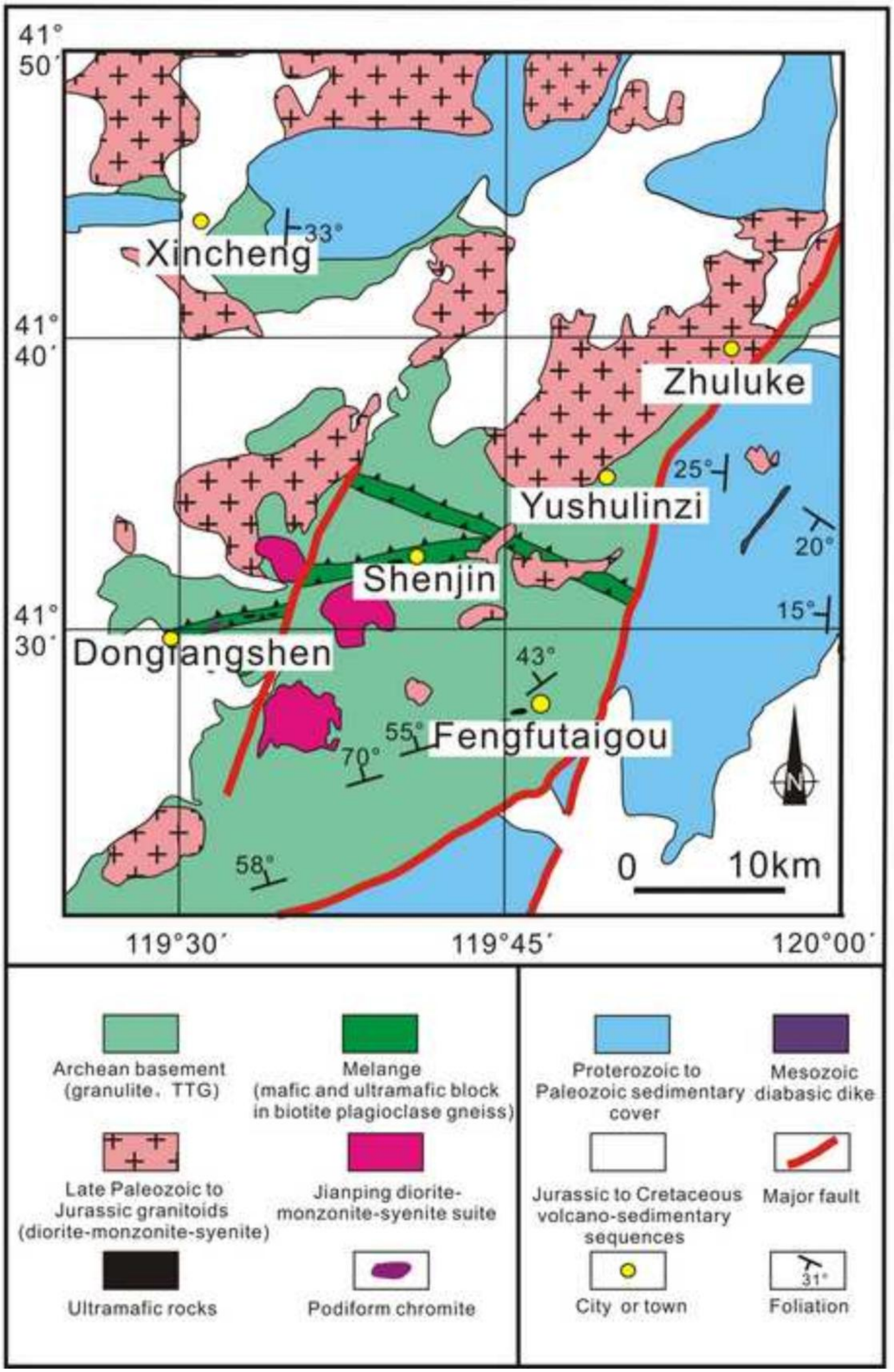
41° 50′
41° 40′
41° 30′
119°30′
119°45′
120°00′
Xincheng
Zhuluke
Yushulinzi
Shenjin
Dongfangshen
Fengfutaigou
33°
25°
20°
15°
43°
55°
70°
58°
0 10km
N
Archean basement (granulite, TTG)
Melange (mafic and ultramafic block in biotite plagioclase gneiss)
Proterozoic to Paleozoic sedimentary cover
Mesozoic diabasic dike
Late Paleozoic to Jurassic granitoids (diorite-monzonite-syenite)
Jianping diorite-monzonite-syenite suite
Jurassic to Cretaceous volcano-sedimentary sequences
Major fault
Ultramafic rocks
Podiform chromite
City or town
31°
Foliation

Figure 13

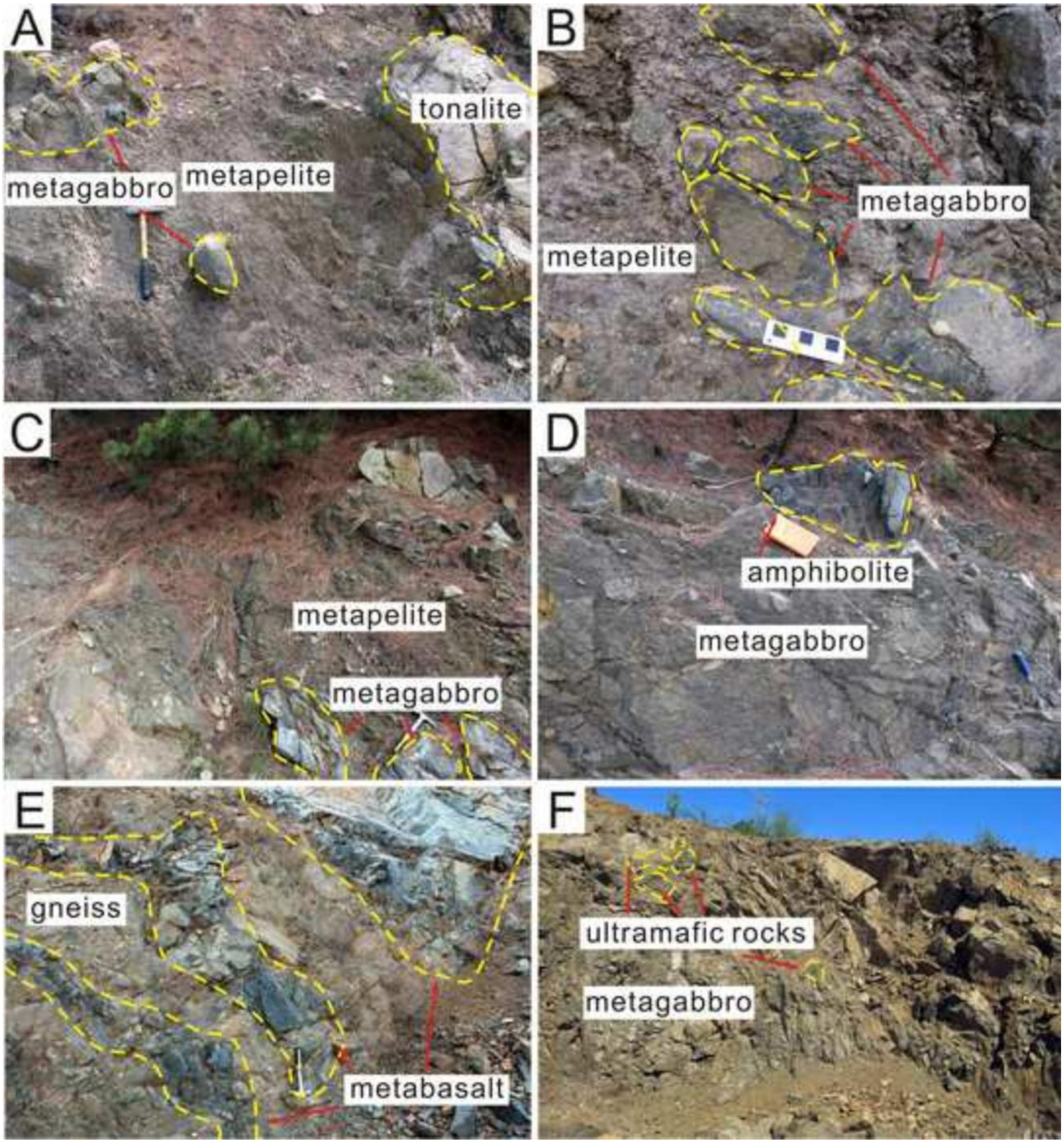
A
B
C
D
E
F
tonalite
metagabbro
metapelite
metagabbro
metapelite
metapelite
metagabbro
amphibolite
metagabbro
gneiss
metabasalt
ultramafic rocks
metagabbro

Figure 14

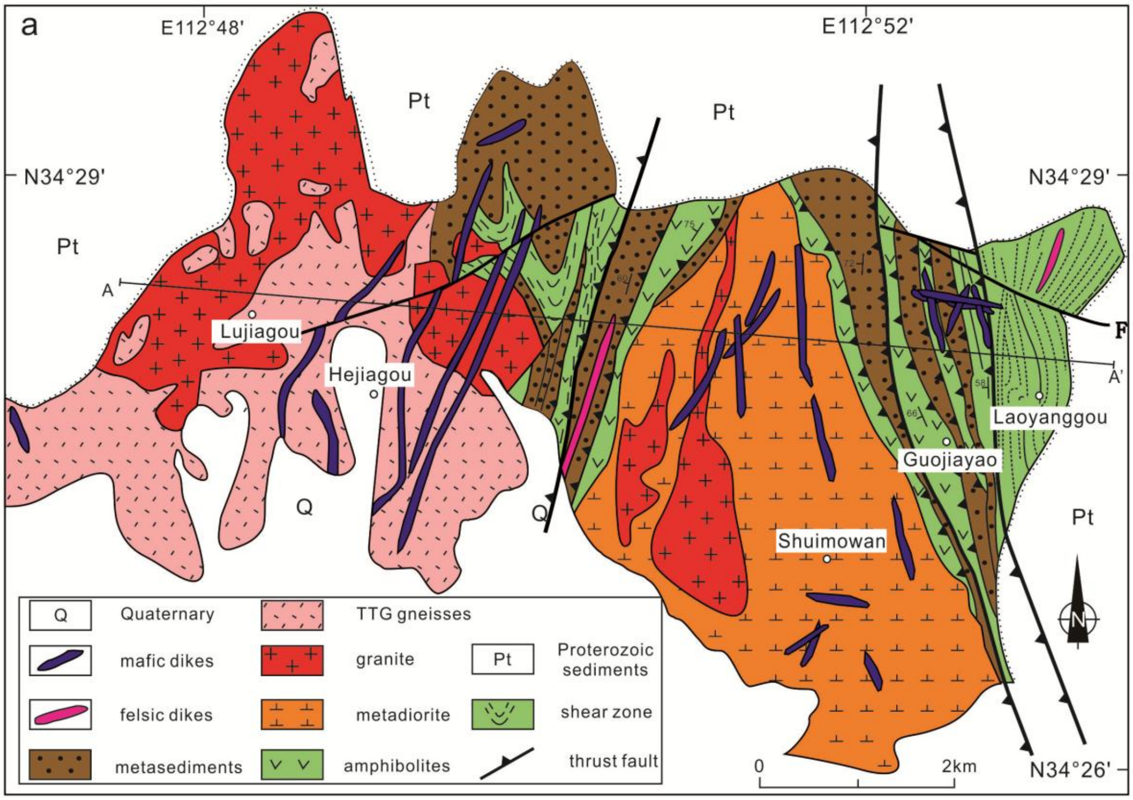
a
E112°48'
E112°52'
N34°29'
N34°29'
N34°26'
Pt
Pt
Pt
Pt
Pt
A
A'
F
Lujiagou
Hejiagou
Q
Q
Shuimowan
Guojiayao
Laoyanggou
Q
Quaternary
TTG gneisses
mafic dikes
granite
Pt
Proterozoic sediments
felsic dikes
metadiorite
shear zone
metasediments
amphibolites
thrust fault
0
2km
N

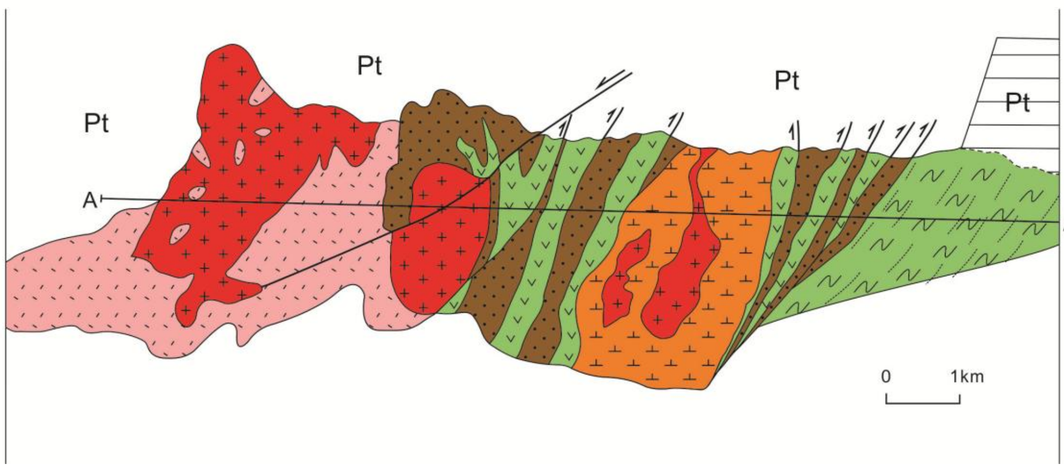
Pt
Pt
Pt
Pt
A
A'
0
1km

Figure 15

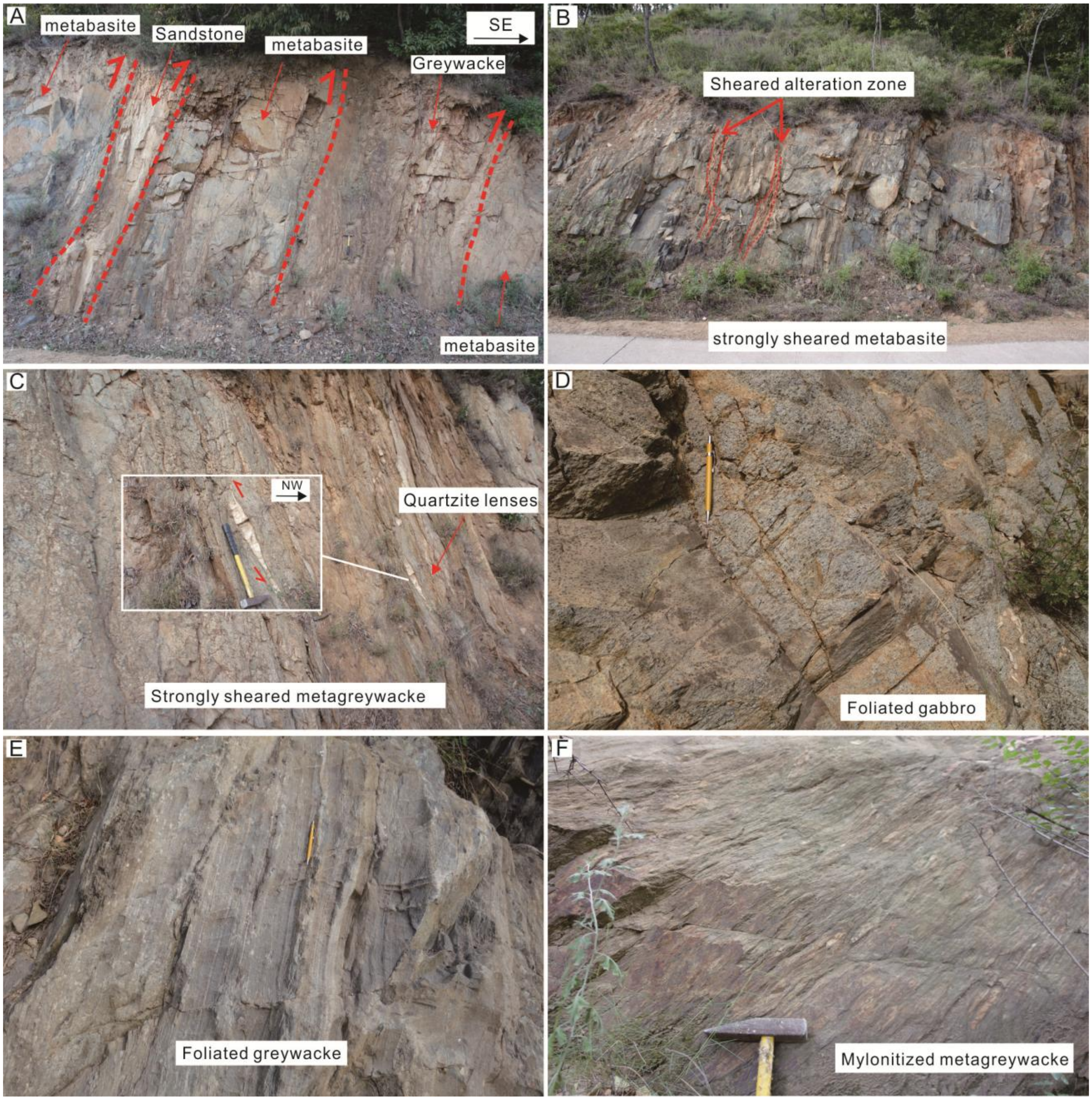
A
metabasite
Sandstone
metabasite
SE
Greywacke
metabasite
B
Sheared alteration zone
strongly sheared metabasite
C
NW
Quartzite lenses
Strongly sheared metagreywacke
D
Foliated gabbro
E
Foliated greywacke
F
Mylonitized metagreywacke

Figure 16

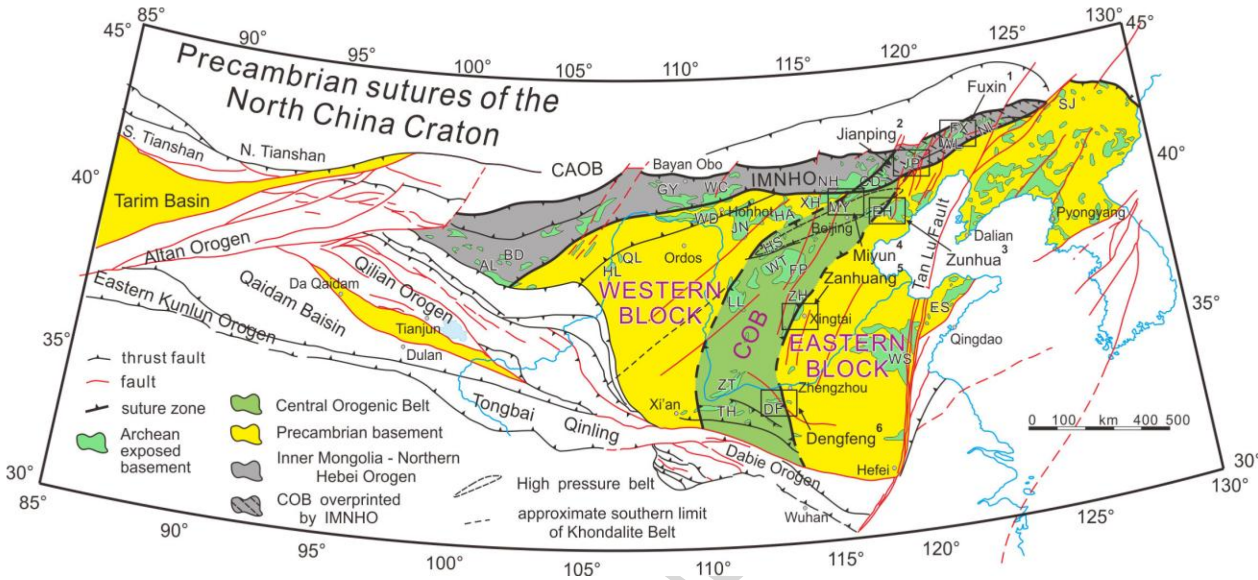
Precambrian sutures of the North China Craton
S. Tianshan
N. Tianshan
Tarim Basin
CAOB
Altan Orogen
Eastern Kunlun Orogen
Qaidam Baisin
Qilian Orogen
Da Qaidam
Tianjun
Dulan
Bayan Obo
IMNHO
Fuxin
Jianping
Hohhot
Beijing
Ordos
WESTERN BLOCK
COB
EASTERN BLOCK
Miyun
Zanhuang
Zunhua
Tan Lu Fault
Dalian
Pyongyang
Qingdao
Xingtai
Zhengzhou
Xi'an
Dengfeng
Tongbai
Qinling
Dabie Orogen
Hefei
Wuhan
thrust fault
fault
suture zone
Archean exposed basement
Central Orogenic Belt
Precambrian basement
Inner Mongolia - Northern Hebei Orogen
COB overprinted by IMNHO
High pressure belt
approximate southern limit of Khondalite Belt
0 100 km 400 500

Figure 17

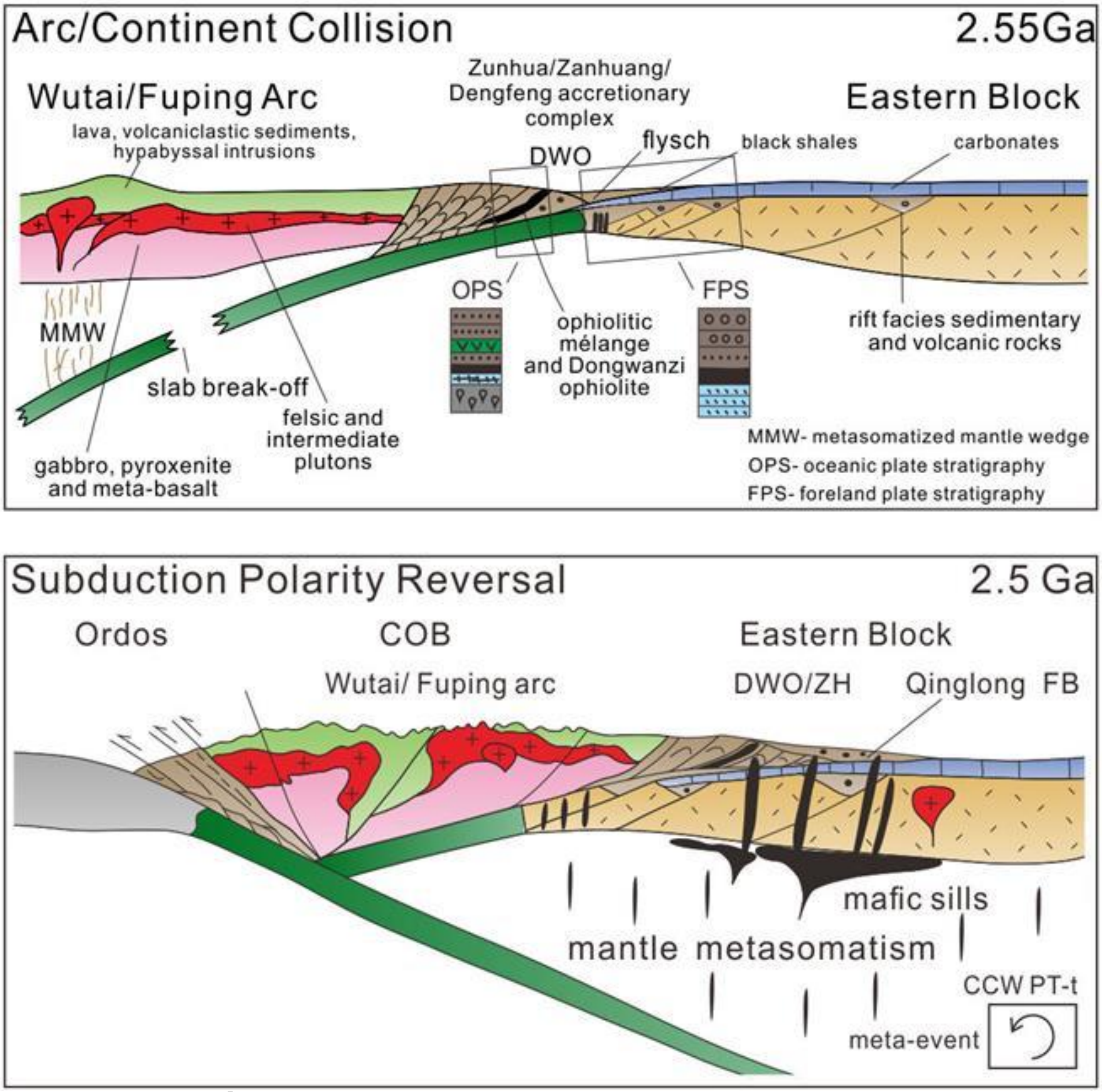

Arc/Continent Collision
2.55Ga
Wutai/Fuping Arc
lava, volcaniclastic sediments, hypabyssal intrusions
Zunhua/Zanhuang/ Dengfeng accretionary complex
Eastern Block
DWO
flysch
black shales
carbonates
OPS
FPS
MMW
ophiolitic mélange and Dongwanzi ophiolite
rift facies sedimentary and volcanic rocks
slab break-off
felsic and intermediate plutons
gabbro, pyroxenite and meta-basalt
MMW- metasomatized mantle wedge
OPS- oceanic plate stratigraphy
FPS- foreland plate stratigraphy
Subduction Polarity Reversal
2.5 Ga
Ordos
COB
Eastern Block
Wutai/ Fuping arc
DWO/ZH
Qinglong FB
mafic sills
mantle metasomatism
CCW PT-t
meta-event

Figure 18

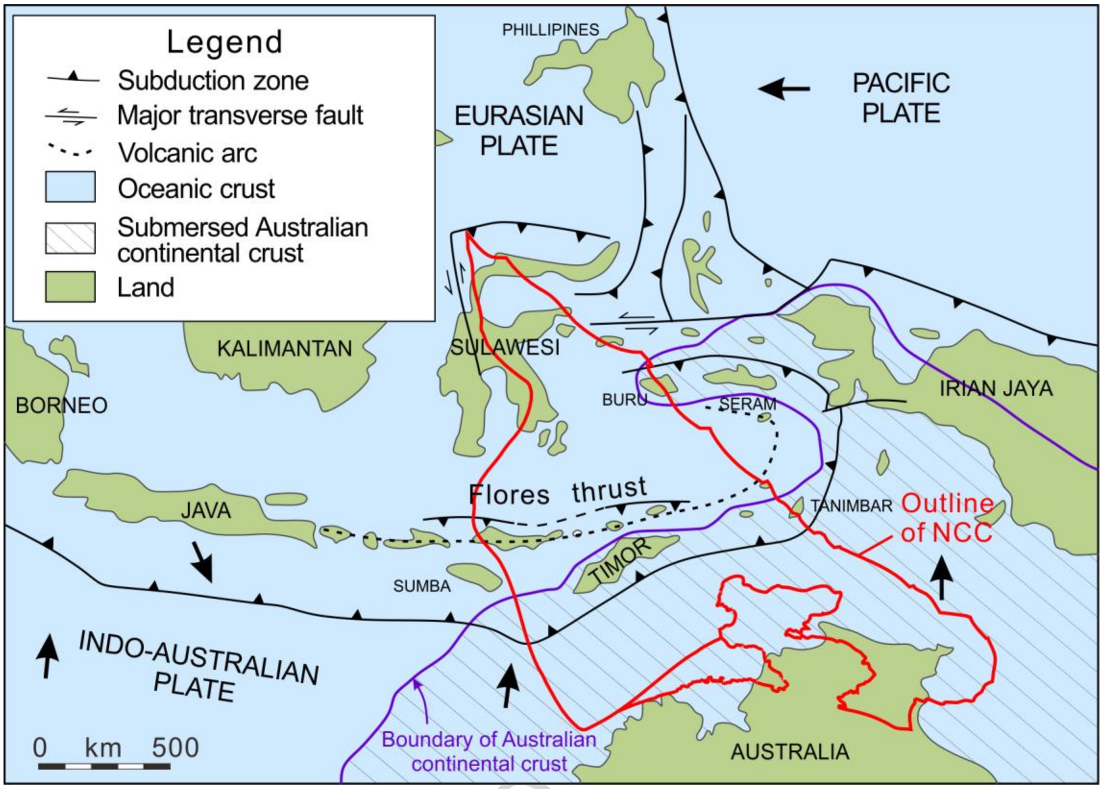

Legend
Subduction zone
Major transverse fault
Volcanic arc
Oceanic crust
Submersed Australian continental crust
Land
PHILLIPINES
EURASIAN PLATE
PACIFIC PLATE
KALIMANTAN
SULAWESI
BORNEO
BURU
SERAM
IRIAN JAYA
JAVA
Flores thrust
TANIMBAR
Outline of NCC
SUMBA
TIMOR
INDO-AUSTRALIAN PLATE
0 km 500
Boundary of Australian continental crust
AUSTRALIA

Figure 19

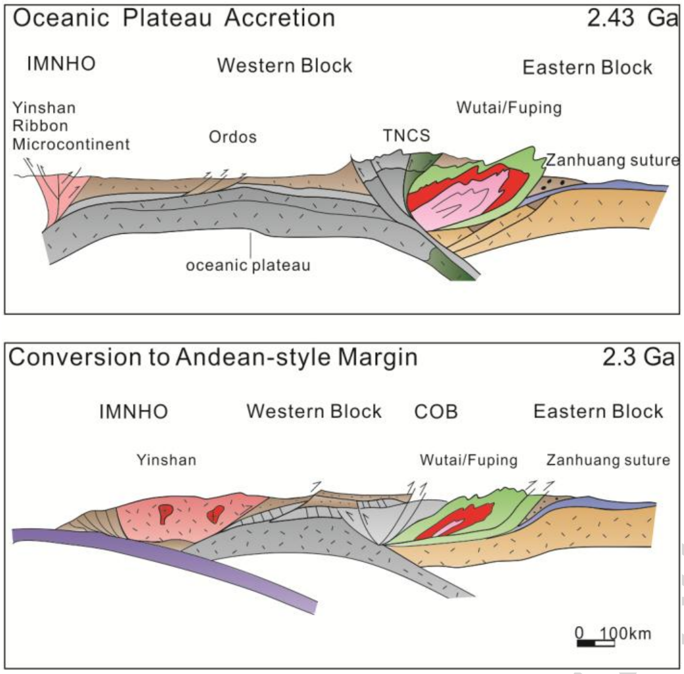
Oceanic Plateau Accretion
2.43 Ga
IMNHO
Western Block
Eastern Block
Yinshan
Ribbon
Microcontinent
Ordos
TNCS
Wutai/Fuping
Zanhuang suture
oceanic plateau
Conversion to Andean-style Margin
2.3 Ga
IMNHO
Western Block
COB
Eastern Block
Yinshan
Wutai/Fuping
Zanhuang suture
0
100km

Figure 20

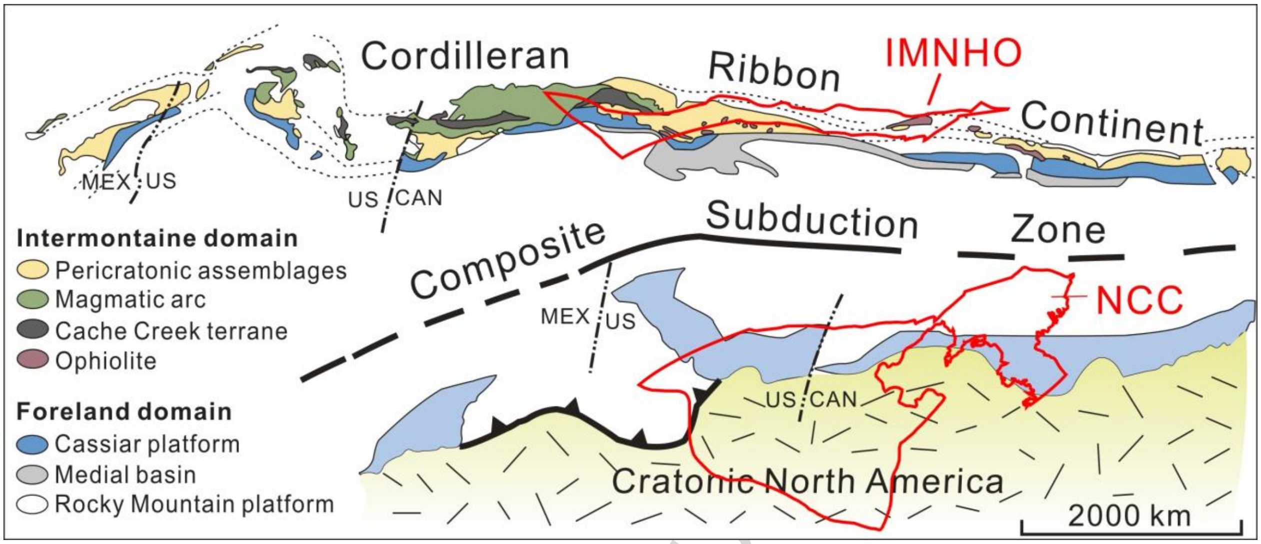

Cordilleran
Ribbon
Continent
IMNHO
MEX
US
US
CAN
Intermontaine domain
Pericratonic assemblages
Magmatic arc
Cache Creek terrane
Ophiolite
Foreland domain
Cassiar platform
Medial basin
Rocky Mountain platform
Composite
Subduction
Zone
MEX
US
NCC
US
CAN
Cratonic North America
2000 km

Figure 21

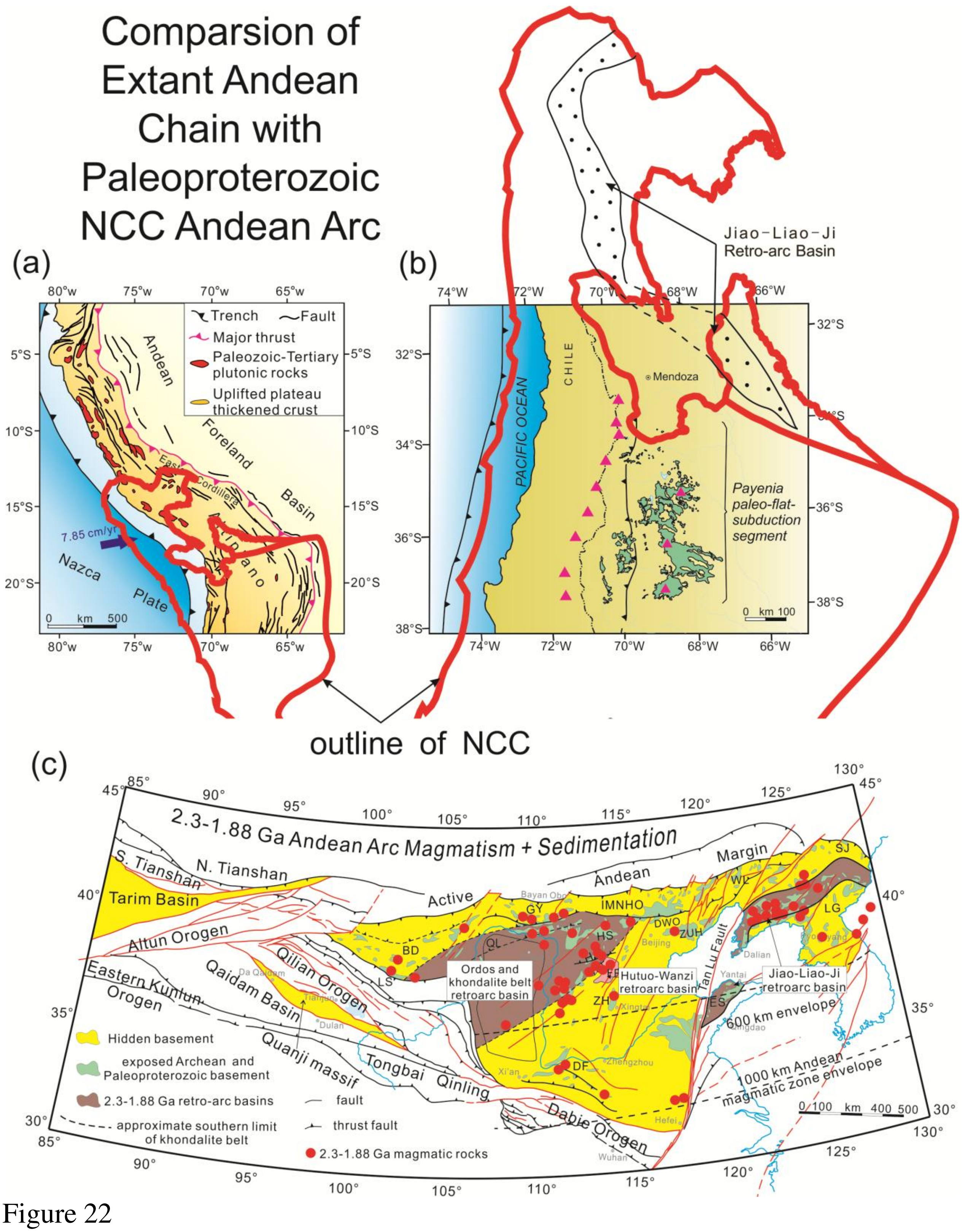

Comparsion of Extant Andean Chain with Paleoproterozoic NCC Andean Arc
(a)
(b)
Trench
Fault
Major thrust
Paleozoic-Tertiary plutonic rocks
Uplifted plateau thickened crust
Andean Foreland Basin
7.85 cm/yr
Nazca Plate
Jiao-Liao-Ji Retro-arc Basin
PACIFIC OCEAN
CHILE
Mendoza
Payenia paleo-flat-subduction segment
outline of NCC
(c)
2.3-1.88 Ga Andean Arc Magmatism + Sedimentation
Active Andean Margin
S. Tianshan
N. Tianshan
Tarim Basin
Altun Orogen
Eastern Kunlun Orogen
Qaidam Basin
Qilian Orogen
Quanji massif
Tongbai
Qinling
Dabie Orogen
Tan Lu Fault
Ordos and khondalite belt retroarc basin
Hutuo-Wanzi retroarc basin
Jiao-Liao-Ji retroarc basin
600 km envelope
1000 km Andean magmatic zone envelope
Hidden basement
exposed Archean and Paleoproterozoic basement
2.3-1.88 Ga retro-arc basins
fault
thrust fault
approximate southern limit of khondalite belt
2.3-1.88 Ga magmatic rocks

Figure 22

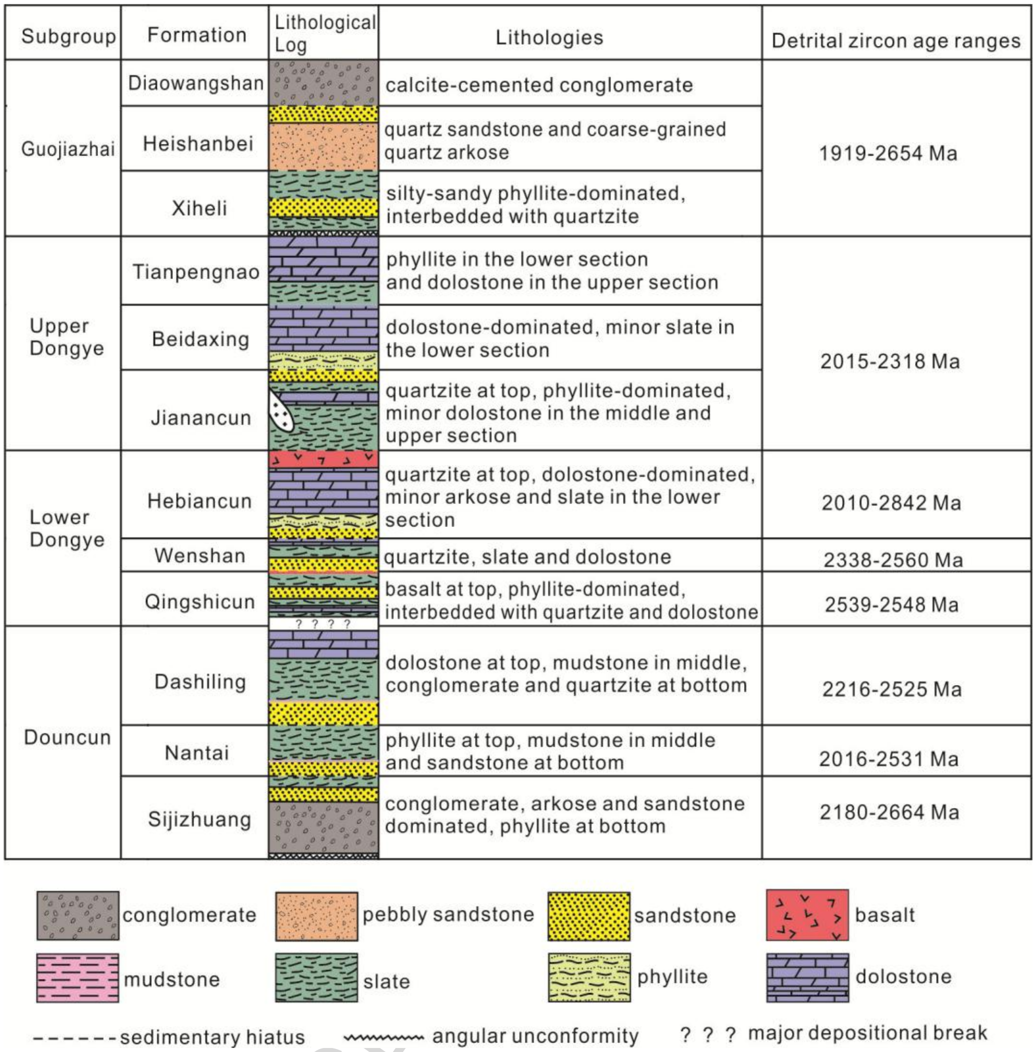
Subgroup
Formation
Lithological Log
Lithologies
Detrital zircon age ranges
Guojiazhai
Diaowangshan
calcite-cemented conglomerate
Heishanbei
quartz sandstone and coarse-grained quartz arkose
Xiheli
silty-sandy phyllite-dominated, interbedded with quartzite
1919-2654 Ma
Upper Dongye
Tianpengnao
phyllite in the lower section and dolostone in the upper section
Beidaxing
dolostone-dominated, minor slate in the lower section
Jianancun
quartzite at top, phyllite-dominated, minor dolostone in the middle and upper section
2015-2318 Ma
Lower Dongye
Hebiancun
quartzite at top, dolostone-dominated, minor arkose and slate in the lower section
2010-2842 Ma
Wenshan
quartzite, slate and dolostone
2338-2560 Ma
Qingshicun
basalt at top, phyllite-dominated, interbedded with quartzite and dolostone
2539-2548 Ma
? ? ? ?
Douncun
Dashiling
dolostone at top, mudstone in middle, conglomerate and quartzite at bottom
2216-2525 Ma
Nantai
phyllite at top, mudstone in middle and sandstone at bottom
2016-2531 Ma
Sijizhuang
conglomerate, arkose and sandstone dominated, phyllite at bottom
2180-2664 Ma
conglomerate
pebbly sandstone
sandstone
basalt
mudstone
slate
phyllite
dolostone
sedimentary hiatus
angular unconformity
? ? ? major depositional break

Figure 23

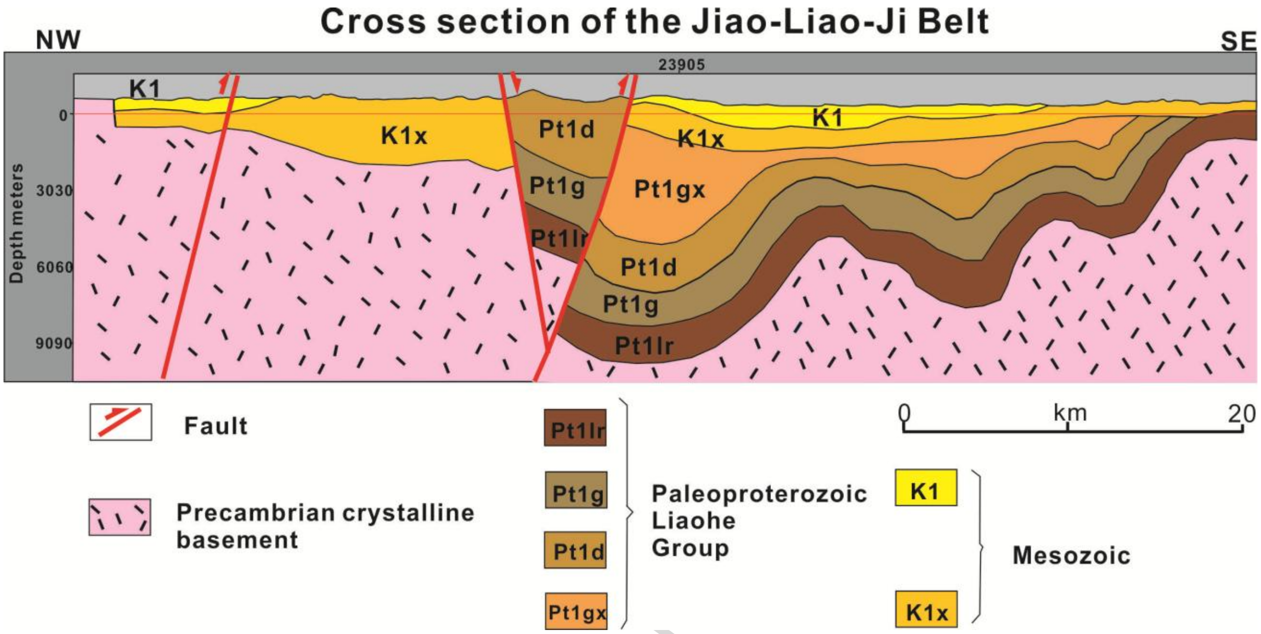
Cross section of the Jiao-Liao-Ji Belt
NW
SE
23905
Depth meters
0
3030
6060
9090
K1
K1x
K1
K1x
Pt1d
Pt1g
Pt1lr
Pt1gx
Pt1d
Pt1g
Pt1lr
Fault
Precambrian crystalline basement
Pt1lr
Pt1g
Pt1d
Pt1gx
Paleoproterozoic Liaohe Group
0 km 20
K1
K1x
Mesozoic

Figure 24

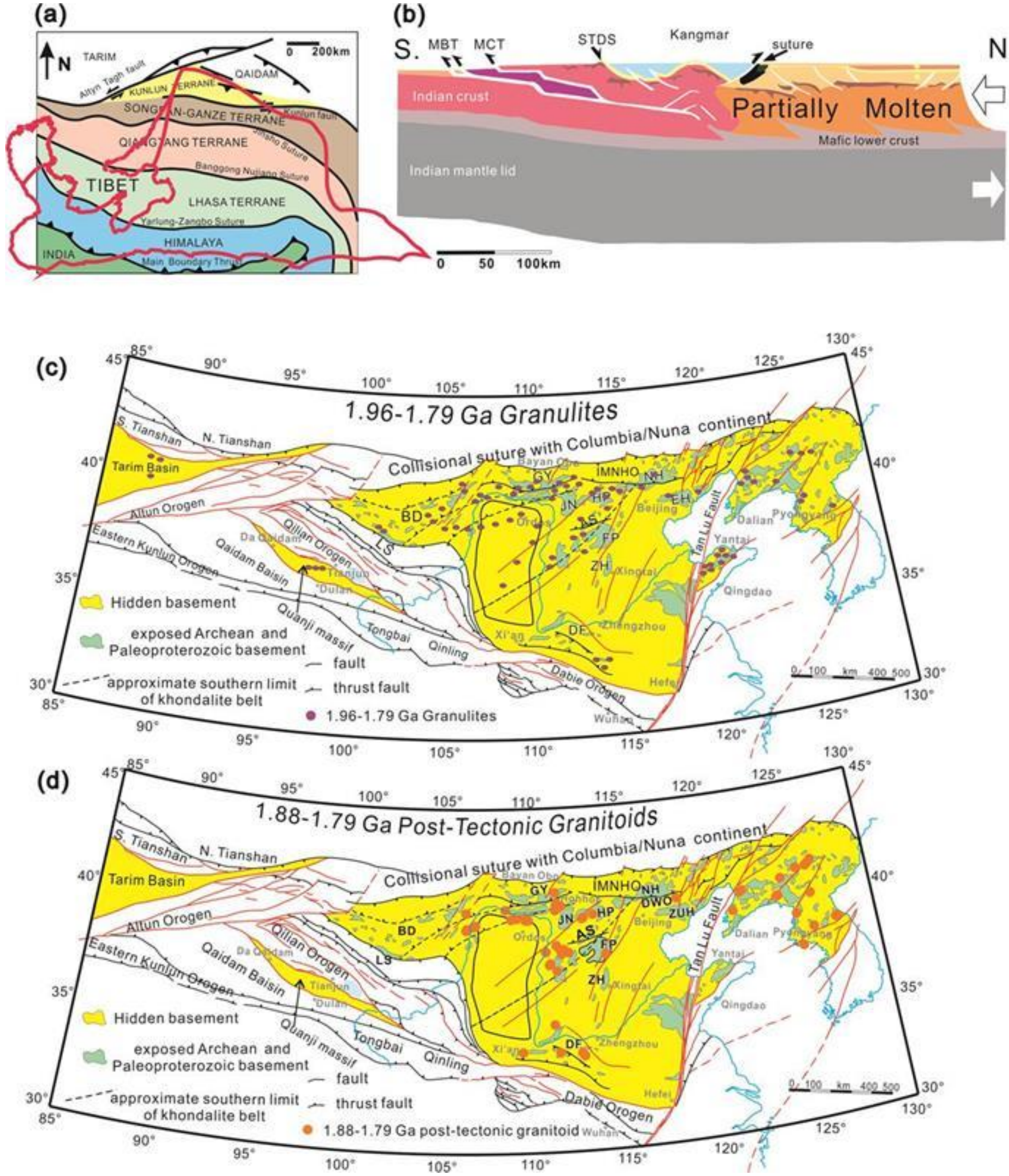
(a)
N
TARIM
0 200km
Altyn Tagh fault
QAIDAM
KUNLUN TERRANE
SONGPAN-GANZE TERRANE
Kunlun fault
QIANGTANG TERRANE
TIBET
Bangong Nujiang Suture
LHASA TERRANE
Yarlung-Zangbo Suture
HIMALAYA
INDIA
Main Boundary Thrust
(b)
S.
MBT
MCT
STDS
Kangmar
suture
N.
Indian crust
Partially Molten
Mafic lower crust
Indian mantle lid
0 50 100km
(c)
1.96-1.79 Ga Granulites
Collisional suture with Columbia/Nuna continent
S. Tianshan
N. Tianshan
Tarim Basin
Altun Orogen
Eastern Kunlun Orogen
Qaidam Baisin
Qilian Orogen
Quanji massif
Tongbai
Qinling
Dabie Orogen
Tan Lu Fault
Hidden basement
exposed Archean and Paleoproterozoic basement
fault
thrust fault
approximate southern limit of khondalite belt
1.96-1.79 Ga Granulites
(d)
1.88-1.79 Ga Post-Tectonic Granitoids
Collisional suture with Columbia/Nuna continent
S. Tianshan
N. Tianshan
Tarim Basin
Altun Orogen
Eastern Kunlun Orogen
Qaidam Baisin
Qilian Orogen
Quanji massif
Tongbai
Qinling
Dabie Orogen
Tan Lu Fault
Hidden basement
exposed Archean and Paleoproterozoic basement
fault
thrust fault
approximate southern limit of khondalite belt
1.88-1.79 Ga post-tectonic granitoid

Figure 25

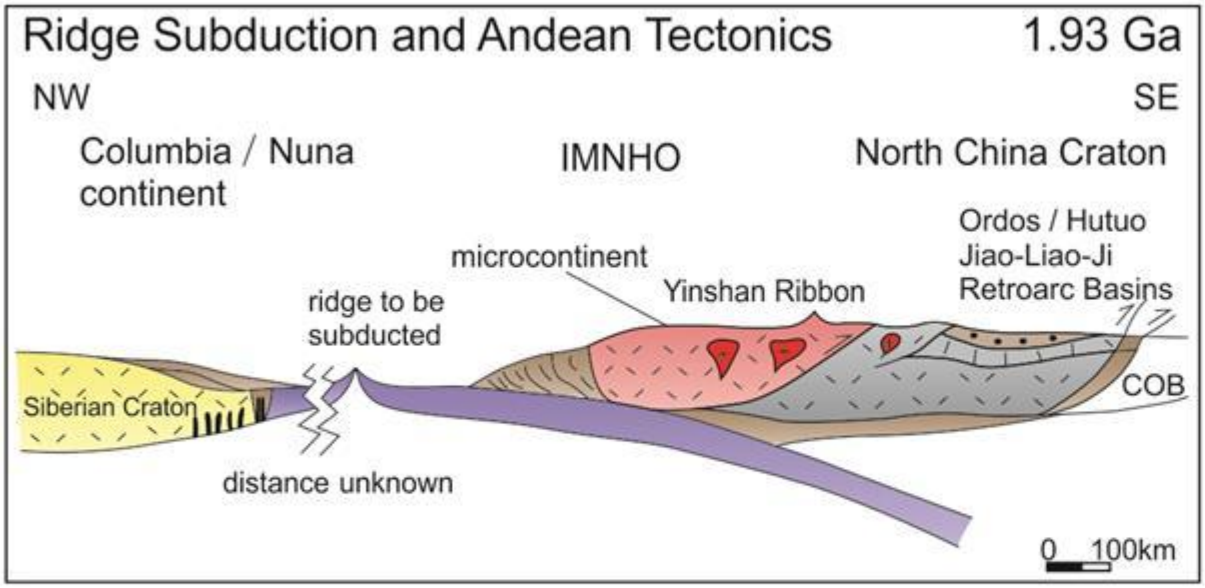
Ridge Subduction and Andean Tectonics
1.93 Ga
NW
SE
Columbia / Nuna continent
IMNHO
North China Craton
Ordos / Hutuo
Jiao-Liao-Ji
Retroarc Basins
microcontinent
Yinshan Ribbon
ridge to be subducted
Siberian Craton
COB
distance unknown
0 100km

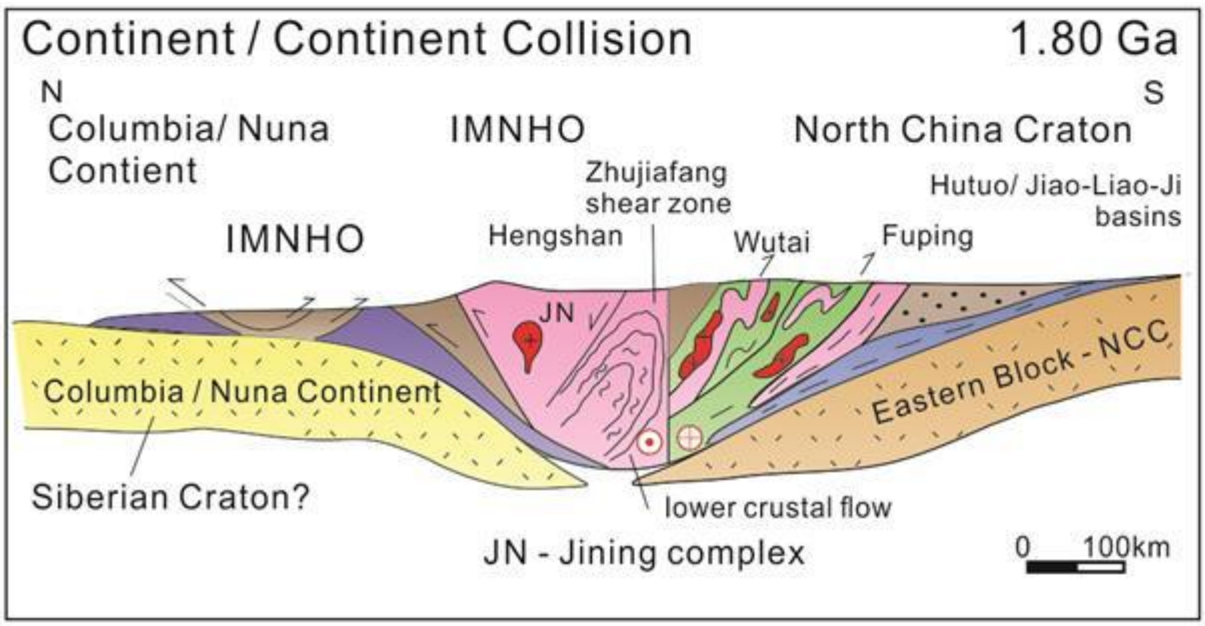
Continent / Continent Collision
1.80 Ga
N
S
Columbia/ Nuna Contient
IMNHO
North China Craton
Zhujiafang shear zone
Hutuo/ Jiao-Liao-Ji basins
IMNHO
Hengshan
Wutai
Fuping
JN
Columbia / Nuna Continent
Eastern Block - NCC
Siberian Craton?
lower crustal flow
JN - Jining complex
0 100km

Figure 26

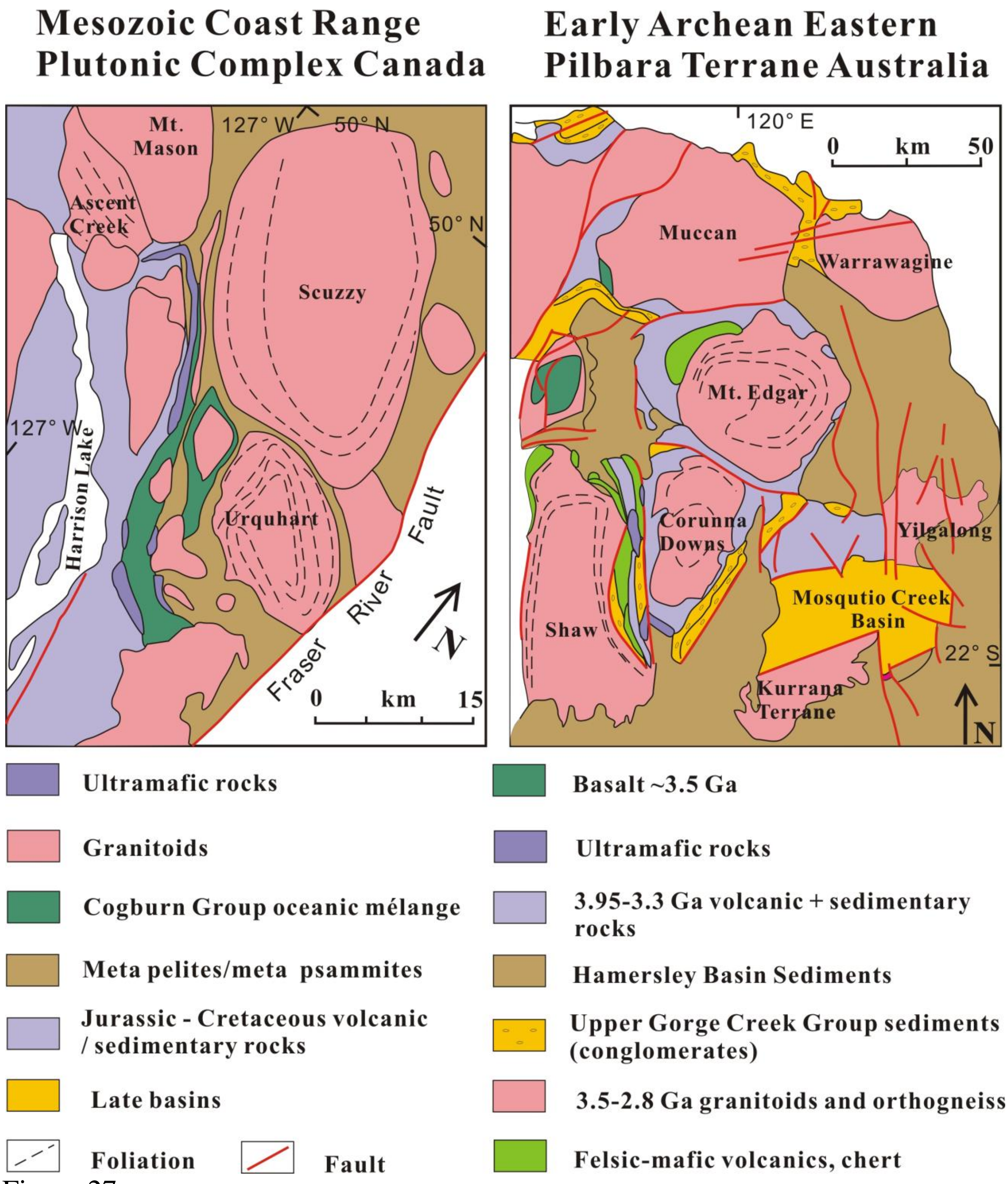
Mesozoic Coast Range
Plutonic Complex Canada
Early Archean Eastern
Pilbara Terrane Australia
Mt. Mason
127° W
50° N
Ascent Creek
Scuzzy
Harrison Lake
Urquhart
Fraser River Fault
0 km 15
N
120° E
0 km 50
Muccan
Warrawagine
Mt. Edgar
Corunna Downs
Yilgalong
Mosqutio Creek Basin
Shaw
22° S
Kurrana Terrane
Ultramafic rocks
Granitoids
Cogburn Group oceanic mélange
Meta pelites/meta psammites
Jurassic - Cretaceous volcanic / sedimentary rocks
Late basins
Foliation
Fault
Basalt ~3.5 Ga
Ultramafic rocks
3.95-3.3 Ga volcanic + sedimentary rocks
Hamersley Basin Sediments
Upper Gorge Creek Group sediments (conglomerates)
3.5-2.8 Ga granitoids and orthogneiss
Felsic-mafic volcanics, chert

Figure 27

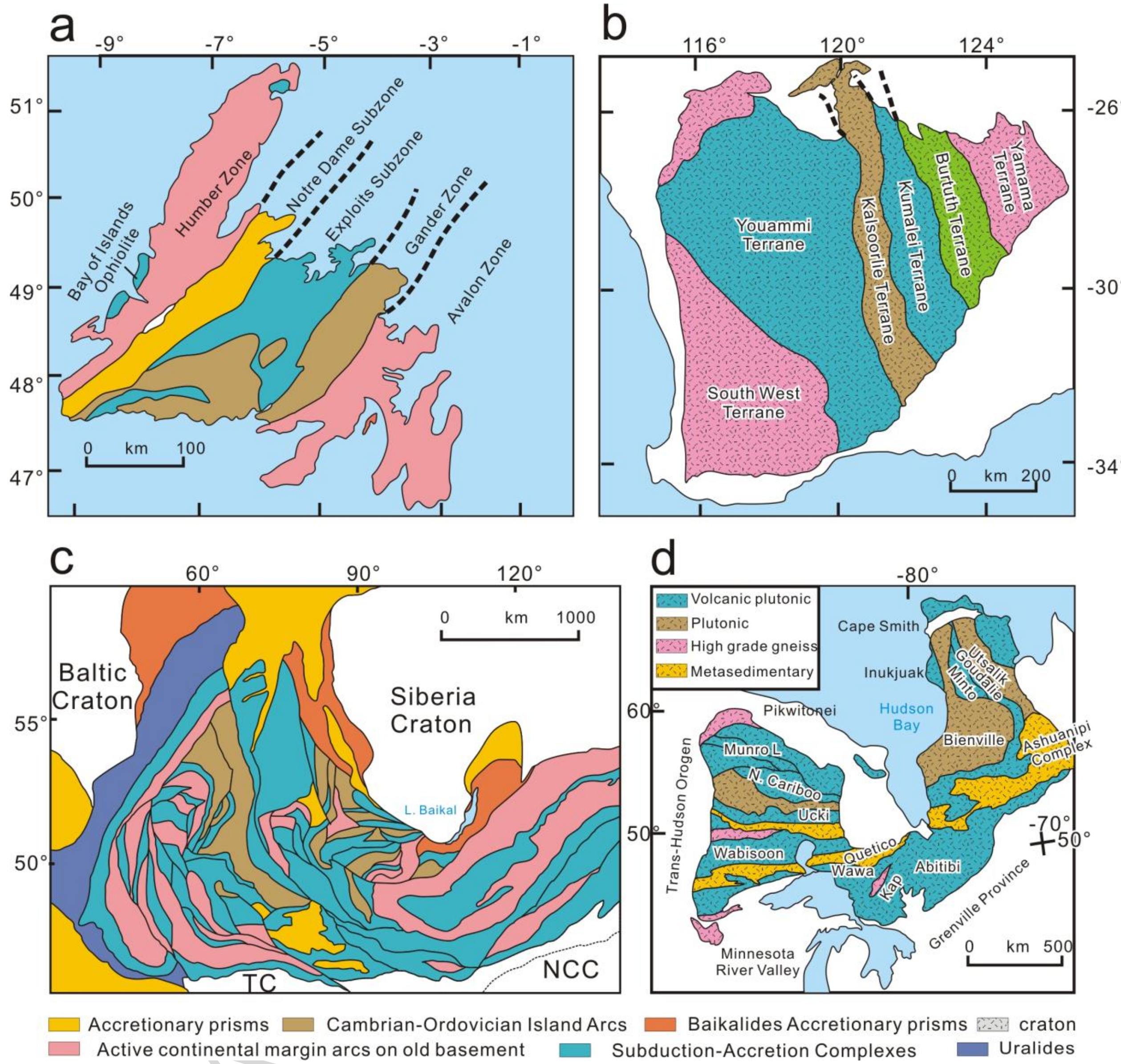
a
-9°
-7°
-5°
-3°
-1°
51°
50°
49°
48°
47°
Bay of Islands Ophiolite
Humber Zone
Notre Dame Subzone
Exploits Subzone
Gander Zone
Avalon Zone
0 km 100
b
116°
120°
124°
-26°
-30°
-34°
Youammi Terrane
Kalgoorlie Terrane
Kurnalei Terrane
Burtuth Terrane
Yamama Terrane
South West Terrane
0 km 200
c
60°
90°
120°
55°
50°
Baltic Craton
Siberia Craton
L. Baikal
TC
NCC
0 km 1000
d
-80°
Volcanic plutonic
Plutonic
High grade gneiss
Metasedimentary
Cape Smith
Inukjuak
Utsalik
Goudalie
Minto
Hudson Bay
Bienville
Ashuanipi Complex
Pikwitonei
Munro L.
N. Cariboo
Ucki
Wabisoon
Quetico
Wawa
Abitibi
Kap
Trans-Hudson Orogen
Grenville Province
Minnesota River Valley
60°
50°
-70°
50°
0 km 500
Accretionary prisms
Cambrian-Ordovician Island Arcs
Baikalides Accretionary prisms
craton
Active continental margin arcs on old basement
Subduction-Accretion Complexes
Uralides

Figure 28

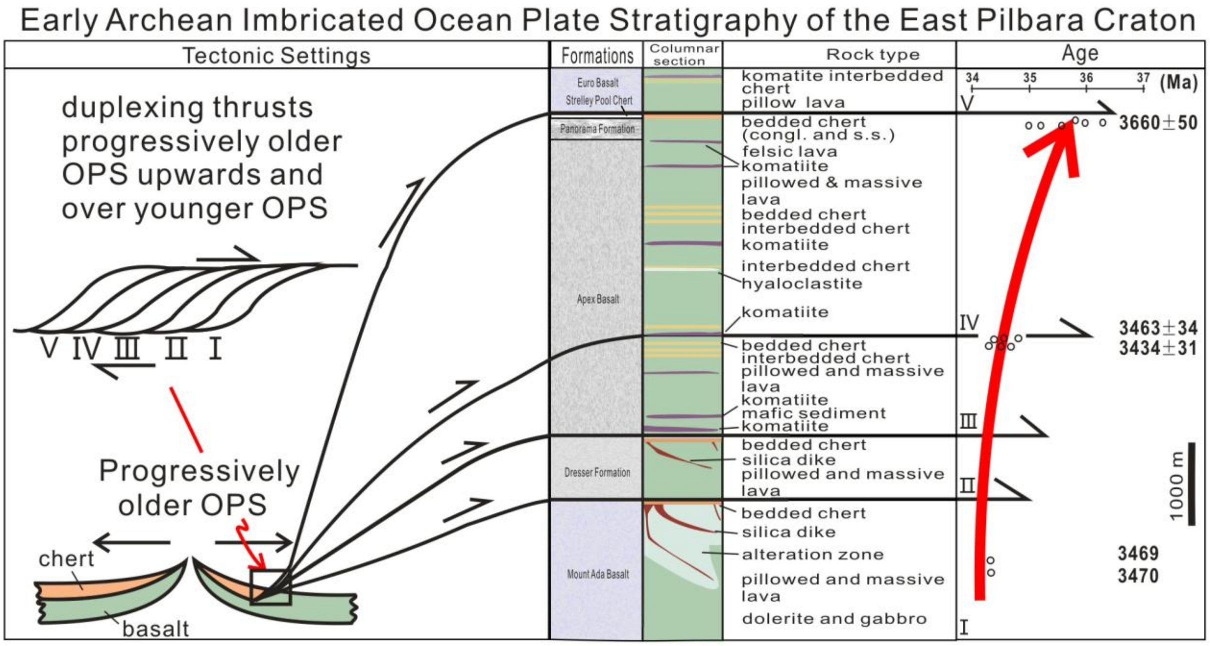

Early Archean Imbricated Ocean Plate Stratigraphy of the East Pilbara Craton
Tectonic Settings
Formations
Columnar section
Rock type
Age
duplexing thrusts progressively older OPS upwards and over younger OPS
V IV III II I
Progressively older OPS
chert
basalt
Euro Basalt
Strelley Pool Chert
Panorama Formation
Apex Basalt
Dresser Formation
Mount Ada Basalt
komatite interbedded chert
pillow lava
bedded chert (congl. and s.s.)
felsic lava
komatiite
pillowed & massive lava
bedded chert
interbedded chert
komatiite
interbedded chert
hyaloclastite
komatiite
bedded chert
interbedded chert
pillowed and massive lava
komatiite
mafic sediment
komatiite
bedded chert
silica dike
pillowed and massive lava
bedded chert
silica dike
alteration zone
pillowed and massive lava
dolerite and gabbro
34 35 36 37 (Ma)
3660±50
3463±34
3434±31
3469
3470
1000 m

Figure 29

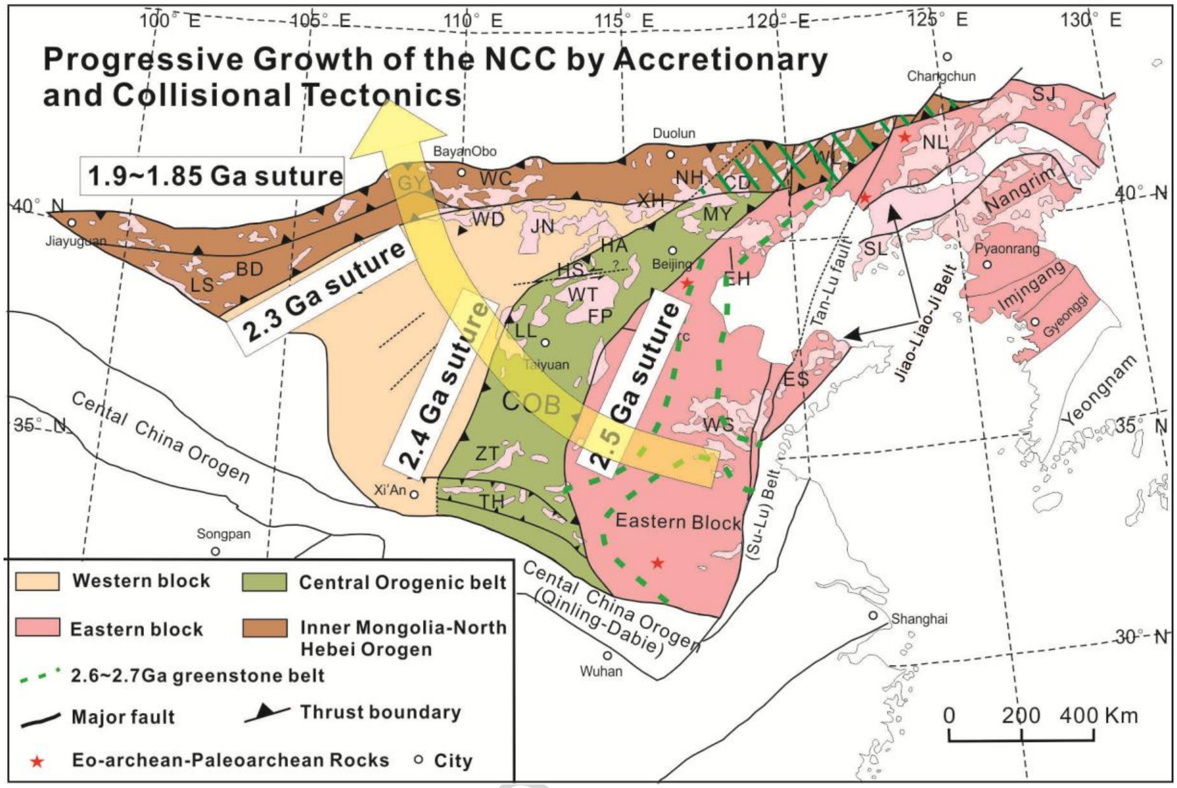

Progressive Growth of the NCC by Accretionary and Collisional Tectonics
1.9~1.85 Ga suture
2.3 Ga suture
2.4 Ga suture
2.5 Ga suture
Western block
Central Orogenic belt
Eastern block
Inner Mongolia-North Hebei Orogen
2.6~2.7Ga greenstone belt
Major fault
Thrust boundary
Eo-archean-Paleoarchean Rocks
City
Eastern Block
Central China Orogen
Cental China Orogen (Qinling-Dabie)
Tan-Lu fault
(Su-Lu) Belt
Jiao-Liao-Ji Belt
COB
Jiayuguan
BayanObo
Duolun
Changchun
Beijing
Taiyuan
Xi'An
Songpan
Wuhan
Shanghai
Nangrim
Pyaonrang
Imjingang
Gyeonggi
Yeongnam
0 200 400 Km

Figure 30